LAYING THE GENETIC AND MOLECULAR FOUNDATION FOR THE STUDY OF *FUSOBACTERIUM NUCLEATUM* IN RELATION TO HUMAN HEALTH AND DISEASE

Michael A. Casasanta

Dissertation submitted to the faculty of Virginia Polytechnic Institute & State University in partial fulfillment of the requirements for the degree of

Doctor of Philosophy in Biochemistry

Daniel J. Slade
Pablo Sobrado
Glenda Gillaspy
Stephen Melville

February 15, 2019
Blacksburg, Virginia

Keywords: *Fusobacterium*, genetics, invasion, phospholipase, host-pathogen interaction, Molecular biology, chemical biology, microbiome

Laying the Genetic and Molecular Foundation for the Study of *Fusobacterium nucleatum* In Relation To Human Health and Disease

Michael A. Casasanta

ABSTRACT

Fusobacterium nucleatum is a Gram-negative, anaerobic bacterium that is a member of the human oral microbiota. Although it is a normal resident of the mouth, it is associated with a number of human diseases including: sepsis, inflammatory bowel disease (IBD), and colorectal cancer (CRC). Despite the important association of *F. nucleatum* with human health and disease, remarkably little is known about the molecular mechanisms underlying these infections. This knowledge gap can, in part, be attributed to a lack of molecular tools and experimental workflows. Creating the genetic tools to fill this knowledge gap is an imperative undertaking for the future development of treatments for diseases involving *F. nucleatum*. Previous work in the field has assigned functions to just a handful of *Fusobacterium* proteins (Fap2, FadA), and only two of those proteins have a well-defined role in the host-pathogen relationship. This dissertation contains work that lays the molecular and genetic foundation for future studies involving *F. nucleatum* by creating a unique gene deletion system while simultaneously establishing broadly applicable experimental workflows and molecular tools to study initial bacterial attachment and invasion processes crucial to *Fusobacterium* virulence. Marker-less gene deletions confirm the importance of Fap2 in host-cell attachment and invasion and suggest a lesser role in invasion for FadA, representing a significant revision to the *Fusobacterium*-host relationship. Also, our system allows for the overexpression and purification of virulence factors directly from *Fusobacterium* for the first time. This permits us to study aspects of *Fusobacterium* protein biology that were previously impossible and will provide further insights into the nature of *Fusobacterium* virulence. A custom suite of molecular tools was also developed to facilitate recombinant expression of these proteins in general laboratory settings using simple *E. coli* protein expression systems. We have used these

new technologies to express and purify a number of potential *Fusobacterium* virulence factors as detailed in this dissertation.

Also contained in this dissertation is the application of these breakthroughs to probe the function of a novel *F. nucleatum* outer membrane phospholipase, FplA. Phospholipases are important virulence factors in a number of well-studied human pathogens including *Pseudomonas aeruginosa* and *Legionella pneumophila*, where they interfere with host cellular signaling processes to increase intracellular bacterial survival. Our data show that FplA is a Class A1 phospholipase (PLA1) with robust catalytic activity capable of binding to and cleaving a number of lipid types. Additionally, we show that it has the ability to bind to important host signaling lipids including phosphatidylinositol 3, 5-bisphosphate and phosphatidylinositol 3, 4, 5-triphosphate. These data suggest FplA may play a role in manipulating the intracellular processes of host cells. Taken together, work in this dissertation provides tools and experimental frameworks for the future study of *F. nucleatum* pathogenesis while identifying and initially characterizing a new, potentially significant, virulence factor in FplA.

Laying the Genetic and Molecular Foundation for the Study of *Fusobacterium nucleatum* In Relation To Human Health and Disease

Michael A. Casasanta

GENERAL AUDIENCE ABSTRACT

Fusobacterium nucleatum is a Gram-negative, anaerobic bacterium that is a member of the human oral microbiota. Although it is a normal resident of the mouth, it is associated with a number of human diseases including: sepsis, inflammatory bowel disease (IBD), and colorectal cancer (CRC). Despite the important association of *F. nucleatum* to human health and disease, remarkably little is known about the molecular mechanisms underlying this relationship. This knowledge gap can be attributed to a lack of molecular tools and experimental workflows to study this association. Developing the genetic tools to fill this gap is imperative for the future development of treatments to diseases involving this pathogen. Previous work in the field has assigned functions to just a handful of *Fusobacterium* proteins, with only two being studied in great detail in human disease models. This dissertation contains work that lays the molecular and genetic foundation for future studies involving *F. nucleatum* by creating a unique gene deletion system while simultaneously establishing broadly applicable molecular tools to study how *F. nucleatum* enters human cells. Gene deletions confirm the importance of Fap2 in host-cell attachment and invasion and suggest a lesser role for invasion in FadA. This revises the roles of the two most well studied *F. nucleatum* proteins in the context of human disease. Also, our system allows for the overexpression and purification of virulence factors directly from *F. nucleatum* for the first time. This permits us to experiment with proteins previously difficult to study using traditional *E. coli* based recombinant systems, which will provide further insights into the nature of *F. nucleatum* virulence. Also contained in this dissertation is the application of these systems to probe the function of a novel *Fusobacterium* outer membrane phospholipase,

FplA. Phospholipases are important virulence factors in a number of well-studied human pathogens including *Pseudomonas aeruginosa* and *Legionella pneumophila*, where they interfere with host cellular signaling processes to increase intracellular bacterial survival. Our data show that FplA is a phospholipase with robust catalytic activity capable of binding to and cleaving a number of lipid types. Additionally, we show that FplA has the ability to bind to important human signaling lipids, suggesting that it may have a role in manipulating processes inside host cells. Taken together, work in this dissertation provides the molecular and genetic tools along with the experimental frameworks for the future study of *F. nucleatum* pathogenesis while identifying and initially characterizing a new, potentially significant, virulence factor in FplA.

To my friends and family...

Acknowledgements

I'd like to express my sincere thanks and appreciation for my advisor Dr. Daniel Slade. His guidance and presence in lab has shown me what it takes to start and build an academic career. His drive has also instilled in me a work ethic that will propel me to success in the future. Late nights in lab may be a necessity, but it makes early Fridays at the Cellar all that much better.

I'd also like to thank the members of my committee: Dr. Pablo Sobrado, Dr. Glenda Gillaspy, and Dr. Stephen Melville for providing much needed insight and guidance. Their input has increased the quality of my work and made me a better, more focused, scientist.

Additionally, I'd like to think my family and friends. My family has been supportive of my career and decision to attend graduate school to pursue and complete my PhD, and for that I am grateful. Completing this process would not have been possible without my friends. They kept me going during the difficult times inherent to any graduate career and provided much needed relief over the last 4.5 years. All of you are awesome.

Table of Contents

List of Figures

List of Tables

Chapter 1

Introduction to Autotransporters as Virulence Factors in *Fusobacterium nucleatum*

Michael A. Casasanta[1], Daniel J. Slade[1]

1. Virginia Polytechnic Institute and State University, Department of Biochemistry, Blacksburg, VA,

USA.

Abstract

The recently sequenced and assembled genomes of *Fusobacterium nucleatum* has revealed a multitude of genes encoding for autotransporters. These secreted, outer membrane proteins are among the most numerous virulence factors in Gram-negative bacteria. Their functions are diverse and have been studied extensively in a number of important human pathogens. Proteins in this family act as adhesins, serine hydrolases, iron scavengers and cytolysins all aiding in the pathogenesis of significant disease-causing organisms including *Escherichia coli*, *Pseudomonas aeruginosa, Bordetella pertussis*. However, the roles these proteins serve in *F. nucleatum* virulence are critically understudied. *F. nucleatum* does not possess large protein export machinies, such as the Type II, III or IV secretion systems. These are typically used by pathogens to secrete virulence factors into their extracellular environment to establish infection and cause disease. The absence of these protein export systems in combination with the overabundance of autotransporter proteins secreted by *F. nucleatum* suggests that autotransporters play a central role in *F. nucleatum* virulence. The methodologies and the suite of molecular tools that we have created for Fusobacterium has provided the foundation for the initial and ongoing study of autotransporters and additional protein families in this bacterium. We have recombinantly expressed, purified and performed initial analysis of proteins from each subclass of the autotransporter family. Thus, we have begun to shed light on the function of these proteins in *F. nucleatum* virulence while providing broadly applicable molecular tools to the greater microbiology community to facilitate work across bacterial genera.

Introduction

Evidence continues to mount illustrating the extent to which *Fusobacterium nucleatum* contributes to disease in humans. It has been shown to cause infections in numerous locations throughout the body, including the brain, liver, lungs, and heart [1–3]. *F. nucleatum* can also invade the placenta and cause still birth in humans [4]. In addition to localized infection, *F. nucleatum* has also been implicated in the development and progression of colorectal cancer (CRC). Infection induces carcinoma formation in the colons of $APC^{min/+}$ mice, and it was shown to be over represented in the carcinomas of patients suffering from CRC [5, 6]. Together, these results suggest a role for *F. nucleatum* in the development or progression of this disease. The mechanisms by which these diverse disease associations take place, however, remain largely unclear (**Figure 1.1**).

The recently sequenced and assembled genome of *F. nucleatum* has helped build a better picture of its virulence factor repertoire [7]. Interestingly, it does not possess the vast majority of protein secretion systems typical of Gram-negative human pathogens [46]. The *F. nucleatum* genome does not contain any genes encoding for a Type 1, 2, 3 or 4 secretion system. These large multi-protein systems facilitate virulence factor secretion from within bacterial cells into either the extracellular environment or directly into host cells where they elicit some effect that aids in pathogenesis [8]. Functions of these effector proteins include adhesion, proteolysis, and lipid hydrolase activity among others. Ultimately, they cause a change in host cell physiology that provides a more conducive environment for pathogen survival and colonization. The role of these large protein secretion machineries in bacterial virulence is filled by members of the Type 5 secretion system, or autotransporters, in *F. nucleatum*.

Autotransporters (ATs) are large, secreted proteins and are among the most commonly possessed virulence factors among Gram-negative bacteria. While most genomes of bacteria that have ATs encode for just a handful of these proteins, *Fusobacterium* species generally have open

reading frames for over 20 [47]. The apparent overabundance suggests an important role for this protein family in *F. nucleatum* pathogenesis. Additionally, their presence in the bacterial outer membrane places them at the host-pathogen interface, making them both prime candidates to manipulate host physiology and potential targets for new therapeutics.

The identification and accurate annotation of ATs in the *F. nucleatum* genome represents the first step in the classification and study of these proteins in this important human pathogen. To fully probe their roles in disease, we need both a genetic system to create in-frame gene deletion strains (reverse genetics) and a suite of molecular tools to recombinantly express, purify and functionally characterize them. Experimental methods for the creation and use of both of these fundamental tools are detailed later in this dissertation. However, to fully appreciate the need the field has for a broadly applicable molecular toolset for the study of large outer membrane proteins, a more detailed understanding of the nature of these proteins is required.

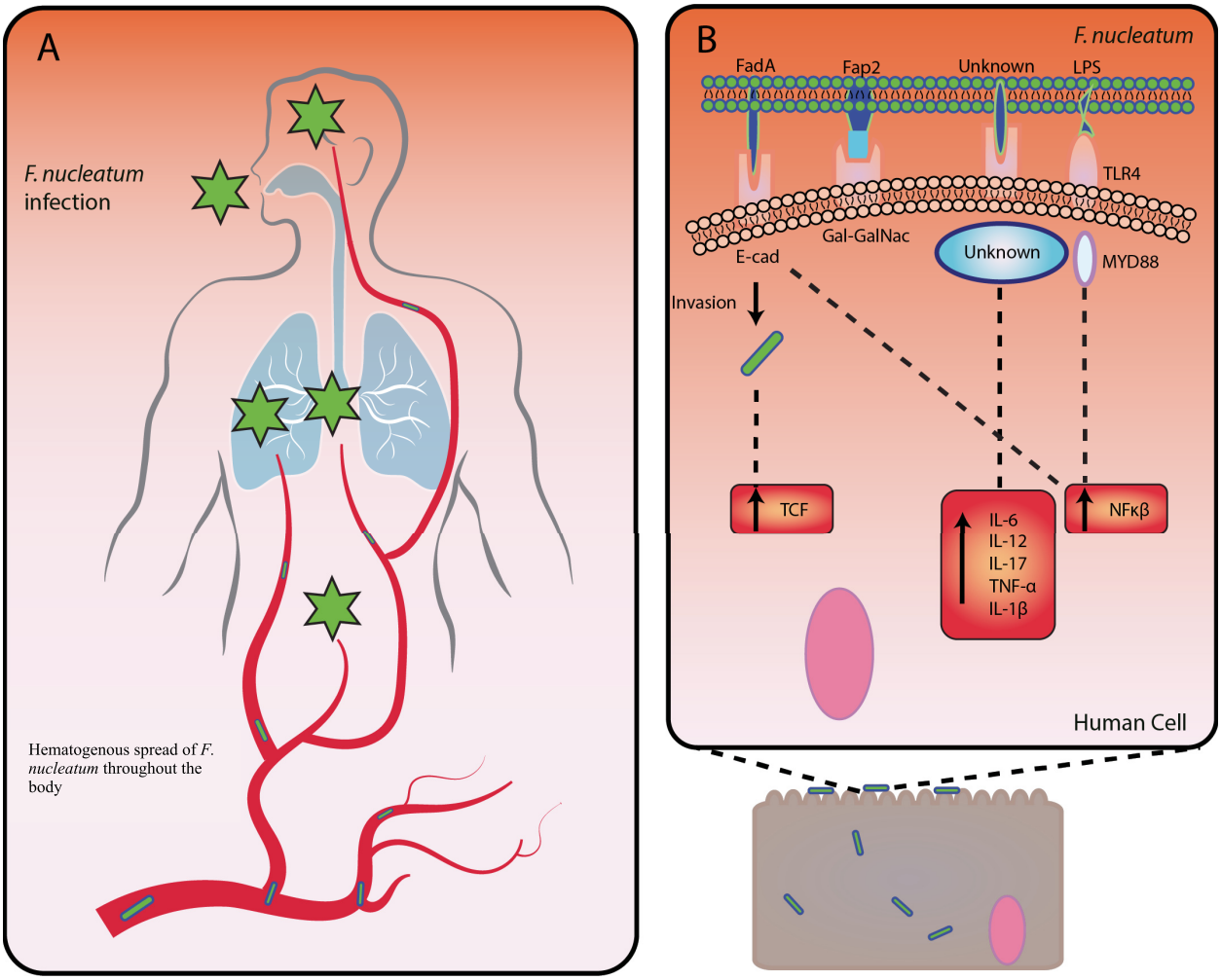

Figure 1.1 The current understanding of *F. nucleatum* infection. (A) *F. nucleatum* causes infection in disparate locations throughout the body. These locations include the mouth, brain, heart, lungs, and liver. Current evidence suggests that these infections are established through hematogenous spread of the bacterium through the body.[9, 10]. (B) Current details about the interactions at the host-pathogen interface are limited. Fap2 and FadA remain the only two virulence factors studied in depth with respect to effects on host cell physiology. Fap2 interacts with Gal-GalNac residues, FadA interacts with E-cad. Together they induce the upregulation of a number of pro-inflammatory markers. E-cad = E-cadherin. Gal-GalNac = N-acetylgalactosamine. Nuclei indicated by pink oval. (B).

Autotransporter Fundamentals

Autotransporters (ATs) are large, Gram-negative bacteria specific proteins that were thought to encode all of the machinery for their own secretion, giving them the name "Autotransporters". However, their secretion is largely dependent on periplasmic chaperones and outer membrane complexes which will be highlighted in the following text, making the autotransporter title misleading. Their protein architecture includes a signal peptide, a functional or 'passenger' domain, and a β-barrel domain (**Figure 1.2**). While secretion of all ATs share some similarities, there are a number of variations in this process among the 5 subcategories of AT that will be described below. However, as a general rule for all ATs, an N-terminal signal peptide directs the unfolded protein to the inner membrane Sec apparatus for translocation into the periplasmic space. Upon translocation, the signal peptide is cleaved from the maturing protein where it then begins to interact with a number of periplasmic chaperone proteins [48]. The exact biophysical details of these processes are unknown, but it is currently thought that these chaperone and outer membrane associated proteins begin to fold and insert the beta barrel of the AT into the outer membrane while simultaneously allowing the passenger domain to translocate to the extracellular environment [49]. Once outside of the cell, the passenger domain may remain anchored to the cell surface or be cleaved and released into the extracellular environment [8, 11]. This elegant system allows for the secretion of a vast, multifunctional array of proteins to the host-pathogen interface with minimal protein machinery required. Detailed descriptions and biophysical schematics of AT biogenesis can be found in the literature [11, 37, 48-50]. The AT family can be divided into 5 subcategories; Type 5a, b, c, d, and e. *F. nucleatum* possesses only type's a-d, so discussion will be limited to details concerning only those types. However, type 5e autotransporters are known as intimins and have been characterized in *E. coli* and shown to be involved in invasion [50].

Type 5a ATs

Structure and Biogenesis

This subcategory represents the monomeric ATs. Both the passenger and β-barrel domains are encoded in one open reading frame and are expressed as a single polypeptide. Their secretion is facilitated through the generalized mechanism described above. Briefly, their domain architecture consists of a signal peptide for protein translocation to the periplasm, a passenger domain which elicits the protein's function and a β-barrel that anchors the protein to the bacterial outer membrane (**Figure 1.2**). After secretion into the periplasm, the unfolded AT interacts with a number of chaperones, including DegP, SurA, FkpA, and Skp, to keep it in an unfolded state [48]. After signal peptide cleavage, the partially unfolded β-barrel domain interacts with the Bam complex in the outer membrane to facilitate AT insertion into the outer membrane. The exact biophysical details are not fully understood about passenger domain translocation, but it is believed to be pulled through the interior of the β-barrel and presented fully folded on the surface of the bacterial cell [49]. At this time, the passenger domain can be cleaved from the cell surface or remain attached to the outer membrane [11]. Many of the enzymatically active monomeric autotransporters are cleaved from the surface of the bacteria. These include the serine protease autotransporters of Enterobacteriaceae (SPATE), which are only expressed in pathogenic Gram-negative bacteria in the colon [51]. Tsh, a monomeric serine protease from an avian pathogenic strain of *E. coli* was used as a model to study the autoproteolytic mechanism of these enzymes.

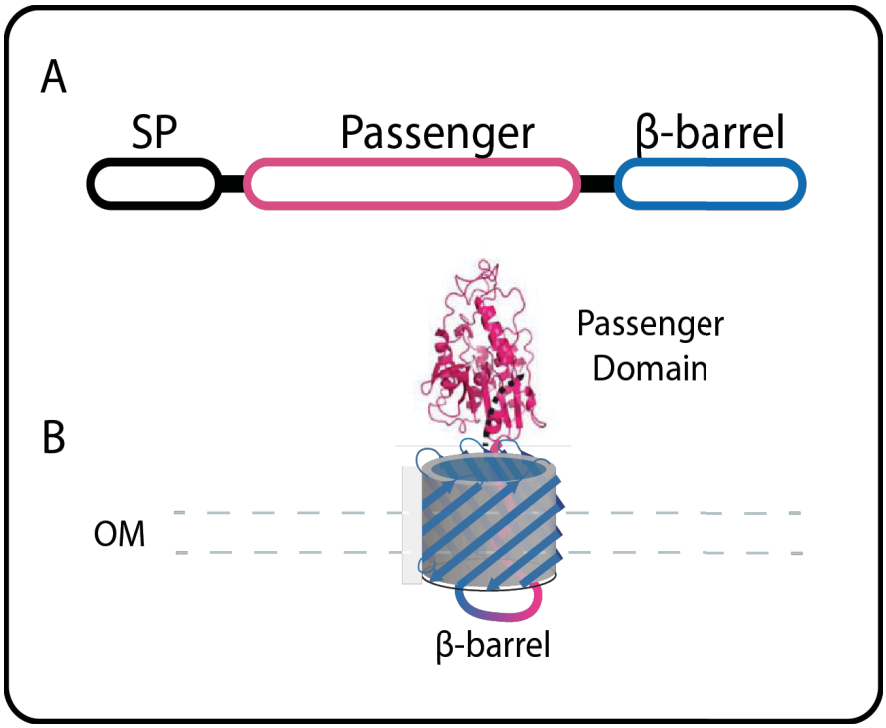

Figure 1.2 The basic domain architecture and subcellular localization of a monomeric autotransporter. (A) The basic domain architecture of a monomeric AT expressed as a cartoon. There is an N-terminal signal peptide (SP) for protein translocation to the periplasm, a passenger domain eliciting the effector function of the AT, and a β-barrel that anchors the protein to the bacterial outer membrane. (B) The subcellular localization of an AT represented by an AT model, FplA, illustrating how the structure of a fully formed Type 5a AT may appear on the outer membrane (OM) (B) [12].

Secretion relies on a 14 amino-acid motif N-terminal to the β-barrel domain relying largely on hydrophobic residues within this motif are needed for autoproteolytic cleavage. Following cleavage, a portion of the α-helical linker is left behind to fill the pore left by the exiting passenger domain [52]. In some instances, cleavage from the bacterial cell surface is dependent upon expression of an accessory enzyme that can cleave the passenger from the β-barrel. IcsP is a serine protease from *Shigella flexneri* that cleaves the actin-nucleation protein IcsA from the surface of the bacterium [53]. Type 5a ATs are functionally diverse and vital to myriad pathogenic bacteria.

Functions in Pathogenic Bacteria

Monomeric ATs are present in many pathogenic bacteria and contribute signficantly to disease. Medically important strains of *E. coli* express multiple Type 5a ATs with a number of different functions. The widely known O157:H7 strain of *E. coli* (EHEC), implicated in severe diarrheal disease, expresses EspP, a serine protease capable of cleaving human coagulation factor V which exacerbates gastrointestinal hemorrhage during infection[13]. Another important *E. coli* virulence factor is AIDA-1. It is a membrane-bound adhesin that facilitates *E. coli* interaction with a wide variety of human host proteins and contributes to biofilm formation and bacterial persistence [14]. *Bordetella pertussis*, the etiologic agent of whooping cough, also utilizes the Type 5a AT pathway to secrete virulence factors. Pertactin is an adhesin expressed by multiple strains of virulent *Bordetella* that is important for the establishment of infection and bacterial persistence. It is also a major component of the acellular *Bordetella* vaccine, further illustrating the importance of ATs in disease and highlighting the promise of exploiting this protein family as a drug target in *F. nucleatum* [54]. *Neisseria meningitidis* also expresses ATs that are important for virulence. MspA is a large surface bound adhesin that mediates bacterial interaction with both endothelial and epithelial cells [15]. *N. meningitidis* also secretes a multifunctional Type 5a serine protease, IgaA1

which is capable of cleaving both human IgA's and NF-κB to promote bacterial persistence during disease [16, 17]. These are just a few examples of Type 5a autotransporters mediating virulent phenotypes in medically significant bacteria.

Examples in *Fusobacterium nucleatum*

The *F. nucleatum* strain used for studies presented in this body of work, ATCC23726, possesses genes for 13 Type 5a ATs, most of which contain unknown functions. However, the number and type of autotransporter varies among species and strain [47]. The most well studied of these proteins is Fap2. Fap2 is a large adhesin (3768AA) anchored to the surface of *F. nucleatum* with an important role in host cell interaction [18]. It binds to Gal-GalNAc residues on cell surface proteins of colon carcinomas where it facilitates invasion [10]. It is also responsible for inactivating NK-T-cells, where it contributes to decreased tumor clearance and impaired immune function [19]. The important role of Fap2 as an adhesin and immune cell modifier highlights the importance of molecular tool development to facilitate advanced study of this protein. Another characterized Type 5a AT in *F. nucleatum* is RadD. While not as well studied as Fap2, it has demonstrated pathogenic potential by inducing cell death in human immune cells [20]. Additionally, it is responsible for *F. nucleatum* aggregation with other bacteria present in its environment. *F. nucleatum* exists in mixed species biofilms in the mouth, and RadD facilitates those interbacterial interactions [21, 22]. Aim1 is yet another understudied AT of *F. nucleatum*. While it induces apoptosis in laboratory cell lines, detailed information about its function in the context of human disease is unknown [23].

The importance of this AT class to *F. nucleatum* virulence is exemplified by the role of Fap2 in host cell invasion, immune system modulation and apoptosis. The pathogenic properties Type 5a ATs confer combined with their outer membrane localization suggest these proteins may

be exploitable as undiscovered vaccine or drug design targets. However, the specific roles *F. nucleatum* proteins play and their functions are largely unknown, representing a sizeable knowledge gap for the field. Unfortunately, modern bioinformatics tools are generally ineffective in assigning predicted functions based on homology to characterized proteins as protein-BLAST and homology searches of functional domains within these ATs provide inconclusive results. Therefore, new functional assays to determine their role in disease are greatly needed.

Type 5b ATs

Structure and Biogenesis

Type 5b ATs, or two partner secretion pairs, are unique among the family in that their passenger and β-barrel domains are encoded by 2 different genes, which are typically denoted *tpsA* and *tpsB* respectively [24]. These gene pairs are located in close proximity on the genome and are expressed together (**Figure 1.3**). Both genes possess signal peptides that direct them to the Sec secretion machinery which facilitates their translocation into the periplasm. Given that these protein pairs are expressed as separate polypeptides, they must have a mechanism for the cognate pairs to find each other in the periplasm. This process is facilitated by the conserved N-terminal region of the TpsA and the tandem polypeptide transport associated (POTRA) domains located just N-terminal to the β-barrel domains in the folded and outer membrane-inserted TpsB. These regions interact to translocate the TpsA to the extracellular environment [25]. However, the exact biophysical mechanisms underpinning this phenomenon of protein pair association and secretion remain largely unknown [26]. The functional effector proteins are typically massive with molecular weights up to 500 kDa, and they possess a largely beta-helical structure. They may be the most functionally diverse subcategory of AT, with members of this widespread protein family possessing adhesive, iron scavenging, cytolytic and hemolytic activities [27–30].

Function in Pathogenic Bacteria

Type 5b secreted ATs are expressed in a several important human pathogens. Perhaps the most well studied of these virulence factors is the filamentous hemagglutinin (FHA) of *B. pertussis*.

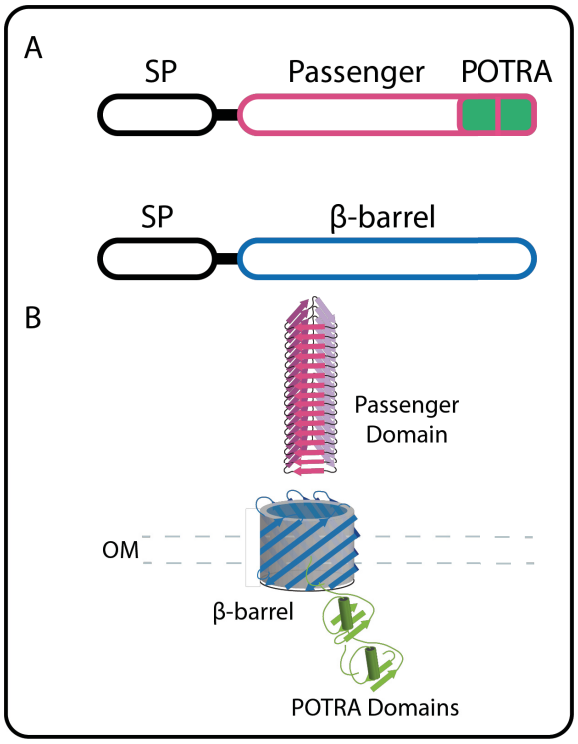

Figure 1.3 The basic domain architecture and subcellular localization of a Type 5b autotransporter. The basic protein domains typical of a Type 5b AT depicted as a cartoon. The passenger and β-barrel of the AT are expressed as two different genes (A). A diagram of what the configuration and localization of a Type 5b AT in the context of a bacterial membrane may look like. The filamentous β-helical structure typical of a TpsA protein is shown in pink as a cartoon and protein interaction domains are shown in green (B).

This protein is responsible for bacterial adherence to epithelial cells in the lungs upon infection. FHA is vital to virulence, as it facilitates colonization and prevents immune system clearance of infection [31]. FHA is also a critical component of the acellular *Bordetella* vaccine, along with the Type 5a, Pertactin, again demonstrating the central role ATs play in the treatment of infectious disease. ShlA of *Serratia marcescens* is a TpsA that elicits cytolytic activity against human epithelial cells and erythrocytes [32]. *Haemophilus influenzae* also expresses the Type 5b secreted AT HMW1 which is a large adhesin responsible for bacterial attachment and colonization of human epithelial cells [33]. Like ShlA and FHA, it is secreted by the aforementioned Type 5b mechanism, however it remains attached to the bacterial cell surface to elicit its function. HMW1 outer membrane attachment is mediated by N-linked glycosylation via a bacterial glycosyltransferase that allows the protein to remain surface attached, thereby interacting with human cell surface proteins. The glycosylation step is imperative for HMW1 effectiveness as an adhesin which suggests that, in specific cases, post-translational modification of ATs is important for virulence [34]. Studying the AT structure-function relationship relative to post translational modification is currently under-studied in the field, and it represents a new avenue of research that can be facilitated by the tools and experimental frameworks presented in this dissertation.

Examples in *F. nucleatum*

The new, corrected genome of *F. nucleatum* assembled by the Slade Lab has uncovered 4 two partner pairs hereafter named VbaA/B, VbbA/B, VbcA/B, and VbdA/B (**Figure 1.4**) [47]. In *F. nucleatum*, however, their functions remain completely unknown. This can be partly attributed to the previous lack of an accurate gene deletion system for *F. nucleatum*. Also, this gene family was critically misannotated in previous genome assemblies which allowed them to go undetected

to bioinformatics classification tools as possible virulence factors. Our recent discovery of these 4 two partner secretion pairs provides the first step in the study of these ATs in *F. nucleatum*. Given the importance of Type 5b ATs to human pathogens like *B. pertussis* and *S. marcescens*, the potential significance of these proteins in *F. nucleatum* pathogenesis is readily apparent [35,36]. Additionally, they represent a pool of potential drug targets that have yet to be examined, again highlighting the need for molecular tools that will facilitate their study. Later chapters of this dissertation detail the creation of these molecular tools, and we have already adapted them for use in studying Type 5b ATs in *F. nucleatum*. Using our suite of custom protein expression and secretion vectors, we have, for the first time, recombinantly expressed and purified a Type 5b protein from *F. nucleatum,* VbaA. Additionally, we have created the first in-frame gene deletion of a protein in this family using our genetic system. We have used the resulting highly purified protein to develop and isolate a custom antibody that can be used to detect the production of VbaA in any number of different cellular contexts (**Figure 1.5**). This, in conjunction with our genetic system, will allow, for the first time, the examination of a Type 5b AT in cellular invasion or host colonization assays and the discovery of a new set of virulence factors in *F. nucleatum*.

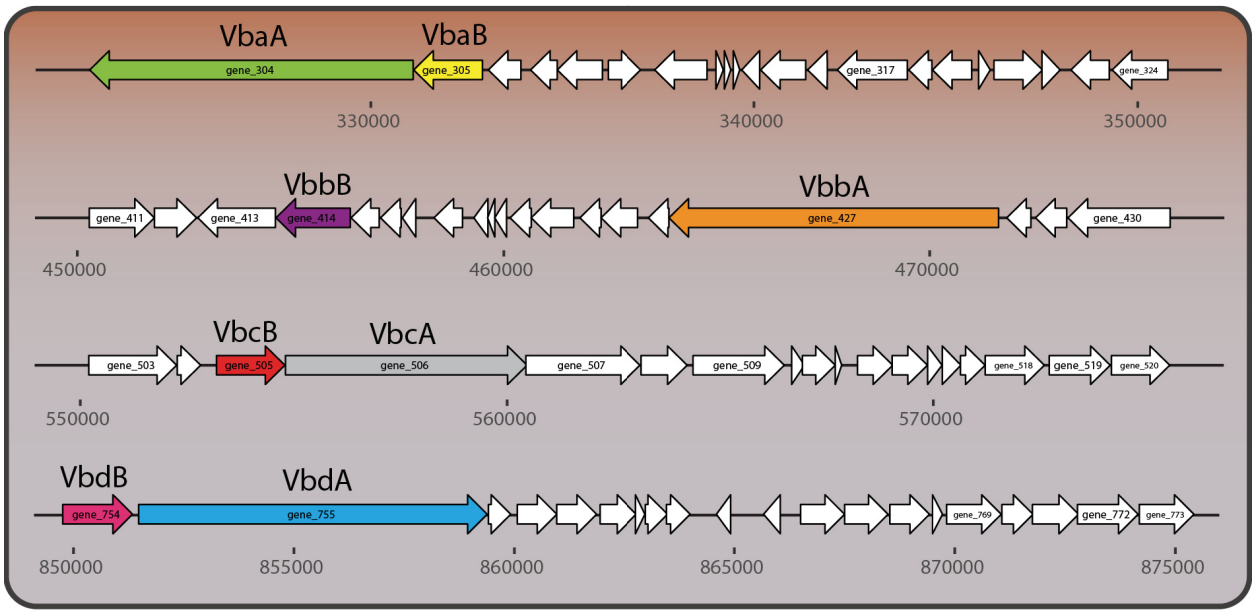

Figure 1.4 The Type 5b Secretion System in *F. nucleatum*. *F. nucleatum* possess 4 two partner secretion pairs. Proteins were predicted to be Type 5b ATs via custom Hidden Markov modeling. In all cases but one, VbbA/B, the TpsA and TpsB are located adjacent to each other in the genome. Their functions have not been discerned, and current bioinformatics classification technologies have been unable to tentatively assign a function.

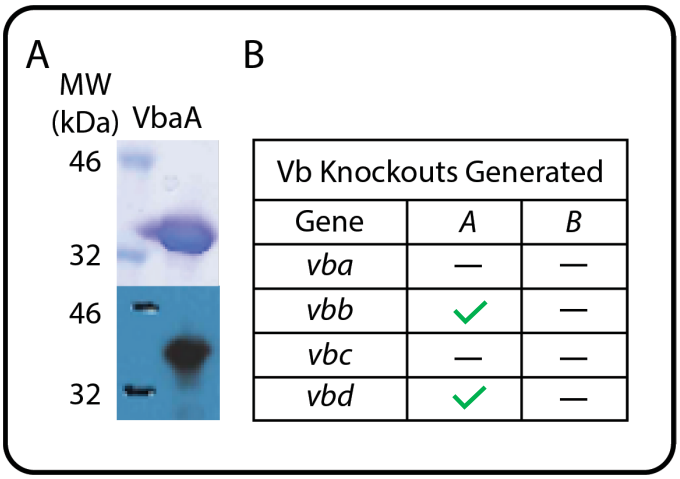

Figure 1.5 The first expression, purification and gene deletions in a Type 5b autotransporter in *F. nucleatum*. We have recombinantly expressed a construct of VbaA (AA 25-325) using our custom expression vectors to >95% purity as shown in a Coomassie stained SDS-PAGE gel. Using this protein, we generated and purified a custom antibody to be used in future biochemical and microbiological assays (A). We have utilized our markerless gene deletion system to generate the first Type 5b knockout strains of *F. nucleatum* by deleting genes *vbbA* and *vbdA*.

Type 5c ATs

Structure and Biogenesis

Type 5c ATs are more commonly known as trimeric ATs. The passenger and β-barrel domains of these proteins are expressed as one peptide and are secreted to the periplasm in a similar manner as Type 5a ATs. The way in which these proteins associate and enter into the outer membrane is what differentiates them from other Type V secreted proteins. After their translocation into the periplasm, the β-barrels of the newly forming AT interact with the Bam complex which facilitates their homo-trimerization. After β-barrel formation and trimerization, passenger domain translocation happens in a similar manner as with the Type 5a ATs (**Figure 1.6**) [11]. Once on the surface, the passenger domain typically displays a repeated, coiled-coil motif that is capable of extending up to 250 nm from the cell surface where they function as adhesins with broad range specificity [37]. The passenger domain of these protein complexes can be further segmented by their 'head' and 'stalk' domains. The globular head domain serves as the interaction point between the adhesin and its substrate. However, in some instances, the stalk domain can also be involved in adhesion [38]. Trimeric ATs are utilitarian proteins that can bind a number of different protein substrates making them versatile, highly functional virulence factors capable of conferring adhesive properties in a wide variety of cellular environments.

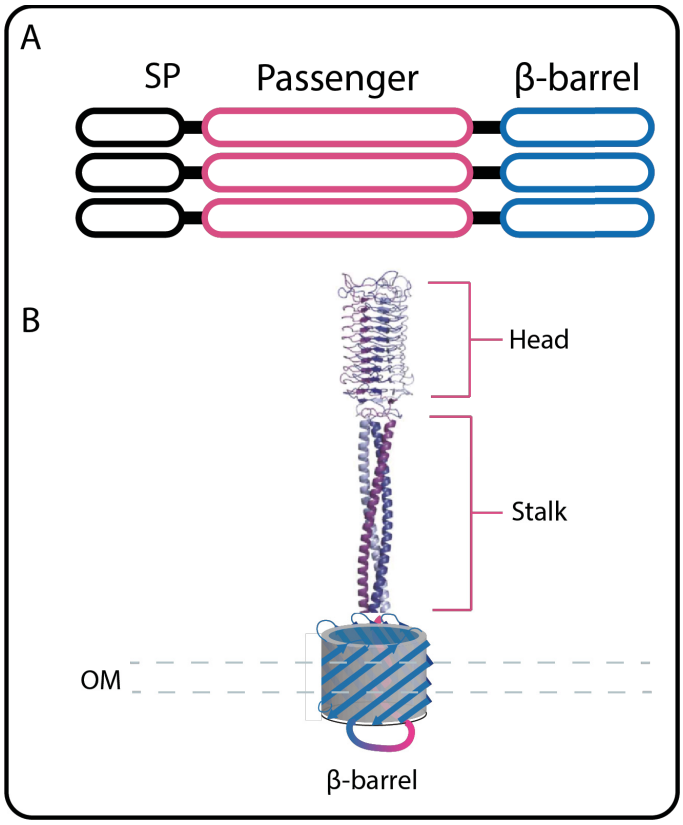

Figure 1.6 The basic domain architecture and subcellular localization of a Type 5c autotransporter. Trimeric ATs are assembled from 3 individual monomers illustrated here as a cartoon (A). Trimerization is initiated when the β-barrel domains interact with the Bam complex and they begin to be inserted in the bacterial outer membrane (OM). A generalized model for trimeric AT insertion and presentation on the bacterial OM is shown as a cartoon depiction (B). This model was adapted from the structure of the trimeric AT, Eip, in *E. coli* [39].

Function in Pathogenic Bacteria

Trimeric ATs are most well characterized in the etiologic agent of the Bubonic plague, *Yersinia pestis*, where YadA demonstrates an ability to bind to a diverse array of human extracellular matrix proteins including collagens, laminin and fibronectin [40, 41]. *Bartonella henselae* produces the trimeric AT, BadA, which contributes to cat scratch fever. In this context BadA is responsible not only for bacterial attachment to extracellular matrix proteins, but it also induces an angiogenic response in immunocompromised patients while conferring antiphagocytic properties to the bacterium [42]. *H. influenzae* secretes two trimeric ATs that contribute to meningitis in Hsf and Hia that mediate bacterial attachment to host cells. *N. meningitidis* also possesses a trimeric AT, NadA, which is responsible for host cell attachment and development of disease in humans. NadA contributes significantly to bacterial colonization, and it has been explored as a potential vaccine candidate making it the third AT subcategory with demonstrated potential as a drug target [43]. These are just some examples in which trimeric ATs are utilized by pathogenic bacteria to infect human tissues, and many more remain to be fully explored.

Examples in *F. nucleatum*

The examination of trimeric ATs in *F. nucleatum* has been completely neglected by the field. This is likely due to genome. We show that *F. nucleatum* 23726 contains 5 trimeric ATs, hereafter named FvcA, B, C, D, and E (**Figure 1.7**). We are the first group to over express and purify proteins in this family in *F. nucleatum* using the molecular tools described in this dissertation (*manuscript in prep)*. These breakthroughs provide the foundation for future studies that will probe the substrate binding specificity and localization of trimeric ATs in a host cell interaction context. We have also created in-frame gene deletion mutants of each individual trimeric AT. In addition to individual gene deletions, we have created strains that have multiple trimeric ATs

deleted to facilitate virulence factor cooperativity studies relative to host cell invasion (*manuscript in prep*). Our advances will prove invaluable for future experimentation with this dynamic and multi-faceted protein family.

Type 5d ATs

Structure and Biogenesis

The Type 5d domain architecture can be described as a hybrid of the Type 5a and b subcategories. The passenger domain and β-barrel are expressed as one polypeptide, and the passenger domain is connected to the β-barrel via a POTRA domain. This region is hypothesized to facilitate protein-protein interactions in the periplasm to initiate and aid in outer membrane insertion, but the exact role of the POTRA domain and the biophysical properties of Type 5d ATs are unknown **(Figure 1.8)** [44]. The effector functions of ATs in this subcategory are the least diverse among the AT family in that they all possess phospholipase activity. Their roles in human disease are completely unknown as only two Type 5d ATs have been studied in any detail, one of which is presented in this dissertation.

Function in Pathogenic Bacteria

Previous to our work, only one Type 5d AT had been studied in PlpD of *P. aeruginosa.* Structure-function analysis of PlpD revealed that it is capable of interacting with phosphatidylinositols, which suggests that it is capable of interfering with host cell signaling processes [44, 45]. However, the exact role of PlpD in *P. aeruginosa* pathogenesis remains unclear. PlpD is a phospholipase with activity demonstrated *in vitro* but its *in vivo* substrate has yet to be elucidated. More work remains to be done to ascertain the role of these understudied proteins in pathogenic bacteria.

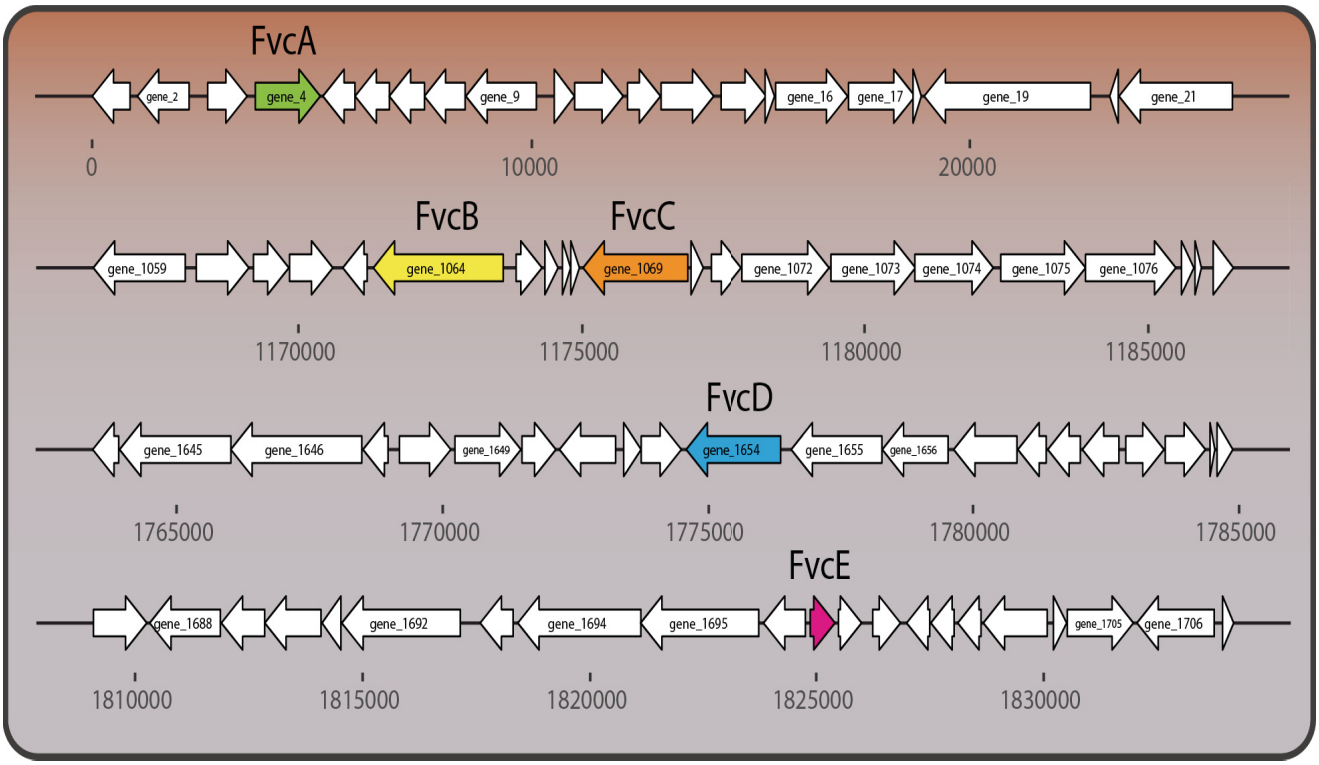

Figure 1.7 The Type 5c secretion system in *F. nucleatum*. *F. nucleatum* possesses 5 trimeric ATs indicated by colored arrows. They are all predicted to be adhesins based on custom HMMR model analysis. Our lab has produced recombinant constructs and knockout mutants of many of these proteins using our custom technologies detailed in this dissertation.

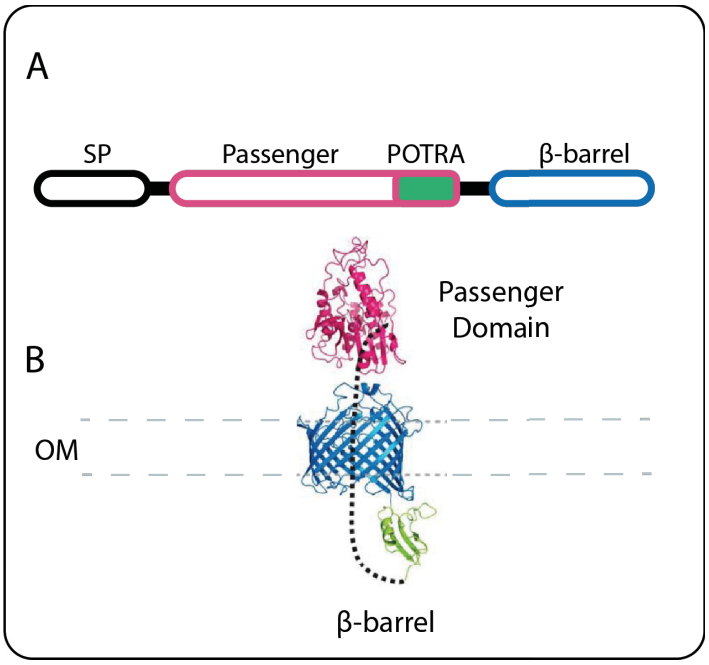

Figure 1.8 The basic domain and subcellular localization of the Type 5d secretion system. The domain architecture is depicted as a cartoon. All domains needed for export are expressed as a single polypeptide. The signal peptide (SP) is shown in black, passenger domain in magenta, POTRA domain in green, and β-barrel domain in blue (A). The 3D representation of this protein system in a biological membrane shown is modified from a model of FplA localization in *F. nucleatum* (B) [12].

Examples in *F. nucleatum*

Almost all strains of *Fusobacterium* possess one Type 5d AT with the exception of strain 27725, *F. varium,* which has two Type 5d genes [47]. Extensive enzymatic and molecular characterization of this protein from *F. nucleatum* 23726, FplA, is presented in chapter 4 [12]. Briefly, FplA is a PLA1 phospholipase with robust *in vitro* catalytic activity. Like PlpD, it is capable of interacting with phosphoinositide lipids, suggesting it may alter human host cell signaling processes. The full extent of this protein's role in disease is not yet known, but we provide the first extensive study of FplA in *F. nucleatum* and perhaps the most extensive study of a Type 5d AT to date. Our results suggest a role for FplA in altering host cell signaling and provide the foundation for future work with this virulence factor and its homologs in other human pathogens.

Discussion

While the very nature of ATs makes production and secretion of virulence factors efficient for the bacterium, it presents a number of challenges for study in the laboratory. Aside from the inherent difficulties of working with an understudied pathogen in *F. nucleatum* (i.e. no established protein over-expression system, genetically recalcitrant strains and anaerobic conditions), experimentation with ATs poses several obstacles. They can be extremely large for bacterial proteins, thus limiting their production in more facile recombinant protein expression systems in *E. coli*. Fap2, for instance, is a 3,768 amino acid protein that is crucial for invasion of and adherence to host cells. Fap2's significance has been known since 2005, but it has yet to be fully expressed and purified in a laboratory setting. Additionally, the hydrophobic, membrane-anchored β-barrel is difficult to express and purify under native conditions. While these portions of ATs have been expressed in inclusion bodies and re-folded *in vitro*, producing them in a more biologically relevant manner in quantities useful for traditional structural biology methodologies has remained challenging.

ATs in *F. nucleatum* represent a large pool of mostly uncharacterized virulence factors that can be targeted by new drugs or vaccines that may eliminate *Fusobacterium*-associated disease in humans. However, previous to work presented in this dissertation the foundation necessary to study these proteins was missing. We have created the molecular and genetic tools needed to gain a full understanding of the mechanisms underpinning *F. nucleatum* pathogenesis, and we present a study that utilizes these tools to begin to understand a never before studied virulence factor in this important human pathogen.

Acknowledgements

Research was supported by startup funding from the Department of Biochemistry at Virginia Tech, the Institute for Critical Technology and Applied Science (ICTAS) at Virginia Tech, and the National Institute for Food and Agriculture.

Author Contributions

MAC and DJS wrote the manuscript.

Competing Interests

The authors declare that they have no conflicts of interest with the contents of this article.

References

1. Heckmann JG, Lang CJG, Hartl H, Tomandl B. Multiple brain abscesses caused by Fusobacterium nucleatum treated conservatively. Can J Neurol Sci. 2003;30: 266–268.
2. Tweedy CR, White WB. Multiple Fusobacterium nucleatum liver abscesses. Association with a persistent abnormality in humoral immune function. J Clin Gastroenterol. journals.lww.com; 1987;9: 194–197.
3. Gedik AH, Cakir E, Soysal O, Umutoğlu T. Endobronchial lesion due to pulmonary Fusobacterium nucleatum infection in a child. Pediatr Pulmonol. 2014;49: E63–5.
4. Han YW, Fardini Y, Chen C, Iacampo KG, Peraino VA, Shamonki JM, et al. Term stillbirth caused by oral Fusobacterium nucleatum. Obstet Gynecol. 2010;115: 442–445.
5. Castellarin M, Warren RL, Freeman JD, Dreolini L, Krzywinski M, Strauss J, et al. Fusobacterium nucleatum infection is prevalent in human colorectal carcinoma. Genome Res. genome.cshlp.org; 2012;22: 299–306.
6. Kostic AD, Chun E, Robertson L, Glickman JN, Gallini CA, Michaud M, et al. Fusobacterium nucleatum potentiates intestinal tumorigenesis and modulates the tumor-immune microenvironment. Cell Host Microbe. 2013;14: 207–215.
7. Sanders BE, Umana A, Lemkul JA, Slade DJ. FusoPortal: an Interactive Repository of Hybrid MinION-Sequenced Fusobacterium Genomes Improves Gene Identification and Characterization. mSphere. 2018;3. doi:10.1128/mSphere.00228-18
8. Costa TRD, Felisberto-Rodrigues C, Meir A, Prevost MS, Redzej A, Trokter M, et al. Secretion systems in Gram-negative bacteria: structural and mechanistic insights. Nat Rev Microbiol. 2015;13: 343–359.
9. Han YW, Redline RW, Li M, Yin L, Hill GB, McCormick TS. Fusobacterium nucleatum

induces premature and term stillbirths in pregnant mice: implication of oral bacteria in preterm birth. Infect Immun. 2004;72: 2272–2279.
10. Abed J, Emgård JEM, Zamir G, Faroja M, Almogy G, Grenov A, et al. Fap2 Mediates Fusobacterium nucleatum Colorectal Adenocarcinoma Enrichment by Binding to Tumor-Expressed Gal-GalNAc. Cell Host Microbe. 2016;20: 215–225.
11. Leo JC, Grin I, Linke D. Type V secretion: mechanism(s) of autotransport through the bacterial outer membrane. Philos Trans R Soc Lond B Biol Sci. 2012;367: 1088–1101.
12. Casasanta MA, Yoo CC, Smith HB, Duncan AJ, Cochrane K, Varano AC, et al. A chemical and biological toolbox for Type Vd secretion: Characterization of the phospholipase A1 autotransporter FplA from Fusobacterium nucleatum. J Biol Chem. 2017;292: 20240–20254.
13. Dziva F, Mahajan A, Cameron P, Currie C, McKendrick IJ, Wallis TS, et al. EspP, a Type V-secreted serine protease of enterohaemorrhagic Escherichia coli O157:H7, influences intestinal colonization of calves and adherence to bovine primary intestinal epithelial cells. FEMS Microbiol Lett. 2007;271: 258–264.
14. Sherlock O, Schembri MA, Reisner A, Klemm P. Novel roles for the AIDA adhesin from diarrheagenic Escherichia coli: cell aggregation and biofilm formation. J Bacteriol. 2004;186: 8058–8065.
15. Turner DPJ, Marietou AG, Johnston L, Ho KKL, Rogers AJ, Wooldridge KG, et al. Characterization of MspA, an immunogenic autotransporter protein that mediates adhesion to epithelial and endothelial cells in Neisseria meningitidis. Infect Immun. 2006;74: 2957–2964.
16. Besbes A, Le Goff S, Antunes A, Terrade A, Hong E, Giorgini D, et al. Hyperinvasive Meningococci Induce Intra-nuclear Cleavage of the NF-κB Protein p65/RelA by Meningococcal IgA Protease. PLoS Pathog. 2015;11: e1005078.
17. Vidarsson G, Overbeeke N, Stemerding AM, van den Dobbelsteen G, van Ulsen P, van der Ley P, et al. Working mechanism of immunoglobulin A1 (IgA1) protease: cleavage of IgA1 antibody to Neisseria meningitidis PorA requires de novo synthesis of IgA1 Protease. Infect Immun. 2005;73: 6721–6726.
18. Coppenhagen-Glazer S, Sol A, Abed J, Naor R, Zhang X, Han YW, et al. Fap2 of Fusobacterium nucleatum is a galactose-inhibitable adhesin involved in coaggregation, cell adhesion, and preterm birth. Infect Immun. 2015;83: 1104–1113.
19. Gur C, Ibrahim Y, Isaacson B, Yamin R, Abed J, Gamliel M, et al. Binding of the Fap2 protein of Fusobacterium nucleatum to human inhibitory receptor TIGIT protects tumors from immune cell attack. Immunity. 2015;42: 344–355.
20. Kaplan CW, Ma X, Paranjpe A, Jewett A, Lux R, Kinder-Haake S, et al. Fusobacterium nucleatum outer membrane proteins Fap2 and RadD induce cell death in human lymphocytes. Infect Immun. 2010;78: 4773–4778.
21. Kaplan A, Kaplan CW, He X, McHardy I, Shi W, Lux R. Characterization of aid1, a novel gene involved in Fusobacterium nucleatum interspecies interactions. Microb Ecol. 2014;68: 379–387.
22. Kaplan CW, Lux R, Haake SK, Shi W. The Fusobacterium nucleatum outer membrane protein RadD is an arginine-inhibitable adhesin required for inter-species adherence and the structured architecture of multispecies biofilm. Mol Microbiol. 2009;71: 35–47.
23. Kaplan CW, Lux R, Huynh T, Jewett A, Shi W, Haake SK. Fusobacterium nucleatum apoptosis-inducing outer membrane protein. J Dent Res. 2005;84: 700–704.
24. Newman CL, Stathopoulos C. Autotransporter and two-partner secretion: delivery of large-size virulence factors by gram-negative bacterial pathogens. Crit Rev Microbiol. 2004;30:

275–286.
25. Jacob-Dubuisson F, Locht C, Antoine R. Two-partner secretion in Gram-negative bacteria: a thrifty, specific pathway for large virulence proteins. Mol Microbiol. 2001;40: 306–313.
26. Grass S, Rempe KA, St Geme JW 3rd. Structural determinants of the interaction between the TpsA and TpsB proteins in the Haemophilus influenzae HMW1 two-partner secretion system. J Bacteriol. 2015;197: 1769–1780.
27. Elsen S, Huber P, Bouillot S, Couté Y, Fournier P, Dubois Y, et al. A type III secretion negative clinical strain of Pseudomonas aeruginosa employs a two-partner secreted exolysin to induce hemorrhagic pneumonia. Cell Host Microbe. 2014;15: 164–176.
28. Schmitt C, Turner D, Boesl M, Abele M, Frosch M, Kurzai O. A functional two-partner secretion system contributes to adhesion of Neisseria meningitidis to epithelial cells. J Bacteriol. 2007;189: 7968–7976.
29. Guérin J, Bigot S, Schneider R, Buchanan SK, Jacob-Dubuisson F. Two-Partner Secretion: Combining Efficiency and Simplicity in the Secretion of Large Proteins for Bacteria-Host and Bacteria-Bacteria Interactions. Front Cell Infect Microbiol. 2017;7: 148.
30. Talà A, Progida C, De Stefano M, Cogli L, Spinosa MR, Bucci C, et al. The HrpB-HrpA two-partner secretion system is essential for intracellular survival of Neisseria meningitidis. Cell Microbiol. 2008;10: 2461–2482.
31. Scheller EV, Cotter PA. Bordetella filamentous hemagglutinin and fimbriae: critical adhesins with unrealized vaccine potential. Pathog Dis. 2015;73: ftv079.
32. Hertle R, Hilger M, Weingardt-Kocher S, Walev I. Cytotoxic action of Serratia marcescens hemolysin on human epithelial cells. Infect Immun. 1999;67: 817–825.
33. St Geme JW 3rd. The HMW1 adhesin of nontypeable Haemophilus influenzae recognizes sialylated glycoprotein receptors on cultured human epithelial cells. Infect Immun. 1994;62: 3881–3889.
34. Grass S, Lichti CF, Townsend RR, Gross J, St Geme JW 3rd. The Haemophilus influenzae HMW1C protein is a glycosyltransferase that transfers hexose residues to asparagine sites in the HMW1 adhesin. PLoS Pathog. 2010;6: e1000919.
35. Renauld-Mongénie G, Cornette J, Mielcarek N, Menozzi FD, Locht C. Distinct roles of the N-terminal and C-terminal precursor domains in the biogenesis of the Bordetella pertussis filamentous hemagglutinin. J Bacteriol. 1996;178: 1053–1060.
36. Konninger UW, Hobbie S, Benz R, Braun V. The haemolysin-secreting ShlB protein of the outer membrane of Serratia marcescens : determination of surface-exposed residues and formation of ion-permeable pores by ShlB mutants in artificial lipid bilayer membranes. Mol Microbiol. 1999;32: 1212–1225.
37. Łyskowski A, Leo JC, Goldman A. Structure and biology of trimeric autotransporter adhesins. Adv Exp Med Biol. 2011;715: 143–158.
38. Campos CG, Byrd MS, Cotter PA. Functional characterization of Burkholderia pseudomallei trimeric autotransporters. Infect Immun. Am Soc Microbiol; 2013;81: 2788–2799.
39. Leo JC, Lyskowski A, Hattula K, Hartmann MD, Schwarz H, Butcher SJ, et al. The structure of E. coli IgG-binding protein D suggests a general model for bending and binding in trimeric autotransporter adhesins. Structure. 2011;19: 1021–1030.
40. Nummelin H, Merckel MC, Leo JC, Lankinen H, Skurnik M, Goldman A. The Yersinia adhesin YadA collagen-binding domain structure is a novel left-handed parallel β-roll. EMBO J. 2004;23: 701–711.
41. Eitel J, Dersch P. The YadA protein of Yersinia pseudotuberculosis mediates high-efficiency uptake into human cells under environmental conditions in which invasin is

repressed. Infect Immun. 2002;70: 4880–4891.
42. Riess T, Andersson SGE, Lupas A, Schaller M, Schäfer A, Kyme P, et al. Bartonella adhesin a mediates a proangiogenic host cell response. J Exp Med. 2004;200: 1267–1278.
43. Comanducci M, Bambini S, Brunelli B, Adu-Bobie J, Aricò B, Capecchi B, et al. NadA, a novel vaccine candidate of Neisseria meningitidis. J Exp Med. 2002;195: 1445–1454.
44. Salacha R, Kovacić F, Brochier-Armanet C, Wilhelm S, Tommassen J, Filloux A, et al. The Pseudomonas aeruginosa patatin-like protein PlpD is the archetype of a novel Type V secretion system. Environ Microbiol. 2010;12: 1498–1512.
45. da Mata Madeira PV, Zouhir S, Basso P, Neves D, Laubier A, Salacha R, et al. Structural Basis of Lipid Targeting and Destruction by the Type V Secretion System of Pseudomonas aeruginosa. J Mol Biol. 2016;428: 1790–1803.
46. Desvaux, Mickaël, Arshad Khan, Scott A. Beatson, Anthony Scott-Tucker, and Ian R. Henderson. 2005. “Protein Secretion Systems in Fusobacterium Nucleatum: Genomic Identification of Type 4 Piliation and Complete Type V Pathways Brings New Insight into Mechanisms of Pathogenesis.” Biochimica et Biophysica Acta 1713 (2): 92–112.
47. Umana, Ariana, Blake E. Sanders, Christopher C. Yoo, Michael A. Casasanta, Barath Udayasuryan, Scott S. Verbridge, and Daniel J. Slade. 2019. “Reevaluating the Fusobacterium Virulence Factor Landscape.” bioRxiv. https://doi.org/10.1101/534297.
48. Nicolay, Toon, Jos Vanderleyden, and Stijn Spaepen. 2015. “Autotransporter-Based Cell Surface Display in Gram-Negative Bacteria.” Critical Reviews in Microbiology 41 (1): 109–23.
49. Dautin, Nathalie, and Harris D. Bernstein. 2007. “Protein Secretion in Gram-Negative Bacteria via the Autotransporter Pathway.” Annual Review of Microbiology 61: 89–112.
50. Wells, Timothy J., and Ian R. Henderson. 2013. “Chapter 16 - Type 1 and 5 Secretion Systems and Associated Toxins.” In Escherichia Coli (Second Edition), edited by Michael S. Donnenberg, 499–532. Boston: Academic Press.
51. Yen, Yihfen T., Maria Kostakioti, Ian R. Henderson, and Christos Stathopoulos. 2008. “Common Themes and Variations in Serine Protease Autotransporters.” Trends in Microbiology 16 (8): 370–79.
52. Yen, Yihfen T., Maria Kostakioti, Ian R. Henderson, and Christos Stathopoulos. 2008. “Common Themes and Variations in Serine Protease Autotransporters.” Trends in Microbiology 16 (8): 370–79.
53. Shere, K. D., S. Sallustio, A. Manessis, T. G. D’Aversa, and M. B. Goldberg. 1997. “Disruption of IcsP, the Major Shigella Protease That Cleaves IcsA, Accelerates Actin-Based Motility.” Molecular Microbiology 25 (3): 451–62.
54. Marr, Nico, David C. Oliver, Vincianne Laurent, Jan Poolman, Philippe Denoël, and Rachel C. Fernandez. 2008. “Protective Activity of the Bordetella Pertussis BrkA Autotransporter in the Murine Lung Colonization Model.” Vaccine 26 (34): 4306–11.

Chapter 2

Reverse genetic dissection of *Fusobacterium nucleatum* cellular invasion and a role in host cell signaling.

Michael A. Casasanta[1], Christopher C. Yoo[1], Blake Sanders[1], Ariana Umana[1], Alison J. Duncan[1], Daniel J. Slade[1]

1. Virginia Polytechnic Institute and State University, Department of Biochemistry, Blacksburg, VA, USA.

Abstract

Fusobacterium nucleatum is an emerging pathogen that commonly resides in the oral microbiome. It was recently coined an 'oncomicrobe' due to its association with the development and progression of colorectal cancer (CRC). *F. nucleatum* induces tumor formation in mice and is over represented in tumor tissues of patients suffering from CRC. Additionally, infection with this organism induces elevated IL-8 secretion which has the potential to create an environment conducive to tumor development and metastasis. These phenotypes were thought to be driven by Fap2 and FadA of *F. nucleatum*. However, experiments detailing and corroborating these findings have been hampered by a lack of genetic and molecular technologies available. These important disease associations highlight the need in the field for easy to use, repeatable genetic and molecular technologies that can facilitate experiments probing the role of this bacterium in disease. Here we present an enhanced genetic system for *F. nucleatum* capable of generating in-frame gene deletions using simple galactose as a secondary selection agent along with protein expression technology to facilitate chromosomal expression of tagged proteins directly from the bacterium. We show in controlled cancer cell models that Fap2 and not FadA is the main driver of both host-pathogen interactions and increased IL-8. Additionally, we demonstrate the utility of this system in the production, purification and detection of virulence factors directly from *F. nucleatum* for the first time. We provide a revised model for how *F. nucleatum* interacts with host cells and the tools to effectively guide and equip researchers with the information necessary to probe *Fusobacterium*-host interactions. Our results demonstrate the importance of biochemical and genetic tool development in the study of new and emerging pathogens and offer a powerful molecular toolkit for future studies involving *F. nucleatum*.

Introduction

Fusobacterium nucleatum is a Gram-negative anaerobic bacterium that is a member of the oral microbiota[1]. In humans, it drives the development of periodontitis and gum disease by facilitating mixed-species biofilm formation with *Porphyromonas gingivalis* and by invading gingival cells directly[2–4]. However, *F. nucleatum* is not limited to pathogenesis within the mouth. It causes infections in disparate locations throughout the body including the brain, heart, liver, lungs, and it can invade the placenta and cause stillbirth in humans[5–10]. In addition to acute infections, *F. nucleatum* is implicated in chronic inflammatory disease. Several high profile studies have shown that *F. nucleatum* contributes to the progression of colorectal cancer (CRC) by inducing tumor formation in $APC^{min/+}$ mice, a commonly used model for CRC, in addition to its overabundance in tumors excised from patients with CRC[11,12]. Despite *F. nucleatum*'s infectious potential in costly human diseases, little is known about the molecular mechanisms underpinning these associations. This gap in knowledge is largely due to the lack of a clear, facile system to genetically dissect *F. nucleatum*.

Most of what is known about *F. nucleatum* pathogenesis is limited to two outer membrane proteins, Fap2 and FadA. Fap2 is a Type 5a secreted autotransporter adhesin that facilitates docking to host cells by binding Gal-GalNAc sugar moieties on membrane proteins which is then followed by bacterial invasion[13,14]. These residues are overexpressed in CRC adenocarcinomas and are thought to aid in *F. nucleatum* targeting of CRC lesions. *F. nucleatum* likely targets CRC lesions, thereby concentrating the bacteria in areas which allows them to contribute to a tumor microenvironment conducive to disease progression by driving up inflammation[11]. FadA is a small adhesin that multimerizes on the bacterial cell surface and interacts with E-cadherin on human epithelial cells to drive invasion and increase IL-8 production[15,16]. The cytokine profile of *F. nucleatum* infected cells is significant, because IL-8 is a known modulator of the tumor

microenvironment. It promotes angiogenesis thereby increasing resource flow to developing tumors which enhances their growth[17,18]. Additionally, newly forming tumors have shown the propensity to express high levels of IL-8 and IL-8 receptors which has a number of implications in the formation and progression of CRC. For instance, IL-8 produced from tumor cells has been shown to initiate tumor cell differentiation to a mesenchymal-type cell which can increase their metastatic potential and make them resistant to immune cell killing[19–21]. Additionally, IL-8 secretion by tumor cells can have paracrine effects by attracting white blood cells to the site of the lesion and decrease the anti-tumor response[22]. Interestingly, Fap2 has also been shown illicit an anti-tumor response by inactivating NK-T cells that have tumor clearing duties by interacting with TIGIT receptors on NK-T cells during infection[23]. Increased IL-8 production from FadA-host interactions combined with the immune-dampening properties resulting from Fap2 mediated reactions potentially act in a synergistic manner to confer pro-CRC properties to *F. nucleatum* during infection.

Recapitulation of these results and furthering the understanding of *F. nucleatum's* role in CRC has proved challenging. These difficulties are largely resulting from the lack of both a facile, repeatable genetic system and molecular tools specific to *F. nucleatum* that can be used to fully probe host-pathogen interactions. Prior to the work presented here, there have only been two studies using a genetic manipulation system capable of creating in-frame gene deletions in *F. nucleatum*. One study probed the biofilm formation dynamics of *F. nucleatum* providing insights on an important aspect of this bacteria's ability to cause disease, particularly in the mouth [24]. The other in-frame deletion mutant was created through a spontaneous recombination event which showed that a small adhesin, FadA, is involved in host cell invasion [16]. We have created a unique, targeted, molecular system with which we used to probe host-pathogen dynamics, thus representing the first study to use such a system to study this aspect of *F. nucleatum* biology. This

methodology relies on a two stage process concluding with a counter selection on galactose to reliably create an unlimited number of mutations in the same strain of *F. nucleatum*. This selection strategy has successfully been exploited in other pathogenic organisms, including *Clostridium perfringens[25]*. Additionally, our system allows for the over-expression and purification of potential virulence factors for *in vitro* studies. Previous to our work, the field has largely relied on traditional recombinant protein expression and purification protocols using *E. coli* based methodologies [26]. This presents a number of challenges as heterologous expression and purification of large membrane proteins, which is the primary means of virulence factor secretion in *F. nucleatum*, presents a sizeable hurdle for the field. Cloning, solubility and toxicity issues abound with these types of proteins presenting challenges that were difficult to overcome prior to work presented here. Our genetic technology utilizes the promoter for a highly expressed ribosomal promoter from *Fusobacterium necrophorum* as the promoter of choice to drive over expression of 6xHis or FLAG tagged versions of putative *F. nucleatum* virulence factors [27,28]. These affinity-tagged proteins can then be purified directly from *F. nucleatum* cultures following simple protocols, and we show the utility of this system with the first over-expression and purification of FadA directly from *F. nucleatum*.

These breakthroughs have allowed us to revisit and revise the roles of Fap2 and FadA in *F. nucleatum* invasion of human epithelial cells. Additionally, we present a clear, concise mechanism for the molecular details of the newly devised selection system. In combination with state-of-the-art imaging flow cytometry and classical microbiological techniques, we show that Fap2 is the main driver in *F. nucleatum* invasion, and that FadA plays no role in invasion through single and tandem gene deletions in the strain *F. nucleatum* 23726. Previous studies, done using *F. nucleatum* 12230, showed that FadA was responsible for invasion and activating pro-inflammatory signaling cascades [15,16] . The results presented here and in other studies suggest

differential roles for FadA in invasion that are strain dependent. We also show, through an unidentified mechanism, that IL-8 secretion is indeed increased by *F. nucleatum* invasion and that it is linked to Fap2 expression. Upon deletion of *fap2*, IL-8 secretion decreases in HCT-116 cells after exposure to *F. nucleatum*. This in conjunction with invasion and host cell binding data suggest that either Fap2 interactions directly cause an increase in IL-8 production, or there is an unidentified mechanism mediated by the bacterial presence in host cells that initializes this response. The latter scenario leaves open the possibility that some unidentified FadA-mediated process is the cause of increased IL-8 secretion, however more work is needed to uncover the full role of FadA in *F. nucleatum* invasion and by which specific means IL-8 secretion is ramped up. Moreover, our invasion and IL-8 findings bolster current evidence that suggests *F. nucleatum* is indeed involved with CRC.

Materials and Methods

Bacterial Strains and Growth Conditions

For plasmid production, *E. coli* strains were grown aerobically at 37°C in LB (10 g/L NaCl, 10 g/L tryptone, 5 g/L yeast extract). When indicated, *E. coli* was grown in SOC recovery media comprised of LB supplemented with 20mM glucose. *F. nucleatum* strain ATCC 23726 was grown at 37°C under anaerobic conditions in CBHK (Columbia broth (Difco) supplemented with hemin (5 μg/mL) and menadione (0.5 μg/mL)) in an anaerobic chamber (90% N_2, 5% CO_2, 5% H_2). Antibiotics were used where appropriate in the following concentrations: Chloramphenicol 25 μg/mL, thiamphenicol 5 μg/mL (CBHK agar plates) and 2.5 μg/mL (CBHK broth). LB components were purchased from Fisher Scientific (Hampton, NH). Bacterial strains were acquired from ATCC (Manassas, VA). Hemin purchased from Alfa Aesar, Haverhill, MA. Menadione purchased from Sigma-Aldrich (St. Louis, MO). Antibiotics, when used, purchased from GoldBio (St. Louis, MO).

Table of Strains	
Genotype	Strain Designation
ATCC 23726	Wild-type *F. nucleatum* (WT)
23726 Δ*galKT*	DJS1
23726 Δ*galKT* Δ*fadA*	DJS2
23726 Δ*galKT* Δ*fap2*	DJS3
23726 Δ*galKT* Δ*fadA* Δ*fap2*	DJS4
23726 Δ*galKT* Δ*fplA*	DJS5

Table 2.1 Table of bacterial strains used in this study.

Human Cell Lines

Both Ca9-22 (gingival squamous cell carcinoma) and HCT-116 (colorectal carcinoma) cell lines were used in this study (ATCC). Ca9-22 cells were grown and maintained in MEM-EBSS media with 10% FBS and penicillin/streptomycin added. HCT-116 cells were grown and maintained in McCoy's 5a media supplemented with 10% FBS and penicillin/streptomycin. Both cell lines were grown in a tissue culture incubator with 5% atmospheric CO_2. Antibiotics were removed immediately prior to infection with *F. nucleatum* strains during infection studies. Both cell lines were grown to 70-80% confluency before use in bacterial attachment and invasion assays. Cell lines acquired from ATCC (Manassas, VA). All media acquired from Caisson Labs (Smithfield, UT)

Competent Cell Creation

E. coli was made competent following the protocol for the Zymo Research (Irvine, CA) Mix and Go Competent cells kit. Briefly, Zymo broth was inoculated 1:100 with fresh overnight *E. coli* growth and incubated at 26°C with 250 rpm shaking (large, refrigerated floor shaker) until the OD_{600}= 0.2. Cells were pelleted and washed using the buffer provided in the kit. After washing, bacterial cells were resuspended in the competency buffer provided and flash frozen in liquid nitrogen before storing at -80°C until used.

F. nucleatum was made electrocompetent using the following protocol: An 8 mL CBHK culture was inoculated with 200 μL of a fresh stationary phase growth of *F. nucleatum*. Cells were grown anaerobically at 37°C with no shaking until the OD_{600} = 0.2. After reaching the desired OD, bacterial cells were pelleted at 1000xG for 15 minutes at 4°C. The 8 mL cell pellet was resuspended in 1 mL of ice-cold wash buffer made in DiH_2O (1mM MOPS + 10% glycerol). The cell resuspension was aliquoted into 1.5 mL microfuge tubes and washed 5 more times at 4°C

following centrifugation at 14,000xG for 2 minutes. After the final wash, the cell pellet was resuspended in 80 µL of the wash buffer and either flash frozen in liquid nitrogen and stored at -80°C for future use or used for electroporation the same day. MOPS was purchased from BioBasic (Amherst, NY).

Transformation and Selection of Bacterial Strains

E. coli was transformed with the appropriate plasmid following the Mix and Go transformation protocol. Briefly, roughly 50 ng of the indicated plasmid was added to a thawed aliquot of competent cells and incubated on ice for 15 minutes. After incubation, 500 µL of SOC recovery media was added to the mixture and the bacteria were incubated at 37°C with 180 rpm shaking for 1 hour under aerobic conditions. After recovery, the bacterial cells were pelleted at 12,000xG for 1 minute. The bacteria were resuspended in approximately 50 µL of SOC and plated on LB plates with the appropriate antibiotic and incubated at 37°C overnight.

F. nucleatum was transformed using standard electroporation procedures. Bacteria were transferred to cold 1 mm electroporation cuvettes (Genesee, USA) and 1.0-3.0 µg ([ ] > 1000 ng/µL) of the indicated plasmid was added immediately before electroporation at 2.5 kV (20 kV/cm), 50 µF, 129 OHMs, using an Electro Cell Manipulator 600 (BTX, USA). Before electroporation, anaerobic recovery media was prepared by adding 2 mL of sterile CBHK supplemented with 1mM $MgCl_2$ to an anaerobic culture tube and pre-warmed to 37°C. The electroporated bacterial cells were added immediately to the anaerobic recovery media via a syringe and incubated at 37°C for 18 hours. After recovery, the 2 mL of bacterial culture was pelleted at 14,000xG for 2 minutes and re-suspended in 200 µL of anaerobic CBHK and were added to CBHK plates with 5ug/mL thiamphenicol, spread evenly over the surface of the plate and incubated in an anaerobic chamber for 48hrs to allow sufficiently large colonies to grow.

Creation of in-frame Gene Deletion Strains

After single crossover chromosomal incorporation and selection on thiamphenicol containing plates, individual colonies of *F. nucleatum* were picked and used to inoculate a 1mL liquid culture (CBHK with 2.5 μg/mL thiamphenicol) in an anaerobic culture tube and incubated overnight at 37°C with no shaking for 18 hours. These cultures were then screened via PCR under the described conditions using the indicated primers to confirm plasmid incorporation onto the chromosome. After PCR confirmation, 100 μL of the overnight liquid culture was added to 2 mL of CBHK in an anaerobic culture tube with no antibiotics and incubated at 37°C with no shaking for 18 hrs. This allows for the second homologous recombination event to take place which removes the plasmid backbone and antibiotic resistance cassette from the chromosome. After the non-selective outgrowth, 100 μL of the overnight growth was added to CBHK plates supplemented with 3% galactose and spread evenly across the surface of the plate. These plates were incubated at 37°C under anaerobic conditions for 48 hours to allow for colonies to form. However, the creation of the DJS1 strain required slightly different conditions. After electroporation with the indicated plasmid, selection with thiamphenicol and the non-selective outgrowth stages, these cells were plated on CBHK plates with 1% 2-deoxygalactose before anaerobic incubation for 48 hours. Colonies were picked from the sugar selectivity plates and used to inoculate 1 mL liquid CBHK growths in anaerobic culture tubes and incubated at 37°C for 18 hrs. These cultures were then screened via PCR using the appropriate primers to confirm the second homologous recombination event.

Imaging Flow Cytometry to monitor *F. nucleatum* host cell invasion

The indicated strains were grown under the conditions described above at 37°C until the OD_{600} = 0.4 before being used to infect human cells. Just before infection, bacterial cells were pelleted,

washed and incubated with 500ng of FM 1-43FX (Thermofisher) lipid dye for 3 minutes. We have shown incorporation of this fluorescent lipid into the outer membrane does not affect cell growth or bacterial invasion (**Figure 2.1**). After lipid staining, bacterial cells were washed, re-suspended in PBS and added to human cells at a MOI of 10:1. Just prior to infection, antibiotic-free cell culture media was added to the human cells. Bacteria were allowed to incubate with human cells for the indicated time at 37°C in a tissue culture incubator with 5% atmospheric CO_2. After the designated infection time, the cell culture media was aspirated and fresh media supplemented with penicillin and streptomycin was added to kill extracellular bacteria for 30 minutes. Next, the infected human cells were dislodged from their culture plates using trypsin containing media and washed in cell culture media containing 10% FBS to neutralize the trypsin. After washing, the cells were fixed in 3.2% paraformaldehyde for 15 minutes and washed in PBS. Upon the last wash, the fixed human cells were resuspended in 15 μL of PBS before analysis by the Amnis Imagestream Mark II (EMD Millipore).

***F. nucleatum* Binding and Invasion Studies:**

A single colony was used to start overnight cultures of *F. nucleatum* 23726 and mutant strains. Stationary phase cultures were back-diluted to OD_{600}= 0.1 in 2 mL of CBHK and grown to exponential phase (OD_{600}= 0.4). Next, bacteria were added at an MOI of 1:1 to the media of the appropriate human cell monolayer cultures in 24 well plates, and incubated for 30 minutes at 37 ˚C in 5% CO_2. Following infection, the monolayer was washed one time with 500 μL of PBS pH 7.4 to remove any unbound bacteria. Next, the human cell monolayer was washed two additional times by adding 500 μL of cell culture media containing no antibiotics to each well plate and placed in a shaking incubator at 100 rpm for 2 minutes at 25 ˚C. After thoroughly washing the cells, the human cells were lysed by adding 200 μL of water to each well, and lysed cells were

transferred to a 1.5 mL conical tube. Serial dilutions were performed and plated on CBHK plates, which were incubated at 37˚C under anaerobic conditions for 48 hours to allow for colony formation.

Results

The creation of a galactose-sensitive strain of *Fusobacterium nucleatum*.

This gene deletion system utilizes a two-stage selection scheme. Second stage selection is based on galactose sensitivity, and that is made possible by exploiting the Leloir pathway in *F. nucleatum* [29, 30]. Briefly, in WT cells, galactose supplied in the media is taken up by the bacteria where it is phosphorylated by galactokinase (GALK). The resulting galactose-1-P is converted into UDP-galactose by galactose-1-phosphate uridylyltransferase (GALT) using UDP-glucose as a substrate. The end product of this pathway is glucose-1-phosphate, which can be used by various metabolic pathways in the bacteria (**Figure 2.1a**). However, upon deletion of *galKT* from the genome and expression of GalK from an introduced plasmid, galactose supplied in the media is converted to galactose-1-phosphate at toxic levels and can be used to select for homologous recombination events excising the *galK*-containing plasmid.

To create the galactose sensitive strain that would become the base strain for all future genetic manipulations (DJS1), initial selection following plasmid-chromosomal integration was first performed on 2-deoxygalactose. A suicide plasmid conferring resistance to thiamphenicol was designed with 1000 base pair regions of homology to the sequence immediately upstream of the start codon of *galK* and the sequence immediately downstream of the *galT* stop codon. Suicide plasmids are used in attempts to genetically manipulate *F. nucleatum* because we hypothesize that robust restriction-modification systems make plasmid maintenance within the bacterium challenging [31]. After electroporation of the knockout plasmid, positive clones were selected on thiamphenicol containing plates, single crossovers validated by PCR, and subsequently grown in the presence of 1% 2-deoxygalactose on solid CBHK agar (**Figure 2.2a-c)**. This artificial substrate was used to create the base strain because it causes toxicity immediately after uptake into the cell

in the presence of GalK and GalT while remaining biologically inert after *galK* and *galT* are successfully excised from the chromosome.

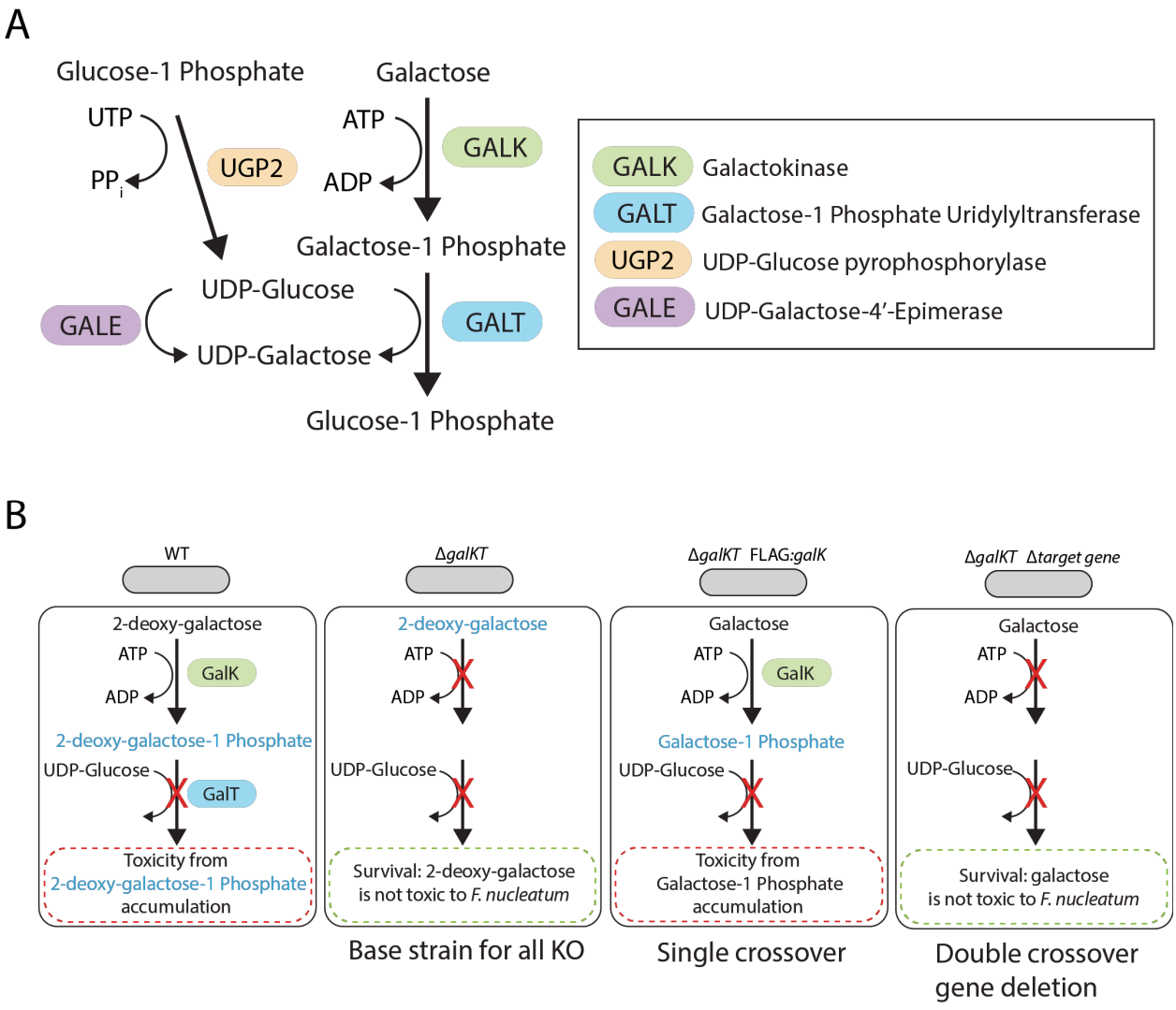

Figure 2.1 The Leloir Pathway in *Fusobacterium nucleatum* and the overall scheme for selection of base strains used in this study. The Leloir pathway uses galactose as a substrate to produce glucose-1-phosphate which can be used in a number of ways in the cell. Our system targets *galK* and *galT* for deletion to create a bacterial strain sensitive to galactose that can be used to create in-frame gene deletion mutants (A). The selection steps and potential outcomes at each stage of mutant construction are outlined (B).

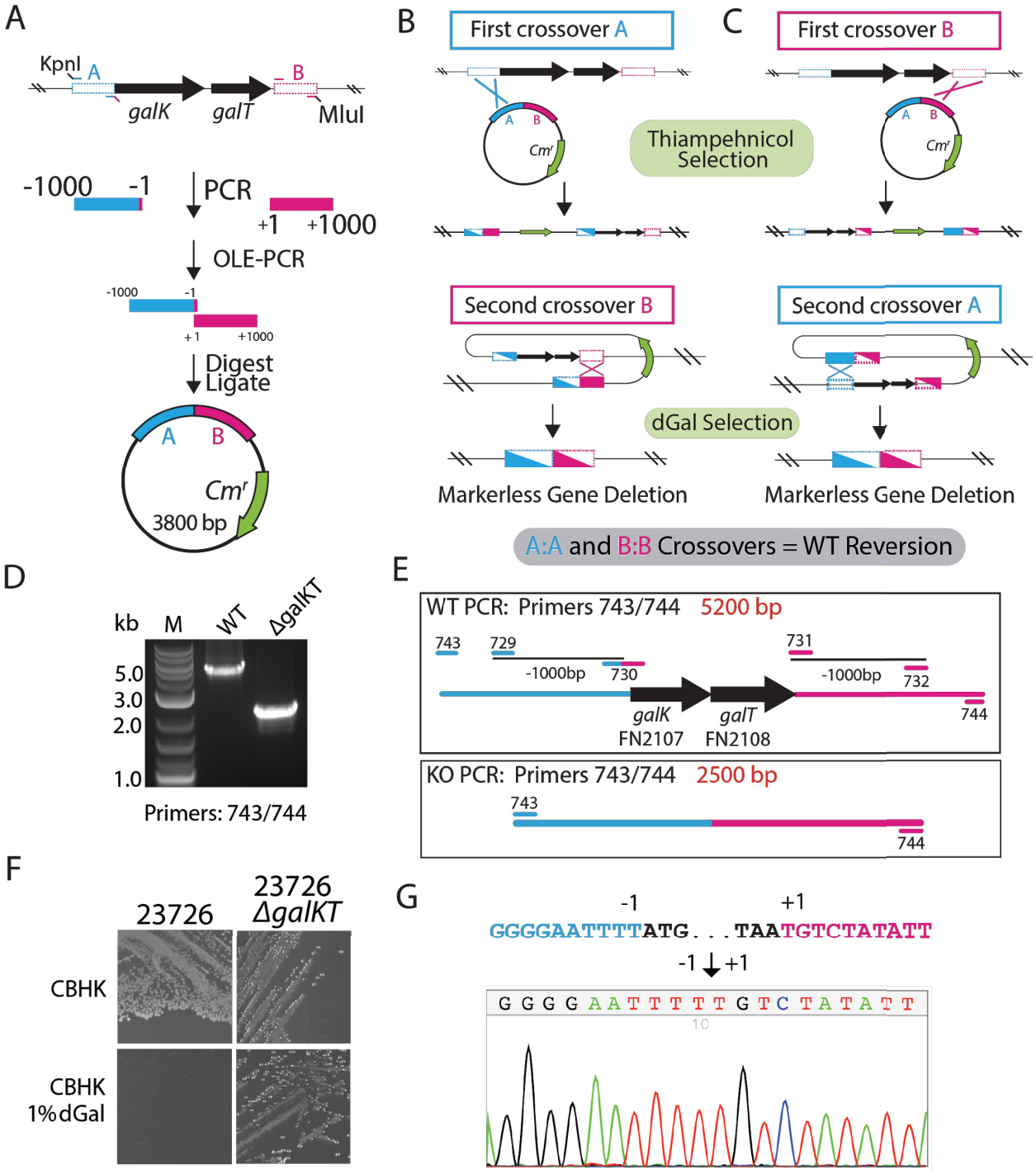

Figure 2.2 The creation of the base strain used for subsequent genetic manipulation. Plasmid design showing the cloning strategy for targeting regions upstream and downstream of *galK* and *galT* (A). The selection scheme highlighting antibiotic and sugar selection measures used and the possible homologous recombination events resulting from each selection stage (B-C). PCR confirmation of *galK* and *galT* excision from the *F. nucleatum* chromosome (D). Primer design and strain verification scheme (E). Bacterial selection on CBHK-agar plates supplemented with the indicated selection agent show expected growth outcomes (F). Sequence verification of successful *galKT* deletion events (G).

Relying on galactose selection is ineffective at this stage as successful gene deletion strains and wild-type reversion strains would show no phenotypic difference in the presence of standard galactose (**Figure 2.1b**). After counter selection on 2-deoxygalactose, chromosomal excision of *galKT* was confirmed via bacterial growth on selective media, PCR, and genomic sequencing (**Figure 2.2d-g**).

Verification of viability of the DJS1 strain.

In order to verify the viability of DJS1, we show that it has growth characteristics comparable to the WT strain. The plasmid-chromosomal integration and homologous recombination event schemes are highlighted in Figure 2.3a-c. Plasmid integration and the resulting gene excision following the two selection stages were verified by PCR (**Figure 2.2d-e).** WT, DJS1::*galKT* and DJS1 strains were all grown on CBHK-agar plates in the presence of thiamphenicol. All three strains show the same ability to grow on CBHK-agar plates. Only DJS1::*galKT* is capable of growing in the presence of thiamphenicol. This confirms the validity of using thiamphenicol as a selection agent by highlighting sensitivity to thiamphenicol. The results also show similar growth characteristics of the WT and DSJ1 strains (**Figure 2.3c**). To provide further assurance that no growth phenotype difference exists between WT and DJS1, both were grown in CBHK liquid cultures and their OD_{600} values were monitored over 12 hrs. The resulting growth curve unearthed no growth differences between the two strains indicating any phenotypic growth defects in response to future experimental conditions are not the result of an underlying physiological problem arising from the deletion of *galK* and *galT* (**Figure 2.3d**).

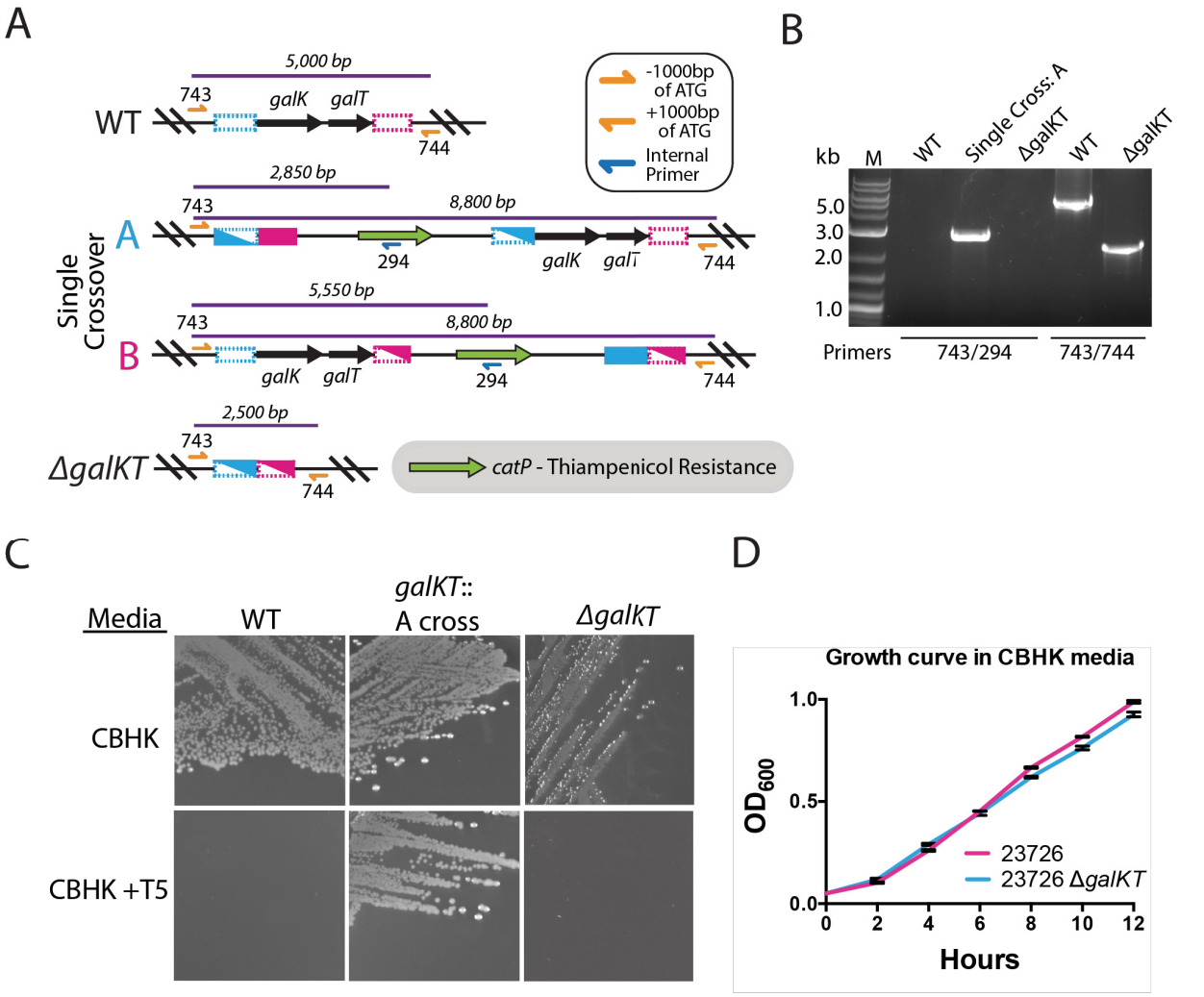

Figure 2.3 Verification of the growth characteristics of Δ*galKT* strain. The identities of the WT, WT with the knockout plasmid incorporated and Δ*galKT* strains were confirmed via PCR as evidenced by the primer screen and resulting DNA amplification (A-B). WT and Δ*galKT* show the same antibiotic sensitivity and growth phenotypes indicating that basic metabolic processes have not been interfered with by genetic manipulation (C-D).

Creation of in-frame gene deletions of virulence factors in *F. nucleatum*

Three previously characterized virulence factors were the first genes targeted for deletion using the DJS1 base strain in *fadA, fplA and fap2*. 750 base pair stretches of homology were designed according to the regions immediately upstream and downstream of the target gene and cloned into a suicide plasmid conferring thiamphenicol resistance (*catP*) and galactose sensitivity (*galK*) (**Figure 2.4a**). Single crossover bacteria were first selected on CBHK-agar plates containing thiamphenicol following electroporation and plasmid integration was confirmed via PCR. Positive clones were then grown in the presence of galactose to select for double homologous recombination events. The possible recombination events and the resulting strains are shown in Figure 2.4b-c. The successful excision of each gene as well as the first stacked mutation of *F. nucleatum* virulence factors were screened and confirmed via PCR (**Figure 2.4d-f**). These strains were then used to highlight the functionality and utility of this genetic system through protein purification and chemical biology experimentation. RT-PCR was performed to confirm there were no defects in the transcription of genes immediately upstream and downstream of each gene targeted for deletion. These results confirm that no polar effects exist in each gene deletion strain. The primer design and results of RT-PCR verification can be seen in Figure 2.5.

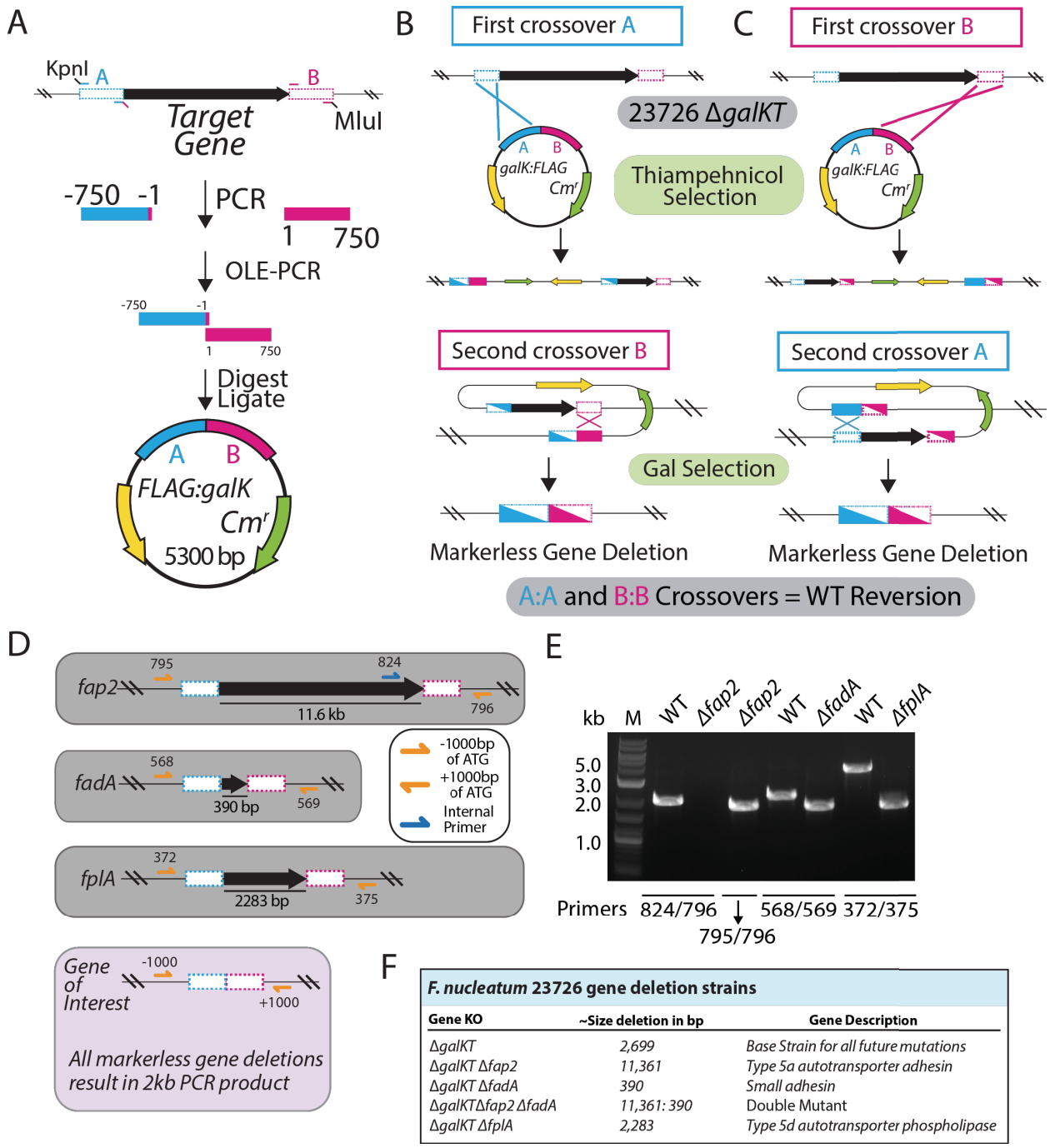

F. nucleatum 23726 gene deletion strains		
Gene KO	**~Size deletion in bp**	**Gene Description**
ΔgalKT	*2,699*	*Base Strain for all future mutations*
ΔgalKT Δfap2	*11,361*	*Type 5a autotransporter adhesin*
ΔgalKT ΔfadA	*390*	*Small adhesin*
ΔgalKTΔfap2 ΔfadA	*11,361: 390*	Double Mutant
ΔgalKT ΔfplA	*2,283*	*Type 5d autotransporter phospholipase*

Figure 2.4 The creation of in-frame gene deletions of *F. nucleatum* virulence factors. The PCR, plasmid integration and homologous recombination event schemes are highlighted (A-C). PCR verification of successful gene deletions affirm successful gene knockouts of each target gene (D-E). An overview of the gene deletion strains caused and the gene description is provided (F)

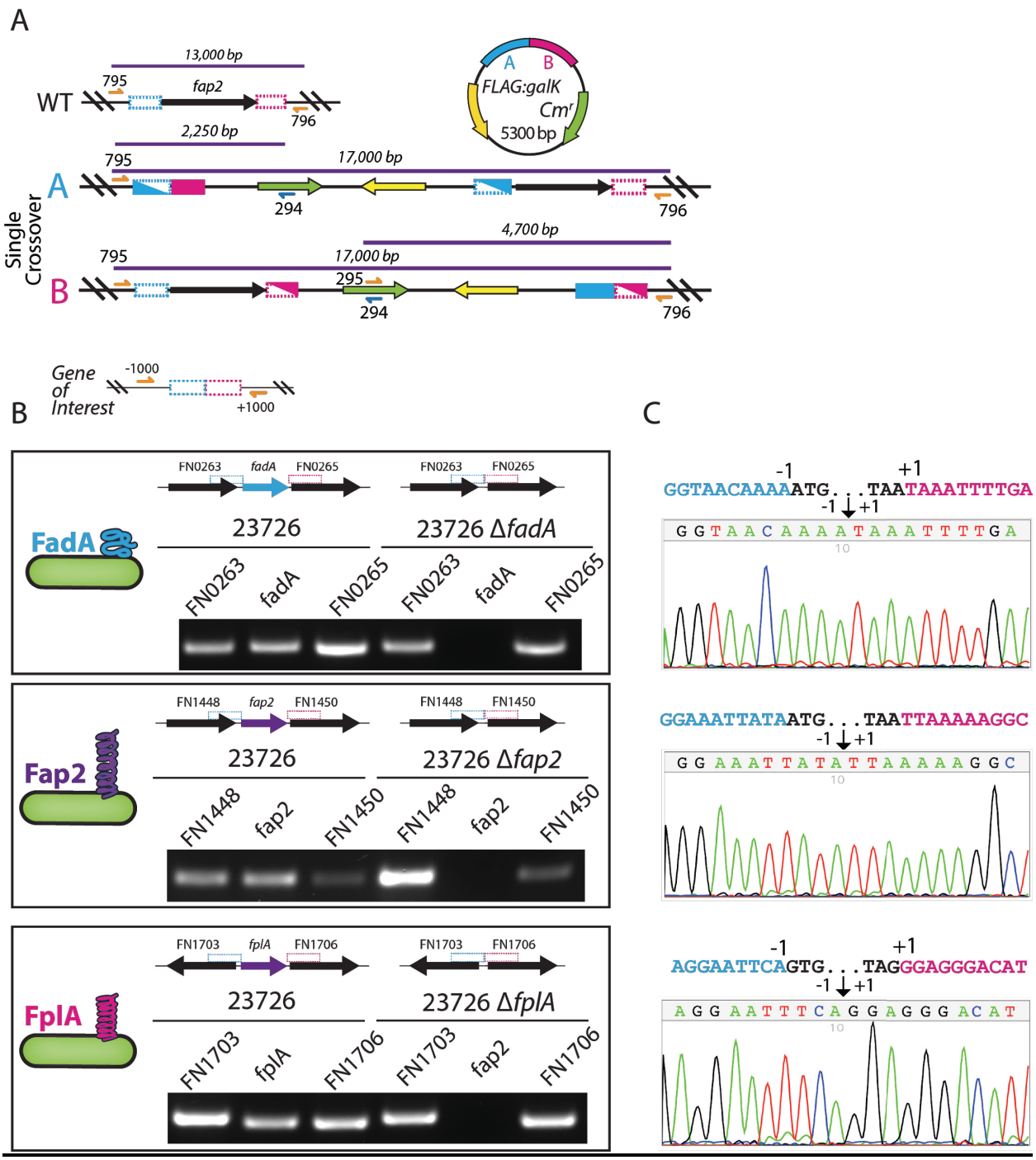

Figure 2.5 RT-PCR verification of the absence of polar effects resulting from gene deletion. An example primer design scheme for RT-PCR verification, here shown for Fap2, is depicted (A). RT-PCR results for each targeted deletion show that transcription of genes immediately upstream and downstream from the gene of interest remain actively transcribed and do not change in their levels of transcription (B). Sequencing data from each strain confirms in-frame gene deletions were achieved beginning at the start codon and ending at the stop codon for DJS2, DJS3, and DJS5 (C).

Developing new molecular technologies using the Δ*galKT* base strain.

We have demonstrated our ability to incorporate various plasmids onto the *F. nucleatum* chromosome, and this can be exploited to create protein over-expression technologies. The genome of *F. nucleatum* ATCC 23726 contains a gene for arsenic transport, *arsB* that is not needed under laboratory conditions. We incorporated a 1000 base pair region of homology to the central portion of *arsB* into our custom over-expression plasmid. This plasmid features a multiple cloning site and thiamphenicol resistance markers. Additionally, it contains an *E. coli* origin of replication to facilitate easy cloning and DNA purification while ensuring plasmid integration on the *F. nucleatum* chromosome. The promoter sequences and their efficiencies have not been explored in *F. nucleatum*, so a promoter from a presumed highly expressed ribosomal protein in *F. necrophorum* D12 was placed upstream of our GOI to drive transcription. Both FLAG and 6xHis affinity tags were cloned into the overexpression plasmid immediately following our GOI for immunoblot detection and affinity capture purification methods (**Figure 2.6a**).

We show that under standard *F. nucleatum* growth conditions, robust levels of protein expression can be detected via immunoblotting for 6xHis-tagged GalT. 200 μL of DJS1::*galK galT*-6xHis grown to stationary phase were lysed and soluble material separated via centrifugation. 1ug of this extract was loaded onto and SDS-PAGE gel and the strength of expression driven by the D12 promoter can be easily seen via immunoblotting (**Figure 2.6b**). In addition to over expression, we present a method to detect active enzymes containing serine hydrolase activity. These enzymes frequently have roles in virulence and metabolic processes, so a clear, straightforward screening technique to generate serine hydrolase activity profiles in response to genetic manipulation will be very useful. Briefly, a rhodamine labeled fluorophosphonate probe (TAMRA-FP) which specifically binds to active enzymes containing serine catalytic residues is added to bacteria to non-specifically interact with these proteins. In this instance, we highlight

this probe's utility in confirming successful gene deletion of *fplA*, and its subsequent application to confirm complementation and expression back into WT (**Figure 2.6c**). Also of note, is that this promoter seems to drive similar levels of FplA expression upon complementation when compared to the levels seen in WT *F. nucleatum*. The FplA expression profile and TAMRA-FP affinity is further detailed in Chapter 4 [32].

Additionally, we show the ability of the D12 promoter in our plasmid to drive expression of FadA to levels that are amenable to affinity purification. After the FadA expression plasmid was transformed and incorporated onto the DJS2 chromosome, 100 mL of bacterial culture was grown to stationary phase. These cells were lysed, and the soluble material was incubated with anti-FLAG resin and standard purification protocols were followed. The resulting elution fraction was run on an SDS-PAGE gel and incubated with Coomassie blue stain. The effectiveness of this methodology and resulting purity can be seen in Figure 2.6d. These proteins can be purified to >95% purity in potentially mg/L quantities through simple, inexpensive protein purification protocols. To our knowledge, this breakthrough represents the first over expression and isolation of an important virulence factor directly from *F. nucleatum* cultures. This method of protein purification preserves post-translational modifications, and it allows this understudied aspect of *F. nucleatum* protein biology to be explored for the first time. We envision overexpression technology to be expanded to include outer membrane proteins, including the autotransporters, in the near future. Membrane protein purification is notoriously difficult in traditional *E. coli*-based systems [33]. Technology presented here will allow for proper membrane insertion as *F. nucleatum* specific chaperones and membrane assembly machinery will be active since protein production is occurring in the natural host. This also eliminates the need for codon optimization, as these production methods no longer need to be done heterologously. The examples presented

here can be easily extended to any protein of interest for future studies of *F. nucleatum* protein biochemistry.

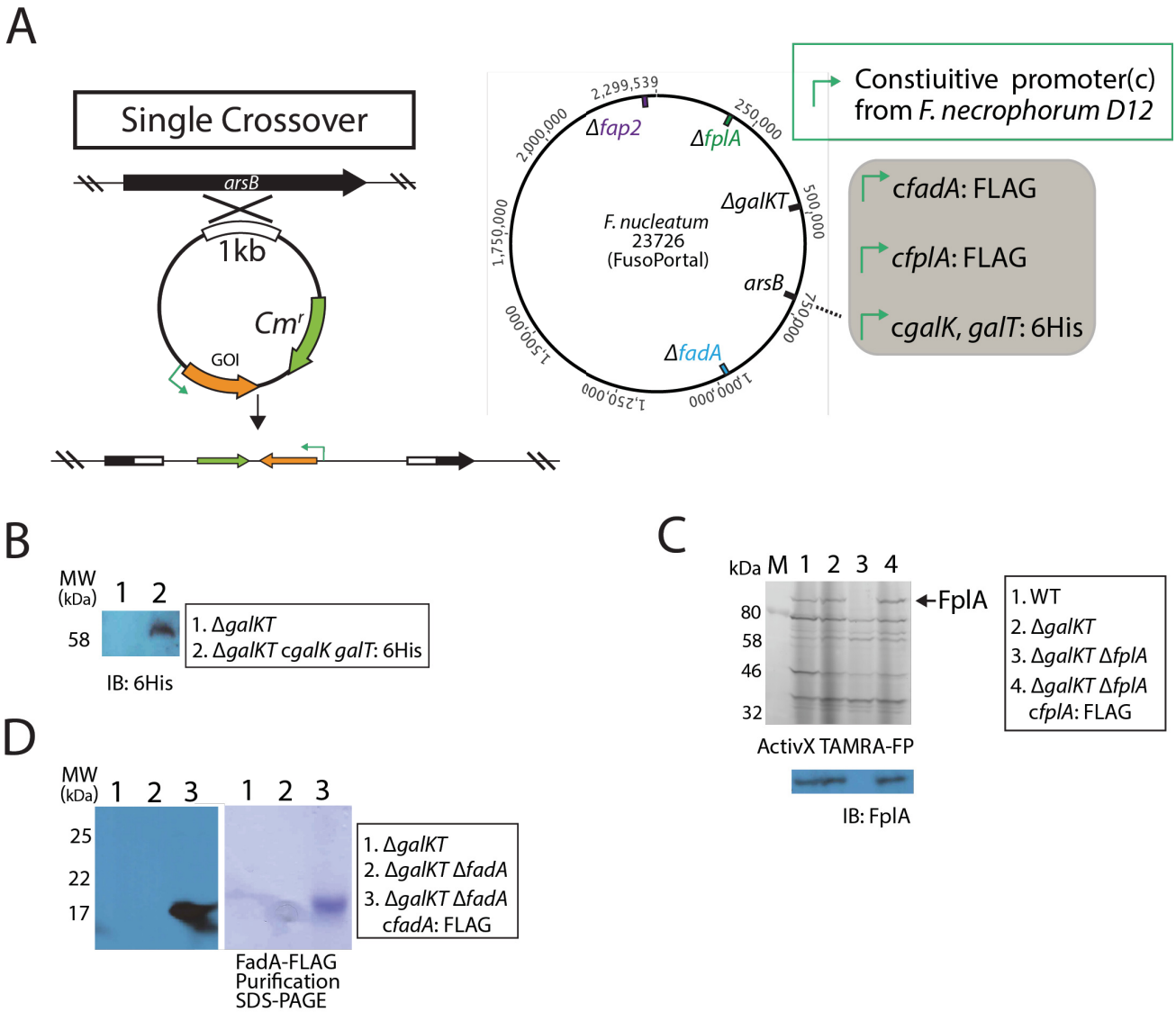

Figure 2.6 Molecular biology possibilities enabled by custom overexpression vectors in *F. nucleatum*. The *arsB* gene of *F. nucleatum* is exploited to introduce plasmids capable of allowing overexpression of any GOI. A diagram of recombination events and the chromosomal location of each GOI deleted in this manuscript are presented (A). Immunoblot for overexpressed GalT via 6xHis tag detection (B). ActiveX TAMRA-FP detection of active serine hydrolases in *F. nucleatum* highlighting FplA production levels in WT, DJS5, and DJS5::*fplA* strains. Immunoblot confirmation of FplA detection is shown below (C). Purification of FadA directly from *F. nucleatum* cultures is shown. Standard anti-FLAG purification methods were followed, and the resulting purified protein is shown via Coomassie staining and α-FLAG immunoblotting (D).

Revisiting the *F. nucleatum* invasion model using reverse genetic dissection and imaging flow cytometry.

We used standard cell culture models to ascertain the roles of Fap2 and FadA in *F. nucleatum* invasion in HCT-116 (cancerous colonocytes) and Ca-922 (cancerous gingival) ATCC typed cells. We determined invasion levels and measured the extent of host-pathogen interaction using both imaging flow cytometry and standard bacterial plating assays respectively. Before determining gene deletion effects on *F. nucleatum* invasion we first compared the WT and DJS1 levels of invasion to ensure that no phenotypic differences exist between the two strains. The indicated cell line was infected at an MOI of 1:1 for 30 minutes after reaching confluency. After the appropriate infection time, cells were washed to remove non-adherent bacteria and dislodged from the tissue culture plate and added to CBHK-agar and incubated under anaerobic conditions at 37°C. Colonies were counted after two days, and the results can be seen in Figure 2.7. These data show there are no differences observed between the WT and DJS1 strains, indicating experiments could move forward without significant confounding effects arising from the deletion of *galK* and *galT*.

Using the strains indicated previously, the same human cell binding and invasion study was performed to test which *F. nucleatum* outer membrane proteins were primarily responsible for initial docking to host cells. After 30 minutes of interaction time, we show that Fap2, and not FadA, is responsible for initial host cell docking in both cell lines tested. There was over a 50% drop in host-pathogen interaction detected in the HCT-116 cell line with DJS3 when compared to DJS1. Similarly, we show a significant decline in the capacity of DJS3 to interact with Ca-922 cells. We do not see these same deficiencies when infecting with DJS2 (**Figure 2.8c**).

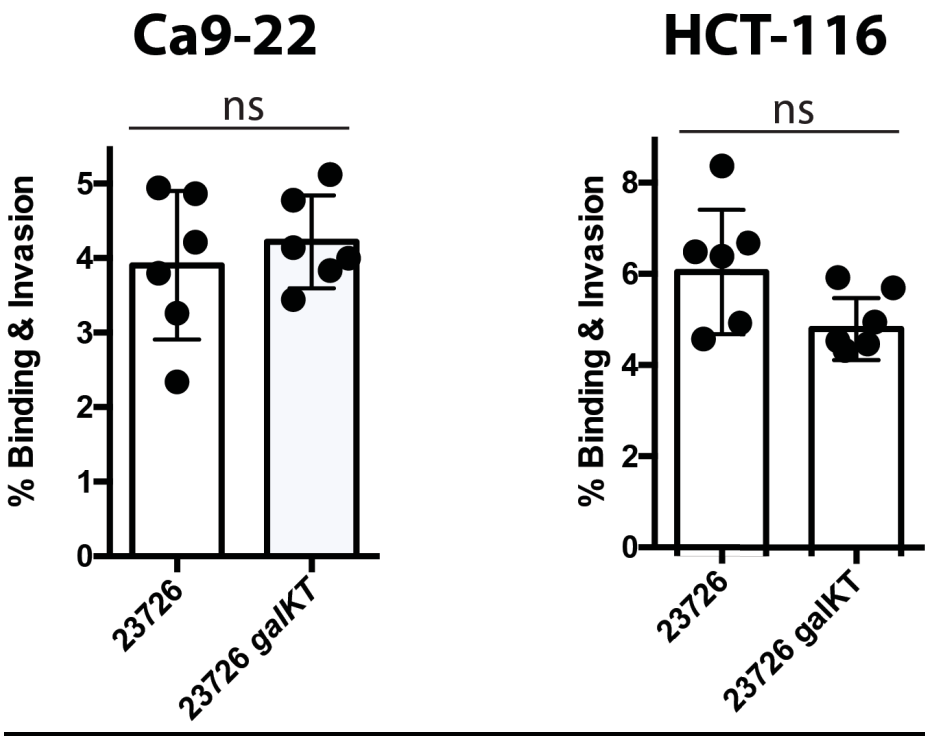

Figure 2.7 *F. nucleatum* 23726 and Δ*galKT* exhibit the same host-pathogen phenotype. The binding and invasion assay of HCT-116 and Ca-922 cell lines reveal that there are no phenotypic differences in the basal host-pathogen interaction between the WT and DJS1 strains used in this infection model. Human cells were infected at an MOI of 1:1 for 30 minutes before washing and plating. Experiments were performed in triplicate. Difference in binding and invasion is not significant (ns, P=0.52).

Next we tested the capacity of each bacterial strain to invade their human host using imaging flow cytometry. An example of the data output from these experiments can be seen in Figure 2.8a. The AMNIS Imagestream instrument generates a phase contrast and fluorescent image of each infection event passing through the flow cell. Cells that fluoresce green are considered to be positively invaded and population counts of positively and negatively infected cells can be generated. Briefly, we performed an antibiotic protection assay on the HCT-116 cell lines using an MOI of 10:1 for the indicated time point followed by killing of extracellular bacteria using penicillin and streptomycin before administering each sample to the instrument. Our data show a strong invasive defect in DJS3 and DJS4 strains at all time points measured when compared with DJS1. Although the infection rates increase as the allowed host-pathogen interaction time increases in DJS3 strains, they never reach the levels of DJS1 (**Figure 2.8d**). We also found that the DJS2 and DJS1 strains have identical infection rates at each time point using these same conditions (data not shown) suggesting a revision to the currently accepted infection model is needed. Together these data confirm that Fap2 is a significant driver of bacterial attachment and invasion of human cells, and that the role of FadA should be reevaluated. This is a large revision to the *F. nucleatum* invasion model as the role of FadA in pathogenesis should be revised in particular model systems when designing future experiments concerning invasion or targeted drug design.

After testing invasion, we wanted to test the effects of Fap2 and FadA on IL-8 secretion in response to *F. nucleatum* infection. Using a commercially available kit to detect levels of secreted cytokines through a standard flow cytometer, we found that IL-8 secretion by HCT-116 cells after infection at an MOI of 10:1 for 4 hours is largely Fap2 mediated. Infection with DJS3 causes a fivefold reduction in IL-8 levels when compared with both DJS1 and DJS2 strains (**Figure2.8e)**.

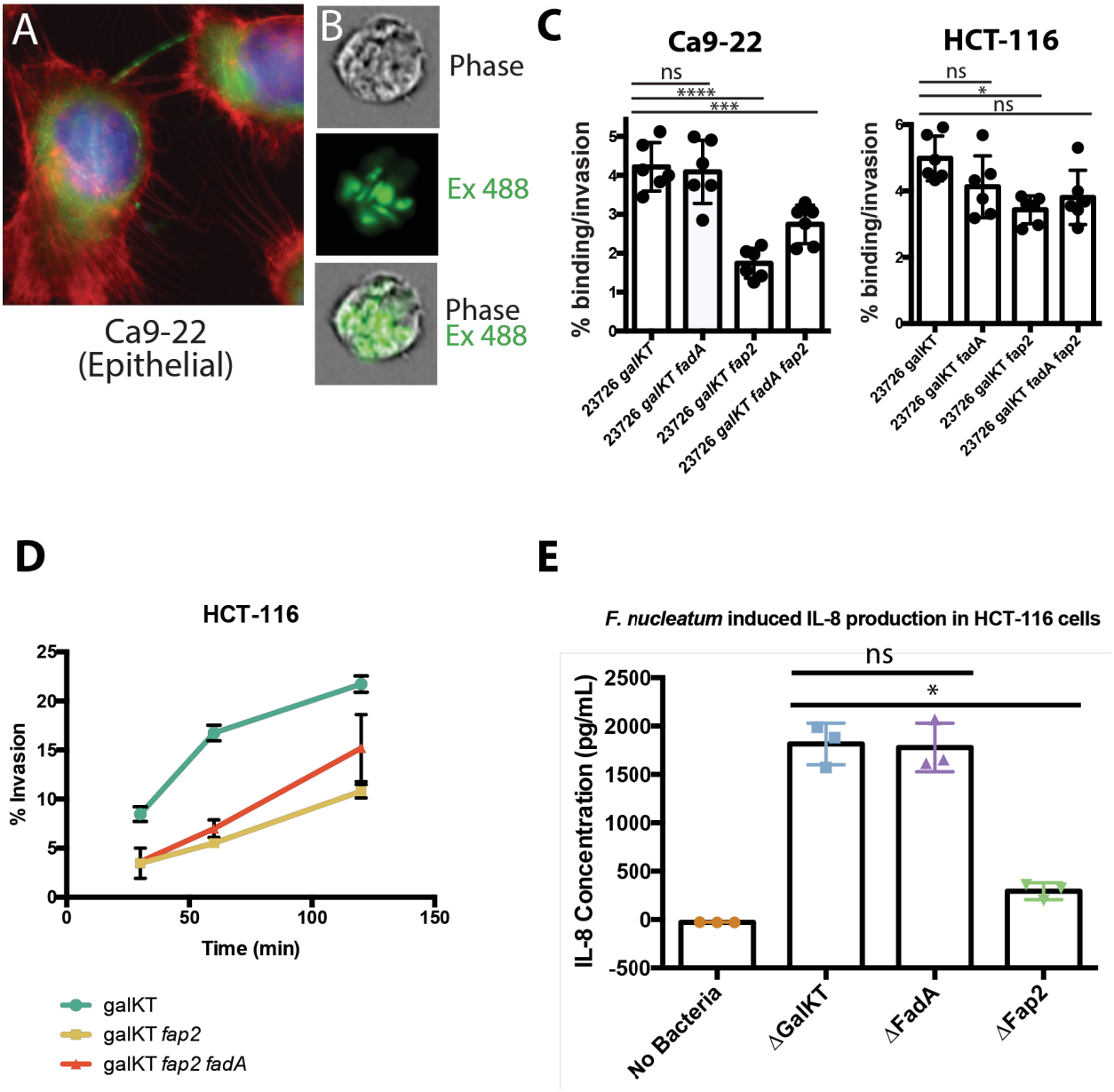

Figure 2.8 *F. nucleatum* host cell interaction, invasion and the resulting IL-8 secretion. Representative image of Ca9-22 cells after 23726 infection for 4 hours at an MOI of 100:1. Image shown to highlight the invasive potential of *F. nucleatum*. Labeling: *F. nucleatum* 23726 (FM1-43FX lipid dye, green), DNA (DAPI, blue), Actin (Phalloidin, red) (A). Invasion of Ca9-22 cells by *F. nucleatum* 23726 at an MOI of 10:1 analyzed by imaging flow cytometry (B). Quantitation of binding and invasion by various strains of *F. nucleatum* in either Ca9-22 or HCT-116 cells at an MOI of 1:1 for 30 minutes (C). Quantitation of invasion by various strains of *F. nucleatum* in HCT-116 cells at an MOI of 10:1 for 2 hours as quantified by imaging flow cytometry (D). Measurement of IL-8 secretion from HCT-116 cells in response to 4 hour infection times by *F. nucleatum* at an MOI of 10:1 for 4 hours (E). Experiments were performed in triplicate. ns (not-significant), $P > 0.5$ *$P \leq 0.01$. ***$P \leq 0.001$, ****$P \leq 0.00001$.

This deficiency can indicate either of two possibilities. There may be some direct Fap2 mediated pathway inside HCT-116 and other human cancerous cells that results in the increase of IL-8 production. Alternatively, the mere presence of *F. nucleatum* in the host cell cytosol may trigger some unidentified host-pathogen interaction that results in increased IL-8 secretion. More work is needed to ascertain the exact mechanism underlying this phenomenon as increased IL-8 production can have significant negative impacts on the CRC outcome. Importantly, these data suggest vastly different roles in invasion for Fap2 and FadA than what has been previously reported. In prior studies, FadA was found to increase IL-8 secretion and drive invasion, but that was not recapitulated here [15, 34]. This is perhaps due to variations in strain or human cell line between the model systems utilized here and the methodologies used to study FadA in the past. These results suggest that the role of FadA may be dependent on strain as FadA was determined important to invasion in *F. nucleatum* 12230 but not in *F. nucleatum* 23726. This implies conclusions made about this protein in one strain may not be applicable to others. Nonetheless, our results suggest a revision to the currently accepted model of *F. nucleatum* infection so that future experiments can be designed more efficiently to yield insightful data.

Discussion

The recent explosion of studies probing the functions of the human microbiome have uncovered new associations between these commensal microorganisms and disease [35–40]. Accordingly, understudied bacterial species are being characterized at the forefront of the microbiology community to help us understand these newly discovered interactions. Unfortunately, moving away from model systems like *E. coli* and *S. epidermidis* frequently presents experimental challenges that can cause bottlenecks and stall progress. Genetically recalcitrant bacteria in the human microbiome are frequently encountered, and the development of effective solutions to genetic manipulation problems are becoming increasingly valuable [41–44]. One such member of the human microbiome that presents all of the above challenges is *F. nucleatum*.

F. nucleatum is an intriguing model organism to study microbiome-induced effects on the development of disease. It has a well demonstrated ability to cause acute infections in locations throughout the body as well as implications in the development and progression of CRC. These disease associations highlight the need to develop technology specific to *F. nucleatum* to facilitate robust molecular and biochemical studies into the molecular underpinnings underlying its pathogenesis. Recent breakthroughs in *F. nucleatum* genome sequencing and assembly provide highly accurate information to guide the development of these technologies [45]. Prior to this study, a well explained, reliable methodology to introduce in-frame gene deletions, which is a fundamental need of pathogenic bacteriology, was wholly unavailable. Unsurprisingly, only one study utilizing such a system has been published to date. While results stemming from that study elucidated key insights into *F. nucleatum* biofilm formation, it did not delve into its pathogenicity [24]. As such, there are lingering questions and sizeable knowledge gaps that remain to be traversed.

Studies attempting to fill these pathogenicity gaps have largely focused on two outer-membrane adhesins, Fap2 and FadA. Both were reported to induce bacterial invasion of human epithelial cells [46, 47]. FadA also had the additional effect of increasing IL-8 secretion of infected cells [15]. IL-8 secretion is of particular importance as it can have significant impacts on the development and metastasis of cancer cells [21]. Since *F. nucleatum* infected tumor cells have been isolated at sites distal to the primary site of infection, mechanistic details are highly sought after concerning the role this bacteria has in the development and progression of cancer [48]. Additional associations between *F. nucleatum* and cancer emphasize the need for technology to study this relationship include decreased patient prognosis and increased disease severity in the presence of *F. nucleatum* infected tumors [49, 50].

Unfortunately, the molecular mechanisms behind these associations have remained elusive. This may be due to incomplete findings resulting from the lack of genetic and molecular resources applicable to *F. nucleatum*. Using the newly developed resources presented here, we have shown that Fap2, and not FadA, is a significant mediator of host-pathogen interaction and host cell invasion by this bacterium. Similarly, we show that IL-8 secretion is dependent on *F. nucleatum* expressing Fap2. These results represent a revision in the host-pathogen interaction model for *F. nucleatum* (**Figure 2.9**). While the difference in the proposed models may be the result of variations in bacterial strain and host cell line used for probing host-pathogen interactions, we are confident that future studies investigating IL-8 secretion and invasion should focus on some yet to be defined Fap2 dependent mechanism. Additionally, these results suggest that more work is needed to understand the role of FadA in *F. nucleatum* pathogenicity. We are confident future work utilizing the straightforward methodologies presented here will begin to yield informative results on *F. nucleatum* induced disease. Details unearthed from experiments utilizing these

technologies may, in turn, lead to enhanced treatment or prevention options for patients suffering from CRC.

Breakthroughs presented in this manuscript provide a new foundation for future exploration of *F. nucleatum*, not only in the context of host-pathogen interaction, but for any study of this bacterium that requires protein and genetic characterization. The recent improvements in genome assembly of *F. nucleatum* in combination with this straightforward molecular technology provide the field with highly accurate, reliable and repeatable methodologies for the dissection of myriad processes that were not possible before. The ability to overexpress and purify proteins directly from *F. nucleatum* will allow researchers to probe the role of post-translational modifications in the effectiveness of various protein families. This aspect of protein biology has been completely neglected in the *F. nucleatum* field. Given its importance to the virulence of *Legionella pneumophila* and *Haemophilus influenzae* among others, elucidating the roles of post-translational modifications in *F. nucleatum* virulence represents an exciting new area of study that can now be adequately explored [51,52]. Additionally, the ability to create multiple gene deletions within the same strain in parallel will allow for the study of virulence factor cooperativity for the first time. *F. nucleatum* 23726 possesses over 20 Type 5 secreted proteins with many of them purported to be involved in virulence [53]. Given the large number of these proteins produced by this bacterium, it is highly possible that they serve redundant roles that would be impossible to study without our addition to the field. Lastly, we highlight the utility of our new methodologies by providing a revision of the current *F. nucleatum* infection model with insights into induced IL-8 secretion and, perhaps, this bacteria's ability to exacerbate CRC.

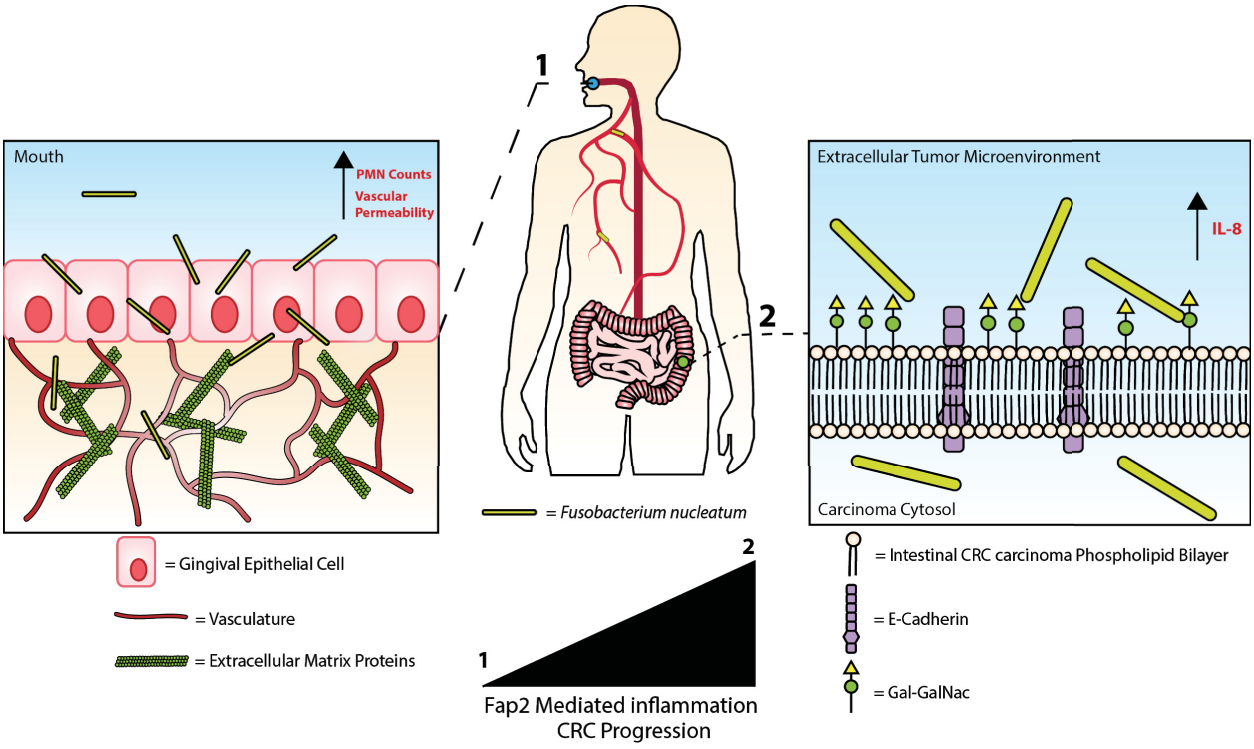

Figure 2.9 A revised model of *F. nucleatum* infection with a proposed role of IL-8 in CRC progression. *F. nucleatum* infects gingival cells and drives up inflammation in the mouth (1). Elevated inflammation corresponds to high PMN counts which increases vascular permeability permitting *F. nucleatum* entry into the bloodstream. Current evidence strongly suggests this bacteria travels hematogenously to gain access to tissues at the systemic level. Elevated expression of Gal-GalNac residues of CRC tumor cells enhances *F. nucleatum*'s affinity for tumor cells via Fap2 mediated interactions. Invasion of tumor cells increases IL-8 secretion which can promote metastasis and decrease patient prognosis (2).

Acknowledgements

Research was supported by startup funding from the Department of Biochemistry at Virginia Tech, the Institute for Critical Technology and Applied Science (ICTAS) at Virginia Tech, and the National Institute for Food and Agriculture.

Author Contributions

MAC, CY and DJS wrote and designed the manuscript. BS, AU, MAC and DJS designed and performed experiments for this manuscript. BS performed RTPCR experiments. AU performed FadA purifications. MAC and CY performed infection assays, and complementation detection assays. MAC, DJS, CY created *F. nucleatum* mutant strains and performed bacterial growth assays.

Competing Interests

The authors declare that they have no conflicts of interest with the contents of this article.

References

1. Kapatral V, Anderson I, Ivanova N, Reznik G, Los T, Lykidis A, et al. Genome sequence and analysis of the oral bacterium Fusobacterium nucleatum strain ATCC 25586. J Bacteriol. Am Soc Microbiol; 2002;184: 2005–2018.
2. Kaplan A, Kaplan CW, He X, McHardy I, Shi W, Lux R. Characterization of aid1, a novel gene involved in Fusobacterium nucleatum interspecies interactions. Microb Ecol. 2014;68: 379–387.
3. Kaplan CW, Lux R, Haake SK, Shi W. The Fusobacterium nucleatum outer membrane protein RadD is an arginine-inhibitable adhesin required for inter-species adherence and the structured architecture of multispecies biofilm. Mol Microbiol. 2009;71: 35–47.
4. Gursoy UK, Könönen E, Uitto V-J. Intracellular replication of fusobacteria requires new actin filament formation of epithelial cells. APMIS. 2008;116: 1063–1070.
5. Gedik AH, Cakir E, Soysal O, Umutoğlu T. Endobronchial lesion due to pulmonary

Fusobacterium nucleatum infection in a child. Pediatr Pulmonol. 2014;49: E63–5.
6. Heckmann JG, Lang CJG, Hartl H, Tomandl B. Multiple brain abscesses caused by Fusobacterium nucleatum treated conservatively. Can J Neurol Sci. 2003;30: 266–268.
7. Tweedy CR, White WB. Multiple Fusobacterium nucleatum liver abscesses. Association with a persistent abnormality in humoral immune function. J Clin Gastroenterol. journals.lww.com; 1987;9: 194–197.
8. Han YW, Fardini Y, Chen C, Iacampo KG, Peraino VA, Shamonki JM, et al. Term stillbirth caused by oral Fusobacterium nucleatum. Obstet Gynecol. 2010;115: 442–445.
9. Liu H, Redline RW, Han YW. Fusobacterium nucleatum induces fetal death in mice via stimulation of TLR4-mediated placental inflammatory response. J Immunol. 2007;179: 2501–2508.
10. Shammas NW, Murphy GW, Eichelberger J, Klee D, Schwartz R, Bachman W. Infective endocarditis due to Fusobacterium nucleatum: case report and review of the literature. Clin Cardiol. 1993;16: 72–75.
11. Abed J, Emgård JEM, Zamir G, Faroja M, Almogy G, Grenov A, et al. Fap2 Mediates Fusobacterium nucleatum Colorectal Adenocarcinoma Enrichment by Binding to Tumor-Expressed Gal-GalNAc. Cell Host Microbe. 2016;20: 215–225.
12. Castellarin M, Warren RL, Freeman JD, Dreolini L, Krzywinski M, Strauss J, et al. Fusobacterium nucleatum infection is prevalent in human colorectal carcinoma. Genome Res. genome.cshlp.org; 2012;22: 299–306.
13. Coppenhagen-Glazer S, Sol A, Abed J, Naor R, Zhang X, Han YW, et al. Fap2 of Fusobacterium nucleatum is a galactose-inhibitable adhesin involved in coaggregation, cell adhesion, and preterm birth. Infect Immun. 2015;83: 1104–1113.
14. Kaplan CW, Ma X, Paranjpe A, Jewett A, Lux R, Kinder-Haake S, et al. Fusobacterium nucleatum outer membrane proteins Fap2 and RadD induce cell death in human lymphocytes. Infect Immun. 2010;78: 4773–4778.
15. Rubinstein MR, Wang X, Liu W, Hao Y, Cai G, Han YW. Fusobacterium nucleatum promotes colorectal carcinogenesis by modulating E-cadherin/β-catenin signaling via its FadA adhesin. Cell Host Microbe. 2013;14: 195–206.
16. Ikegami A, Chung P, Han YW. Complementation of the fadA mutation in Fusobacterium nucleatum demonstrates that the surface-exposed adhesin promotes cellular invasion and placental colonization. Infect Immun. Am Soc Microbiol; 2009;77: 3075–3079.
17. Li A, Dubey S, Varney ML, Dave BJ, Singh RK. IL-8 directly enhanced endothelial cell survival, proliferation, and matrix metalloproteinases production and regulated angiogenesis. J Immunol. 2003;170: 3369–3376.
18. Scheibenbogen C, Möhler T, Haefele J, Hunstein W, Keilholz U. Serum interleukin-8 (IL-8) is elevated in patients with metastatic melanoma and correlates with tumour load. Melanoma Res. 1995;5: 179–181.
19. Palena C, Hamilton DH, Fernando RI. Influence of IL-8 on the epithelial-mesenchymal transition and the tumor microenvironment. Future Oncol. 2012;8: 713–722.
20. Bates RC, DeLeo MJ 3rd, Mercurio AM. The epithelial-mesenchymal transition of colon carcinoma involves expression of IL-8 and CXCR-1-mediated chemotaxis. Exp Cell Res. 2004;299: 315–324.
21. Fernando RI, Castillo MD, Litzinger M, Hamilton DH, Palena C. IL-8 signaling plays a critical role in the epithelial-mesenchymal transition of human carcinoma cells. Cancer Res. 2011;71: 5296–5306.
22. David JM, Dominguez C, Hamilton DH, Palena C. The IL-8/IL-8R Axis: A Double Agent in Tumor Immune Resistance. Vaccines (Basel). 2016;4. doi:10.3390/vaccines4030022

23. Gur C, Ibrahim Y, Isaacson B, Yamin R, Abed J, Gamliel M, et al. Binding of the Fap2 protein of Fusobacterium nucleatum to human inhibitory receptor TIGIT protects tumors from immune cell attack. Immunity. 2015;42: 344–355.
24. Wu C, Al Mamun AAM, Luong TT, Hu B, Gu J, Lee JH, et al. Forward Genetic Dissection of Biofilm Development by Fusobacterium nucleatum: Novel Functions of Cell Division Proteins FtsX and EnvC. MBio. 2018;9. doi:10.1128/mBio.00360-18
25. Nariya H, Miyata S, Suzuki M, Tamai E, Okabe A. Development and application of a method for counterselectable in-frame deletion in Clostridium perfringens. Appl Environ Microbiol. 2011;77: 1375–1382.
26. Nithianantham S, Xu M, Yamada M, Ikegami A, Shoham M, Han YW. Crystal structure of FadA adhesin from Fusobacterium nucleatum reveals a novel oligomerization motif, the leucine chain. J Biol Chem. 2009;284: 3865–3872.
27. Narayanan SK, Nagaraja TG, Chengappa MM, Stewart GC. Cloning, sequencing, and expression of the leukotoxin gene from Fusobacterium necrophorum. Infect Immun. 2001;69: 5447–5455.
28. Nagaraja TG, Narayanan SK, Stewart GC, Chengappa MM. Fusobacterium necrophorum infections in animals: pathogenesis and pathogenic mechanisms. Anaerobe. 2005;11: 239–246.
29. Leloir LF, Trucco RE. [35] Galactokinase and galactowaldenase. Methods in Enzymology. Academic Press; 1955. pp. 290–294.
30. Frey PA. The Leloir pathway: a mechanistic imperative for three enzymes to change the stereochemical configuration of a single carbon in galactose. The FASEB Journal. Federation of American Societies for Experimental Biology; 1996;10: 461–470.
31. Kinder Haake S, Yoder S, Gerardo SH. Efficient gene transfer and targeted mutagenesis in Fusobacterium nucleatum. Plasmid. 2006;55: 27–38.
32. Casasanta MA, Yoo CC, Smith HB, Duncan AJ, Cochrane K, Varano AC, et al. A chemical and biological toolbox for Type Vd secretion: Characterization of the phospholipase A1 autotransporter FplA from Fusobacterium nucleatum. J Biol Chem. 2017;292: 20240–20254.
33. Smith SM. Strategies for the purification of membrane proteins. Methods Mol Biol. 2011;681: 485–496.
34. Manson McGuire A, Cochrane K, Griggs AD, Haas BJ, Abeel T, Zeng Q, et al. Evolution of invasion in a diverse set of Fusobacterium species. MBio. Am Soc Microbiol; 2014;5: e01864.
35. Turnbaugh PJ, Ley RE, Hamady M, Fraser-Liggett CM, Knight R, Gordon JI. The Human Microbiome Project. Nature. 2007;449: 804–810.
36. Valdez Y, Brown EM, Finlay BB. Influence of the microbiota on vaccine effectiveness. Trends Immunol. 2014;35: 526–537.
37. Dejea CM, Wick EC, Hechenbleikner EM, White JR, Mark Welch JL, Rossetti BJ, et al. Microbiota organization is a distinct feature of proximal colorectal cancers. Proceedings of the National Academy of Sciences. 2014; doi:10.1073/pnas.1406199111
38. Grice EA, Segre JA. The skin microbiome. Nat Rev Microbiol. 2011;9: 244–253.
39. Yamamura K, Baba Y, Nakagawa S, Mima K, Miyake K, Nakamura K, et al. Human Microbiome Fusobacterium Nucleatum in Esophageal Cancer Tissue Is Associated with Prognosis. Clin Cancer Res. 2016; doi:10.1158/1078-0432.CCR-16-1786
40. Hieken TJ, Chen J, Hoskin TL, Walther-Antonio M, Johnson S, Ramaker S, et al. The Microbiome of Aseptically Collected Human Breast Tissue in Benign and Malignant Disease. Sci Rep. 2016;6: 30751.

41. Serafini F, Turroni F, Guglielmetti S, Gioiosa L, Foroni E, Sanghez V, et al. An efficient and reproducible method for transformation of genetically recalcitrant bifidobacteria. FEMS Microbiol Lett. 2012;333: 146–152.
42. Coico R, Kowalik T, Quarles J, Stevenson B, Taylor R, editors. Genetic Manipulation of Mycobacterium tuberculosis. Current Protocols in Microbiology. Hoboken, NJ, USA: John Wiley & Sons, Inc.; 2005. p. 3007.
43. Coico R, Kowalik T, Quarles J, Stevenson B, Taylor R, editors. Genetic Manipulation of Campylobacter jejuni. Current Protocols in Microbiology. Hoboken, NJ, USA: John Wiley & Sons, Inc.; 2005. p. 1.3.1.
44. Sander JD, Joung JK. CRISPR-Cas systems for editing, regulating and targeting genomes. Nat Biotechnol. 2014;32: 347–355.
45. Sanders BE, Umana A, Lemkul JA, Slade DJ. FusoPortal: an Interactive Repository of Hybrid MinION-Sequenced Fusobacterium Genomes Improves Gene Identification and Characterization. mSphere. 2018;3. doi:10.1128/mSphere.00228-18
46. Kaplan CW, Lux R, Huynh T, Jewett A, Shi W, Haake SK. Fusobacterium nucleatum apoptosis-inducing outer membrane protein. J Dent Res. 2005;84: 700–704.
47. Han YW. Fusobacterium nucleatum: a commensal-turned pathogen. Curr Opin Microbiol. 2015;23: 141–147.
48. Bullman S, Pedamallu CS, Sicinska E, Clancy T, Ogino S, Tabernero J, et al. Abstract 5129: Fusobacterium and co-occurring microbes in primary and metastatic colorectal cancer. Cancer Res. American Association for Cancer Research; 2018;78: 5129–5129.
49. Mima K, Nishihara R, Qian ZR, Cao Y, Sukawa Y, Nowak JA, et al. Fusobacterium nucleatum in colorectal carcinoma tissue and patient prognosis. Gut. 2016;65: 1973–1980.
50. Nosho K, Sukawa Y, Adachi Y, Ito M, Mitsuhashi K, Kurihara H, et al. Association of Fusobacterium nucleatum with immunity and molecular alterations in colorectal cancer. World J Gastroenterol. 2016;22: 557–566.
51. Michard C, Doublet P. Post-translational modifications are key players of the Legionella pneumophila infection strategy. Front Microbiol. 2015;6: 87.
52. Grass S, Lichti CF, Townsend RR, Gross J, St Geme JW 3rd. The Haemophilus influenzae HMW1C protein is a glycosyltransferase that transfers hexose residues to asparagine sites in the HMW1 adhesin. PLoS Pathog. 2010;6: e1000919.
53. Nicolay T, Vanderleyden J, Spaepen S. Autotransporter-based cell surface display in Gram-negative bacteria. Crit Rev Microbiol. 2015;41: 109–123.

Chapter 3

A vector suite for the overexpression and purification of tagged outer membrane, periplasmic, and secreted proteins in *E. coli*

Michael A. Casasanta[1] and Daniel J. Slade[1]

1. Department of Biochemistry, Virginia Polytechnic Institute and State University, Blacksburg, VA, USA.

Abstract

Outer membrane and secreted proteins in Gram-negative bacteria constitute a high percentage of virulence factors that are critical in disease initiation and progression. Despite their importance, it is often difficult to study these proteins due to challenges with expression and purification. Here we present a suite of vectors for the inducible expression of N-terminally 6His tagged outer membrane, periplasmic, and secreted proteins in *E. coli*, and show this system to be capable of producing milligram quantities of pure protein for downstream functional and structural analysis. This system can not only be used to purify recombinant virulence factors for structural and functional studies, but can also be used to create gain-of-function *E. coli* for use in phenotypic screens, and examples of each are provided herein.

Introduction

Protein secretion from the cytoplasm to the periplasm, outer membrane, and extracellular environment, is an important mechanism for bacterial pathogenesis.[1–3] While a complete overview of all multi-component protein secretion systems in bacteria is beyond the scope of this chapter,[2] we will provide background and techniques used in Gram-negative bacteria for the initial export of proteins through the inner membrane. The two main systems for the export of proteins from the cytoplasm to the periplasm are the general secretion route termed the Sec pathway (unfolded proteins), and the Twin-Arginine Translocation (Tat) pathway (folded proteins).[4] Both the Sec and Tat systems rely on translocated proteins to have an N-terminal signal peptide (~15-40 AA), that is used for initial binding and initiation of inner membrane translocation. These signal peptides can be bioinformatically identified by online servers such as SignalP or PREDTAT (*see Note 1*).

E. coli is the most common bacterial strain for recombinant protein expression, and this bacterium contains both Sec and Tat systems for protein translocation. Our experience is that while a protein from a non-*E. coli* genus of bacteria might be predicted to have a signal sequence, it is often not efficiently recognized by the *E. coli* machinery, which results in a lack of robust recombinant protein expression. To rectify this gap, we have developed a suite of vectors (**see Figure 3.1, Table 3.1 and Note 2**) with signal sequences from highly expressed *E. coli* proteins, thereby facilitating the translocation of recombinant proteins through the inner membrane using either the Sec or Tat pathways. A similar method was previously used for the successful production of highly pure protein for the structure determination of EstA; a *Pseudomonas aeruginosa* outer membrane protein of the Type 5 secreted autotransporter family.[5] To facilitate Sec secretion, we used the signal sequences from *E. coli* OmpA (residues 1-27) and TamA (residues 1-27), and for the TAT system we used SufI (FtsP) (residues 1-30). To add flexibility to our vectors, we created

versions that have variations of ampicillin or chloramphenicol antibiotic resistance, and multiple origins of replication (p15A, ColE1). All versions of these vectors result in proteins that contain an N-terminal 6His tag for purification and detection. These vectors provide flexibility by allowing replication in a variety of *E. coli* hosts, and in addition, will allow for the simultaneous expression of two proteins by concurrently transforming compatible plasmids of interest.

Methods

A Vector Suite for the Expression of Tagged Extra-Cytoplasmic Proteins

After predicted cleavage of the signal sequence by Signal peptidase I (SPaseI) as proteins are transported to the bacterial extracytoplasmic space,[6] recombinant proteins will retain a minimal N-terminal extension and a 6His tag before the amino acids of your gene of interest. For vectors pDJSVT86 and pDJSVT87 which contain an OmpA 1-27 tag, the residues will be: N-APKDNTHHHHHHxxxxxx, where xxxxxx begins the amino acids from the gene the user cloned into the vector. For vectors pDJSVT89 and pDJSVT90 which contain a TamA 1-27 tag, the residues will be: N- ANVRLQHHHHHHxxxxxx. For vector pDJSVT91, which contains a SufI 1-30 tag, the residues will be: N- AGQHHHHHHxxxxxx. For a graphical summary describing protein products, please refer to **Figure 3.1**. All five vectors have been submitted to the Addgene non-profit plasmid repository, and can be obtained by requesting the ID number in **Table 3.1**.

Plasmid	Addgene ID
pDJSVT86	108965
pDJSVT87	109302
pDJSVT89	109303
pDJSVT90	109304
pDJSVT91	109305

Table 3.1. Addgene ID's for plasmids used in these methods

Required Instrumentation for the following methods:

Thermocycler, refrigerated centrifuge (capable of 15,000 RCF), refrigerated ultracentrifuge (capable of 100,000 RCF), swinging bucket centrifuge capable of spinning 12 well plates, cell sonifier or pressure cell (EmulsiFlex-C3, Avestin) for bacterial lysis, DNA and protein electrophoresis apparatus, Western blot transfer apparatus, glass column for protein purification, exponential decay electroporator, Fast-protein liquid chromatography (FPLC) system (ÄKTA pure system, GE Healthcare, USA), Fluorescent microscope with 63-100x objective (GFP and DAPI filters), 500 mL and 4 L baffled bottom flasks, Stir plate, cold room or cold box for protein purification, Stirred ultrafiltration cell, heating and cooling shaking incubator.

General Materials:

All solutions should be made using high quality deionized water. Unless otherwise stated, store all solutions at room temperature. No sodium azide is added to any reagent. All *E. coli* should be properly handled by following BSL-1 specific guidelines.

PCR and Cloning - Materials:

1. 50x TAE buffer: 242g Tris base, 100mL of 500mM EDTA (pH 8.0) solution, 57.1mL glacial acetic acid in a final volume of 1 liter.
2. Agarose gels for DNA separation: 1g of agarose per 100 ml of 1x TAE buffer (1% gel) with 0.5 μg/ml ethidium bromide for visualization on a standard UV light box or digital gel visualization system.
3. High fidelity polymerase with proofreading activity to ensure accurate cloning of your target gene.
4. T4 DNA ligase (NEB)

5. Synthetic oligonucleotides for PCR.
6. EZ-10 Spin Column Plasmid DNA Miniprep Kit (BioBasic)
7. EZ-10 Spin Column PCR Products Purification Kit (BioBasic)

Growth Medium and Supplements - Materials:

1. LB Broth: 10g Tryptone (1% w/v), 5g Yeast Extract (0.5% w/v), 10g NaCl (1% w/v) per liter of media. Autoclave for sterility. Use baffled bottom shaking flasks at ≤25% occupancy to ensure proper aeration during growth.
2. LB agar: add 15 g/L Bacto agar to LB broth prior to autoclaving. LB agar plates should contain an appropriate antibiotic for transformant selection. Add the antibiotic once the agar has cooled to 50°C prior to pouring plates.
3. Isopropyl β-D-1-thiogalactopyranoside (IPTG) for the induction of protein expression under T7 promoters: Final concentration of 25-250 μM in LB media.
4. ZYP-5052 auto-induction media. 1% tryptone, 0.5% yeast extract, 50 mM Na_2HPO_4, 50 mM KH_2PO_4, 25 mM $(NH_4)_2SO_4$, 0.5% glycerol, 0.05% glucose, 0.2% α-lactose, 2 mM MgSO4, 0.2x trace elements (Please see the following reference: Studier, 2005, Protein Expression and Purification)[7]
5. Carbenicillin (ampicillin) and chloramphenicol are used to maintain plasmids during expressions at 100 μg/ml and 25 μg/ml final concentrations, respectively. Store at -20 ˚C

Competent Cells and Transformation - Materials:

1. DH5α or TOP10 *E. coli* for cloning and stable storage of plasmid backbones and clones.
2. BL21(DE3) and ArcticExpress (DE3) RIL *E. coli* for protein expression (Agilent Technologies)

3. Liquid nitrogen to freeze extra aliquots of electrocompetent cells.
4. 10% glycerol (sterile filtered)
5. SOC broth medium: 20 g/L tryptone, 5 g/L yeast extract, 0.5 g/L NaCl. Adjust to pH 7.0 by addition of 5 N NaOH, sterilize by autoclaving, and then add 20 mL of sterile 1 M glucose (final concentration of 20 mM).
6. Optional: Competent cell preparation using a Mix & Go! *E. coli* Transformation Kit (Zymo Research)
7. 1 mM gap electroporation cuvettes

Secreted Protein Purification - Materials:

1. 1 M Tris pH 7.5
2. 4 M NaCl
3. Stirred Ultrafiltration cell with pump for pressure-based sample concentration.
4. Ultracell® 10 kDa Ultrafiltration Discs (Millipore).
5. Chelating sepharose fast flow resin (GE Life Sciences) charged with nickel chloride for purification of 6His tagged proteins.
6. Econo-Column® Chromatography Columns, 2.5 × 10 cm (BioRad).
7. Ni-Sepharose wash buffer: 20 mM Tris pH 7.5, 50 mM imidazole, 400 mM NaCl.
8. Ni-Sepharose elution buffer: 20 mM Tris pH 7.5, 250 mM imidazole, 50 mM NaCl.
9. Optional ion exchange chromatography columns for additional protein purification.
10. Size-exclusion column: HiPrep 16/60 Sephacryl S-200 HR (GE Healthcare).
11. Size-exclusion chromatography buffer: 20 mM Tris pH 7.5, 150 mM NaCl, 10% glycerol.
12. Amicon Ultra Centrifugal Filter Units (GE Life Sciences).

Membrane Protein Purification - Materials:

1. Sarkosyl (Sigma-Aldrich) (additional detergents can be screened to optimize purification).
2. *E . coli* lysis and membrane fraction dilution buffer: 20 mM Tris pH 7.5, 20 mM imidazole, 400 mM NaCl, 1 mM PMSF.
3. Membrane pellet resuspension buffer: 20 mM Tris pH 7.5, 2% Sarkosyl.
4. Chelating sepharose fast flow resin (GE Life Sciences) charged with nickel chloride for purification of 6His tagged proteins.
5. Econo-Column® Chromatography Columns, 2.5 × 10 cm (BioRad).
6. Ni-Sepharose membrane wash buffer: 20 mM Tris pH 7.5, 50 mM imidazole, 400 mM NaCl, 0.2% Sarkosyl.
7. Ni-Sepharose membrane elution buffer: 20 mM Tris pH 7.5, 250 mM imidazole, 50 mM NaCl, 0.2% Sarkosyl.
8. Size-exclusion column: HiPrep 16/60 Sephacryl S-200 HR (GE Healthcare)
9. Size-exclusion chromatography buffer: 20 mM Tris pH 7.5, 150 mM NaCl, 10% glycerol, 0.2% Sarkosyl
10. Amicon Ultra Centrifugal Filter Units (GE Life Sciences)

Immunoblotting - Materials:

1. Precast 4-20% acrylamide precast gels (CBS Scientific) for SDS-PAGE analysis of protein expression and purification.
2. Color Prestained Protein Standard, Broad Range (11–245 kDa) (NEB)
3. Polyvinylidene difluoride (PVDF)(preferred) or nitrocellulose membranes.
4. Western blot transfer buffer (Towbin buffer): 25 mM Tris, 192 mM glycine, pH 8.3, 20% methanol (vol/vol)

5. Tris-buffered saline (10x TBS): 1.5 M NaCl, 0.1 M Tris-HCl, pH 7.4
6. TBST: 1x Tris buffered saline with 0.1% Tween-20
7. Methanol
8. Blocking and diluent solution: TBST with 3% BSA
9. THE^{TM} His Tag Antibody, mAb, Mouse (Genscript, USA)
10. Anti-mouse m-IgGκ BP-HRP secondary antibody (Santa Cruz)
11. ECL western blotting substrate (Thermo Scientific)
12. Lucent Blue X-ray film (Advansta). Optional: Digital gel and blot imaging system to replace exposure on film.

Immunofluorescence microscopy - Materials:

1. 10 mm round #1.5 thickness coverslip glass (Fisher Scientific)
2. Standard glass microscopy slides (Fisher Scientific)
3. 0.1 mg/ml Poly-L-lysine (Sigma-Aldrich)
4. PBS with 0.2% Gelatin pH 7.5
5. PBS with 3.2% paraformaldehyde
6. THE^{TM} His Tag Antibody, mAb, Mouse (Genscript)
7. Goat anti-Rabbit IgG (H+L) Secondary Antibody, Alexa Fluor 488 (Thermo Fisher)
8. ProLong Gold Antifade mountant (Thermo Fisher)
9. 1000x (100 μg/ml) DAPI (4',6-Diamidino-2-Phenylindole, Dihydrochloride) (Sigma-Aldrich)
10. Nail polish to seal coverslip to the slide

The methods outlined describe the use of the described suite of vectors to clone target genes for expression (see *Note 2*), purification, characterization, and development of gain-of-function *E. coli* strains. For simplicity, all of the results shown in **Figure 3.2** have used plasmid pDJSVT86, [8] which contains an OmpA signal sequence, ampicillin resistance, T7 promoter, and the lac operator DNA sequence for IPTG induction.

Targeted Gene Cloning:

Standard molecular cloning methods for cohesive-end ligations should be used for inserting your gene of interest into the multiple cloning site (MCS), which contain the restriction enzyme sites NotI, KpnI, XhoI, and BamHI (Plasmids pDJSVT86, pDJSVT89, pDJSVT91) and NotI, KpnI, XhoI (pDJSVT87, pDJSVT90)(**Figure 3.1**). In detail, you will generally include either a NotI or KpnI site in the design of your 5' primer, or either a KpnI, XhoI, or BamHI site in the 3' reverse primer when amplifying your gene of interest by PCR (see Note 5). For example, to clone your gene of interest using NotI and XhoI restriction sites, design your primers as follows:

Forward primer (NotI): 5' GACTAC**GCGGCCGC**gXXXXXXXXXXXXX 3'

Underlined: Extra bases added at the end of the primer to increase restriction enzyme cleavage efficiency. They don't change the construct at all and will be cleaved by the enzyme and not incorporated into the plasmid.

Bold: NotI restriction site. You need to add a single guanine nucleotide (g) after this site to keep your protein in frame for translation (See **Figure 3.1d**).

XXXXXXX: The sequence of your gene of interest. This should start with the first amino acid that comes after the predicted Sec or Tat signal sequence (*see Note 1*). We recommend making this

sequence long enough to have a melting temperature of 50-60 ˚C. Do not include the restriction site or extra 5' bases in the melting temperature determination when designing the primer.

Reverse primer (XhoI): ** This primer should be ordered 5' to 3', but we will help you first design it in the 3' to 5' orientation for simplicity:

3' XXXXXXXXXXXXXXX*TAG***CTCGAG**ATCTAG 5'

XXXXXXX: The sequence of your gene of interest. This should be the final amino acids in the protein (or final residues you want to clone). We recommend making this sequence long enough to have a melting temperature of 50-60 ˚C. Do not include the restriction site or extra 5' bases in the melting temperature determination when designing the primer.

Italics: Include a stop codon after your final amino acid encoding nucleotides.

Bold: XhoI restriction site

Underlined: Extra bases added at the end of the primer to increase restriction enzyme cleavage efficiency. They don't change the construct at all and will be cleaved by the enzyme and not incorporated into the plasmid.

For ordering from your supplier of choice, you need to reverse and complement the sequence, and the primer above would result in the following sequence:

5' CTAGAT**CTCGAG***CTA*XXXXXXXXXXXXXXX 3'

After polymerase chain reaction (PCR) with the designed primers and template DNA of your target gene, analyze 5 µl of the 50 µl reactions on a 1% agarose gel and visualize with a UV light source if using ethidium bromide in the gel. If the desired products were obtained, purify the remaining 45 µl of PCR product using a DNA spin column specific for PCR product purification.

Both the purified base vector and PCR product of your gene of interest should be digested with the proper restriction enzymes for 1-16 hours, and we recommend dephosphorylating the vector with Antarctic phosphatase as outlined in the manufacturers recommendations. Post

digestion and dephosphorylation, vector and insert should be purified using a Plasmid DNA Miniprep Kit. Purified DNA can be quantified by either analysis on an agarose gel, via NanoDrop (Thermo Scientific), or Qubit (Thermo Scientific). DNA is now ready for ligation with T4 DNA ligase (NEB), and subsequent transformation into competent DH5α or TOP10 E. coli. These strains can be made electrocompetent by a simple and robust protocol.[9] In brief, this protocol grows *E. coli* in SOC media and uses ice cold 10% glycerol to produce competent cells. We have found an alternate method by using the Mix & Go! *E. coli* Transformation Kit (Zymo Research). This has the advantage of not having to desalt ligations before transformation, as you need to do with electrocompetent cells.

After successful cloning of your construct and verification by restriction digest with enzymes used to insert the gene of interest, we recommend using Sanger sequencing to verify a correct insert with a proper in frame DNA sequence. This can be achieved by using T7 promoter and T7 Terminator primers for plasmids pDJSVT86, 89, 91, and ACYCDuetUP1 and T7 Terminator for plasmids pDJSVT87, 90.

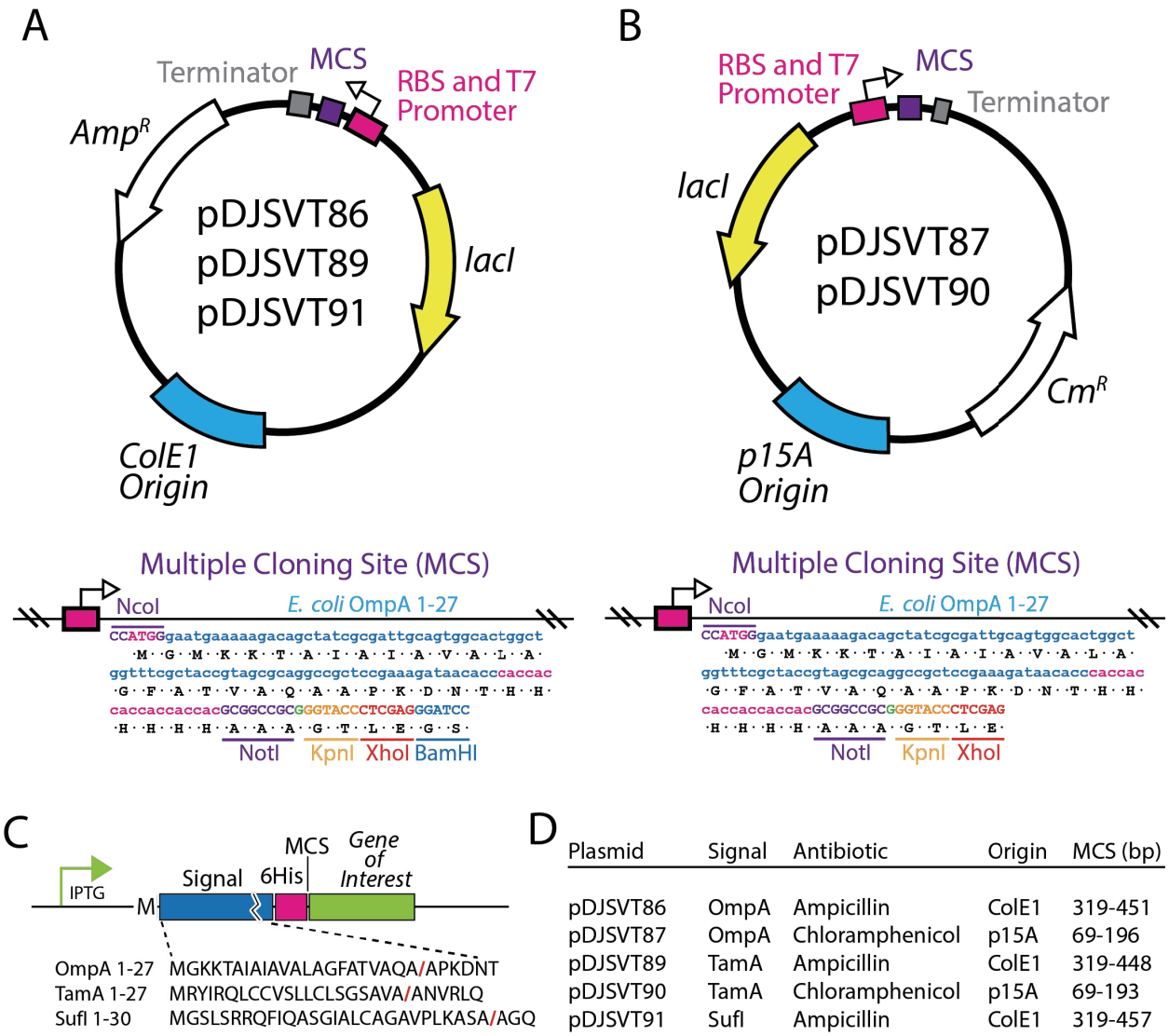

Plasmid	Signal	Antibiotic	Origin	MCS (bp)
pDJSVT86	OmpA	Ampicillin	ColE1	319-451
pDJSVT87	OmpA	Chloramphenicol	p15A	69-196
pDJSVT89	TamA	Ampicillin	ColE1	319-448
pDJSVT90	TamA	Chloramphenicol	p15A	69-193
pDJSVT91	SufI	Ampicillin	ColE1	319-457

Figure 3.1 Overview of *E. coli* expression vectors and Multiple Cloning Sites (MCS) for the production of recombinant proteins secreted to extracytoplasmic spaces. A) Overview showing features of vectors created from a pET-16b base vector. B) Overview showing features of vectors created from a pACYCduet-1 base vector. C) Representation of the protein products created by both vectors. D) Table describing vector specific features for each of the five vectors described in this chapter.

Protein Expression:

We have successfully used LB with IPTG, or ZYP-5052 auto-induction media for robust expression and purification of secreted and membrane proteins. *E. coli* have been used with success (BL21 (DE3)) for proteins secreted into the media. In addition, we found that outer membrane proteins expressed and purified well from ArcticExpress (DE3) RIL *E. coli*. While it has not been tested, combining the vectors described herein with recently reported *E. coli* strains designed specifically for robust production of outer membrane proteins could increase target protein yield.[10]

DNA from positively cloned constructs were transformed into either BL21 (DE3) or ArcticExpress (DE3) RIL *E. coli* for protein expression. A single colony was picked and transferred to a sterile tube containing five mL of LB media supplemented with carbenicillin (pDJSVT86, 89, 91) or chloramphenicol (pDJSVT87, 90) at 100 or 25 μg/ml, respectively, and grown overnight at 37 ˚C with 250 RPM shaking. Overnight growths were used to inoculate 100 mL of autoinduction media in a 500 mL baffled bottom flask (1:100 inoculation), and then grown overnight (≥ 16 hours) at 37 ˚C with 250 RPM shaking. If the yield of your protein is low, you can scale up to 1 L of media in a 4 L baffled bottom flask and follow the same protocol. In addition, if autoinduction of protein expression at 37 ˚C does not produce enough protein, we recommend using ArcticExpress (DE3) RIL *E. coli* for protein expression at 8 ˚C overnight with 25 μM IPTG added at an OD_{600}=0.6 before lowering the temperature for > 16 hours. The following morning, *E. coli* are harvested by centrifugation at 5k RCF for 15 minutes to pellet cells. Media was then poured off and sterile filtered using a 0.3 μm filter and a vacuum flask. The 100 mL of collected media was adjusted to 20 mM Tris pH 7.5 and 400 mM NaCl before purification over Ni-sepharose beads. Optionally, if larger cultures are required to yield the desired amount of protein, the pH

and salt adjusted media can then be concentrated using a Stirred ultrafiltration cell and the desired molecular weight cutoff filters (e.g. 10 kDa) to facilitate an easier purification.

Media is next incubated with 5 mL of packed Ni-sepharose beads while stirring at 4 ˚C for one hour in a glass beaker. Media and Ni-Sepharose beads are then poured into a 2.5 x 10 cm glass purification column with an adjustable flow stop cock. Allow the beads to pack into a uniform resin bed and then slowly pass the media containing your 6His tagged protein back through the resin bed to ensure efficient protein capture. Wash the beads with 100-300 mL of Ni-Sepharose wash buffer, followed by elution of your target protein in 10-20 ml of Ni-Sepharose elution buffer. Purified protein can now be further purified using ion exchange or size-exclusion chromatography on a Fast-protein liquid chromatography (FPLC) system. In addition, the initial affinity purification using Ni-Sepharose resin can be run on an FPLC. Post purification, check for yield and purity by SDS-PAGE and a bicinchoninic acid assay (BCA) or Qubit instrument. To ensure the protein is your target and contains a 6His tag, a western blot can be run using a 6His primary antibody as described below. Protein can be further concentrated for downstream experiments using Amicon spin concentrators (GE Life Sciences).

Expression and Purification of Outer Membrane Proteins:

As with all membrane proteins, there are vast differences in optimal expression and purification conditions, and we recommend reading a comprehensive review by SM Smith [11] or other sources of your choice. For the following studies, we reference a paper that addressed the purification of membrane proteins in *Campylobacter jejuni*.[12] The researchers reported that purification of outer membrane proteins using N-lauroylsarcosine (Sarkosyl) produced the purest protein, and therefore we used a hybrid strategy for the purification of FplA; a Type 5d secreted outer membrane protein that contains a 50 kDa soluble portion extracellular to the membrane.[8] This

likely makes the protein act less like a true embedded outer membrane protein, which we address during the following methods.

DNA from positively cloned constructs were transformed into either BL21 (DE3) or ArcticExpress (DE3) RIL *E. coli* for protein expression. A single colony was picked and transferred to a sterile tube containing five mL of LB media supplemented with carbenicillin (pDJSVT86, 89, 91) or chloramphenicol (pDJSVT87, 90) at 100 or 25 μg/ml, respectively, and grown overnight at 37 ˚C with 250 RPM shaking. Overnight growths were used to inoculate 100 ml of autoinduction media in a 500 mL baffled bottom flask (1:100 inoculation), and then grown overnight (≥ 16 hours) at 37 ˚C with 250 RPM shaking. If the yield of your protein is low, you can scale up to 1 L of media in a 4 L baffled bottom flask and follow the same protocol. In addition, if autoinduction of protein expression at 37 ˚C does not produce enough protein, we recommend using ArcticExpress (DE3) RIL *E. coli* for protein expression at 8 ˚C overnight with 25 μM IPTG added at an OD_{600}=0.6 before lowering the temperature for > 16 hours. The following morning, *E. coli* are harvested by centrifugation at 5k RCF for 15 minutes to pellet cells. We recommend using these pellets immediately instead of freezing as your protein of interest could be on the surface and may be sensitive to freeze thaw cycles.

Resuspend the pellet in 10 mL of *E. coli* lysis buffer per 1 gram of cell pellet and lyse on a french press or pressure cell for 5-10 passes at maximum pressure of 20,000psi. Alternatively, a sonfier could be used but is harsher on proteins. After lysis, centrifuge the lysate at 4 ˚C and 12,000 RCF for 15 minutes. Remove the supernatant and transfer to ultracentrifuge tubes for centrifugation 4 ˚C and 100,000 RCF for 1 hour. This will produce a pellet of total membranes, which should be resuspended in 10 ml of membrane pellet resuspension buffer by pipetting to resuspend pellets in all tubes and recombining into a small beaker and stirring at 4 ˚C for 1 hour to solubilize the membranes. At this point, most protocols would have you re-centrifuge this

mixture to pellet the outer membrane proteins, but we have found that our outer membrane protein with soluble extracellular domains partially fractionate into the Sarkosyl containing buffer; a trait usually reserved for inner membrane proteins. Therefore, we then dilute the 10 ml of total membrane containing buffer with 90 ml of membrane fraction dilution buffer (same at the initial lysis buffer), to bring the final concentration of Sarkosyl to 0.2%.

Protein in membrane purification buffer is next incubated with 5 mL of packed Ni-sepharose beads while stirring at 4˚C for one hour in a glass beaker. Media and Ni-Sepharose beads are then poured into a 2.5 x 10 cm glass purification column with an adjustable flow stop cock. Allow the beads to pack into a uniform resin bed and then slowly pass the media containing your 6His tagged protein back through the resin bed to ensure efficient protein capture. Wash the beads with 100-300 ml of Ni-Sepharose membrane wash buffer, followed by elution of your target protein in 10-20 ml of Ni-Sepharose membrane elution buffer. Purified protein can now be further purified using ion exchange or size-exclusion chromatography on a Fast-protein liquid chromatography (FPLC) system. In addition, the initial affinity purification using Ni-Sepharose resin can be run on an FPLC. Post purification, check for yield and purity by SDS-PAGE and a bicinchoninic acid assay (BCA) or Qubit instrument. To ensure the protein is your target and contains a 6His tag, a western blot can be run using a 6His primary antibody as described below. To further concentrate protein for downstream experiments, we recommend using Amicon Ultra Centrifugal Filter Units (GE Life Sciences).

Immunoblotting:

To detect the production of secreted, periplasmic, or outer membrane proteins using the vectors described here, we recommend taking advantage of the N-terminal 6His tag that remains on the

proteins after passing through the Sec or Tat secretion systems. In addition, you can also use antibodies specific for your protein of interest using the following protocol:

In brief, separate the desired protein purification fractions or purified proteins by SDS-PAGE using a pre-cast 4-20% gel. Load 5 μL of Color Prestained Protein Standard, Broad Range (11–245 kDa) to the gel to ensure that you can identify the molecular weight of your target protein by western blot. Transfer proteins to a methanol activated Polyvinylidene difluoride (PVDF) membrane using western blot transfer buffer. Post transfer, incubate the membrane in 10 mL of blocking buffer (TBST 3% BSA) in a plastic container (ensure the blot is submerged) for >2 hours with gently rocking at room temperature or overnight at 4 ˚C. Remove the blocking buffer and add in 10 mL of a 1:1000 dilution of THE™ His Tag Antibody, mAb, Mouse (Genscript) in blocking buffer. Incubate for 1 hour at room temperature with light rocking. Discard of the primary antibody solution and wash extensively with TBST. Add in 10 mL of a 1:5000 dilution of Anti-mouse m-IgGκ BP-HRP secondary antibody (Santa Cruz) in blocking buffer. Incubate for 1 hour at room temperature with light rocking. Discard the secondary antibody solution and wash extensively with TBST. Remove the membrane from the TBST wash solution and place on a flat surface covered in aluminum foil. Add 3 ml of properly mixed ECL western blotting substrate and ensure that the entire blot is covered in liquid for ~3 minutes. Carefully pick up the blot with tweezers and transfer to a western blot developing cassette. Use either Lucent Blue X-ray film or a digital gel and blot imaging system to visualize 6His tagged proteins on the gel.

Immunofluorescence Microscopy of Outer Membrane Proteins:

We provide a protocol for visualizing 6His tagged domains on the surface of *E. coli* using the commercially available THE™ His Tag Antibody, mAb, Mouse (Genscript). In addition, you can also use antibodies specific for your protein of interest using the following protocol:

DNA from positively cloned constructs were transformed into either BL21 (DE3) or ArcticExpress (DE3) RIL *E. coli* for protein expression. A single colony was picked and transferred to a sterile tube containing five mL of LB media supplemented with carbenicillin (pDJSVT86, 89, 91) or chloramphenicol (pDJSVT87, 90) at 100 or 25 µg/ml, respectively, and grown overnight at 37 ˚C with 250 RPM shaking. Overnight growths were used to inoculate 100 ml of autoinduction media in a 500 mL baffled bottom flask (1:100 inoculation), and then grown overnight (≥ 16 hours) at 37 ˚C with 250 RPM shaking. In addition, if autoinduction of protein expression at 37 ˚C does not produce enough protein, we recommend using ArcticExpress (DE3) RIL *E. coli* for protein expression at 8 ˚C overnight with 25 µM IPTG added at an OD_{600}=0.6 before lowering the temperature for > 16 hours. The following morning, *E. coli* are back diluted to OD_{600}=0.2 and 1 mL is centrifuged at 5,000 RCF for five minutes. The pelleted bacteria are washed twice with 500 µL of PBS 0.2% Gelatin pH 7.5 followed by centrifuging at 5,000 RCF for five minutes. Resuspend cells in 500 µL of PBS with 3.2% paraformaldehyde and fix for 20 minutes. Concurrently, incubate round 10 mm #1.5 coverslips with 0.1mg/mL poly-L-lysine for 20 minutes at room temperature. After bacteria are fixed, transfer a single coverslip to a 12 well plate and then place the 500 µL of bacteria into the well on top of the coverslip. Next, add 2 mL of PBS to the well and swirl to make sure the coverslip is submerged. Transfer the 12 well plate into a swinging bucket centrifuge and pellet bacteria onto coverslips at 2,000 RCF for 10 minutes. Post-centrifugation, transfer coverslips to a fresh well in a 12 well plate and wash the coverslip 2x with 2 mL of PBS 0.2% Gelatin pH 7.5.

Prepare a 100 µL solution of 1:100 dilution of your antibody of choice (THE™ His Tag Antibody, mAb, Mouse Genscript) in PBS 0.2% Gelatin pH 7.5. Place 20 µl of the solution on a piece of parafilm, and invert the coverslip on the antibody solution for one hour at room temperature. To maintain moisture, place a small container over the coverslip with a wet sponge

taped to the lid. After incubation in primary antibody, transfer the coverslip bacteria up into a new well in a 12 well plate and wash 2x with PBS 0.2% Gelatin pH 7.5. Next, add 1 ml of PBS 0.2% Gelatin to each well and add 2 drops from the dropper of Goat anti-Rabbit IgG (H+L) Secondary Antibody, Alexa Fluor 488. Incubate at room temperature for 30 minutes, followed by two washes with 2 mL of PBS 0.2% Gelatin pH 7.5, and two washes with 2 mL of PBS pH 7.5. Add 4 µL of ProLong Gold Antifade mountant to a glass slide and invert the cover slip on top. Gently press down and remove excess liquid from the edges of a coverslip with a delicate task wipe. Seal the coverslip to the slide with nail polish around the edges. Store the slide in a dark case until you are ready to image.

Image the fluorescently green labeled bacteria using a fluorescent microscope and either a GFP or FITC filter under 63x or 100x magnification. Obtaining images using either brightfield or phase contrasts (better) will help to determine the percentage of cells that expressed your protein in the outer membrane. Representative results can be seen in **figure 3.2**.

Notes

1. Web servers for signal peptide prediction: PREDTAT (http://www.compgen.org/tools/PRED-TAT/submit), SignalP: We find the most accurate predictions use SignalP v 3.0 with the Hidden Markov Model (HMM) option selected (http://www.cbs.dtu.dk/services/SignalP-3.0/)
2. Plasmids presented in Figure 1 are available through Addgene (www.addgene.org/Daniel_Slade/) as outlined in **Table 1**, and all sequences and details of plasmids and their development can be found on our Open Science Framework (https://osf.io/n7tmj/) data repositories.

3. Note that these plasmid were created to maximize cloning efficiency for AT rich genomes by utilizing the GC rich restriction enzyme sites NotI (GCGGCCGC), KpnI (GGTACC), XhoI (CTCGAG).
4. These vectors can also be used for expression of cytoplasmic proteins by cloning into the vector using the NcoI site located 5' of the signal sequence DNA. The NotI, KpnI, or XhoI site can then be used as the 3' restriction site. Note, this will also remove the 6His tag located in the vector. This will also partially revert the plasmids back to their parent vectors of pET-16b (pDJSVT86, 89, 91) and pACYCDuet-1 (pDJSVT87, 90)
5. We prefer to clone all of our genes through polymerase chain reaction (PCR), but users can also choose to synthesize genes if desired, which would allow for codon optimization in *E. coli*.

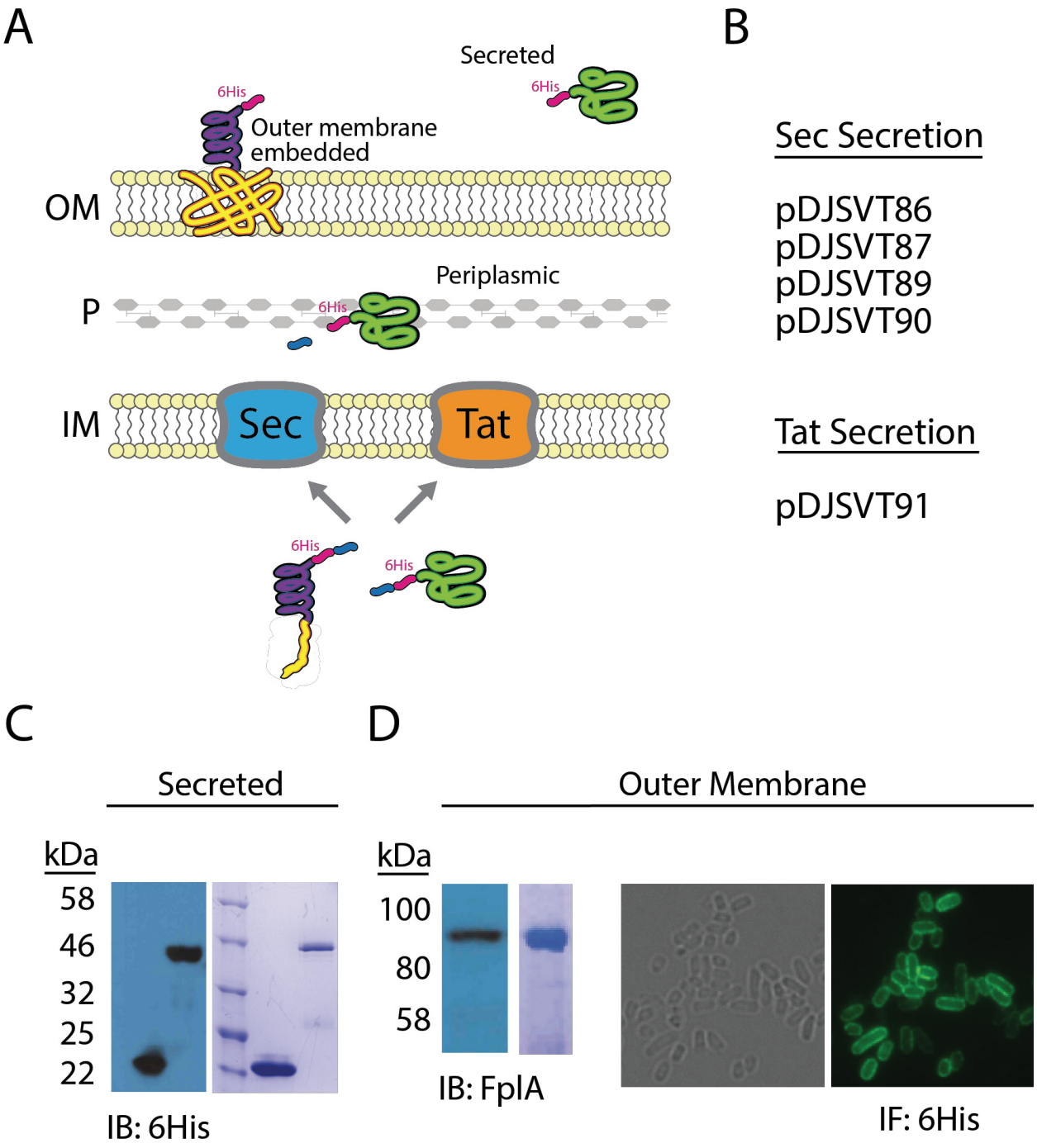

Figure 3.2: Expression of recombinant, extracytoplasmic proteins in *E. coli* using a suite of vectors described herein. A) Overview of protein export and the potential sub- and extracellular location of proteins. B) Description of vectors and the secretion systems used by each. C) Detection by 6His western blot and purification of two secreted proteins directly from the media of an overnight autoinduction growth. D) Immunoblot detection and purification of the *Fusobacterium nucleatum* outer membrane protein FplA, and detection of its expression on the surface of *E. coli* as detected by immunofluorescence using the same FplA antibody used in the immunoblot.

Acknowledgements

Research was supported by startup funding from the Department of Biochemistry at Virginia Tech, the Institute for Critical Technology and Applied Science (ICTAS) at Virginia Tech, and the National Institute for Food and Agriculture.

Author Contributions

MAC and DJS designed, performed, analyzed experiments, and wrote the manuscript.

Competing Interests

The authors declare that they have no conflicts of interest with the contents of this article.

References

1. Lee VT, Schneewind O. Protein secretion and the pathogenesis of bacterial infections. Genes Dev. 2001;15: 1725–1752.
2. Green ER, Mecsas J. Bacterial Secretion Systems: An Overview. In: Kudva IT, Cornick NA, Plummer PJ, Zhang Q, Nicholson TL, Bannantine JP, et al., editors. Virulence Mechanisms of Bacterial Pathogens, Fifth Edition. American Society of Microbiology; 2016. pp. 215–239.
3. Dautin N, Bernstein HD. Protein secretion in gram-negative bacteria via the autotransporter pathway. Annu Rev Microbiol. 2007;61: 89–112.
4. Natale P, Brüser T, Driessen AJM. Sec- and Tat-mediated protein secretion across the bacterial cytoplasmic membrane--distinct translocases and mechanisms. Biochim Biophys Acta. 2008;1778: 1735–1756.
5. van den Berg B. Crystal structure of a full-length autotransporter. J Mol Biol. 2010;396: 627–633.
6. Auclair SM, Bhanu MK, Kendall DA. Signal peptidase I: cleaving the way to mature proteins. Protein Sci. 2012;21: 13–25.
7. Studier FW. Protein production by auto-induction in high density shaking cultures. Protein Expr Purif. 2005;41: 207–234.
8. Casasanta MA, Yoo CC, Smith HB, Duncan AJ, Cochrane K, Varano AC, et al. A chemical and biological toolbox for Type Vd secretion: Characterization of the phospholipase A1 autotransporter FplA from Fusobacterium nucleatum. J Biol Chem. 2017; doi:10.1074/jbc.M117.819144
9. Woodall CA. Electroporation of E. coli. Methods Mol Biol. 2003;235: 55–69.
10. Meuskens I, Michalik M, Chauhan N, Linke D, Leo JC. A New Strain Collection for

Improved Expression of Outer Membrane Proteins. Front Cell Infect Microbiol. 2017;7: 464.
11. Smith SM. Strategies for the purification of membrane proteins. Methods Mol Biol. 2011;681: 485–496.
12. Hobb RI, Fields JA, Burns CM, Thompson SA. Evaluation of procedures for outer membrane isolation from Campylobacter jejuni. Microbiology. 2009;155: 979–988.

Chapter 4

A chemical and biological toolbox for Type Vd secretion: Characterization of the phospholipase A1 autotransporter FplA from *Fusobacterium nucleatum*

Michael A. Casasanta[1], Christopher C. Yoo[1], Hans B. Smith[1], Alison J. Duncan[1], Kyla Cochrane[2], Ann C. Varano[3], Emma Allen-Vercoe[4], Daniel J. Slade[1]

1. Virginia Polytechnic Institute and State University, Department of Biochemistry, Blacksburg, VA, USA.

2. British Columbia Cancer Agency Genome Sciences Centre, University of British Columbia Department of Medical Genetics, Simon Fraser University Department of Biochemistry and Molecular Biology, Vancouver, British Columbia, Canada.

3. Virginia Tech Carilion Research Institute, Roanoke, VA, USA.

4. Molecular and Cellular Biology, University of Guelph, Guelph, Ontario, N1G 2W1 Canada

*Correspondence: Dr. Daniel J. Slade, Department of Biochemistry, Virginia Polytechnic Institute and State University, Blacksburg, VA 24061. Telephone: +1 (540) 231-2842. Email: dslade@vt.edu

Abstract

Fusobacterium nucleatum is an oral pathogen that is linked to multiple human infections and colorectal cancer. Strikingly, *F. nucleatum* achieves virulence in the absence of large, multi-protein secretion systems (Type I, II, III, IV, and VI) which are widely used by Gram-negative bacteria for pathogenesis. By contrast, *F. nucleatum* strains contain genomic expansions of Type V secreted effectors (autotransporters) that are critical for host cell adherence, invasion, and biofilm formation. Here we present the first characterization of a *F. nucleatum* Type Vd phospholipase class A1 autotransporter (strain ATCC 25586, gene FN1704) that we hereby rename *Fusobacterium* phospholipase autotransporter (FplA). Biochemical analysis of multiple *Fusobacterium* strains revealed that FplA is expressed as a full-length 85 kDa outer membrane embedded protein, or as a truncated phospholipase domain that remains associated with the outer membrane. While the role of Type Vd secretion in bacteria remains unidentified, we show that FplA binds with high affinity to host phosphoinositide signaling lipids, revealing a potential role for this enzyme in establishing a *F. nucleatum* intracellular niche. To further analyze the role of FplA we developed an *fplA* gene knockout strain, which will guide future *in vivo* studies to determine its potential role in *F. nucleatum* pathogenesis. In summary, using recombinant FplA constructs we have identified a biochemical toolbox that includes lipid substrates for enzymatic assays, potent inhibitors, and chemical probes to detect, track, and characterize the role of Type Vd secreted phospholipases in Gram-negative bacteria.

Introduction

Fusobacterium nucleatum is an emerging oral pathogen that is involved in periodontitis[1], and also readily disseminates, presumably through hematogenous spread[2,3], to cause potentially fatal infections of the brain[4], liver[5], lungs[6], heart[7], appendix[8], and amniotic fluid where it causes preterm birth[2,9,10]. Recent studies have uncovered a correlation between colorectal cancer tumors and an overabundance of *F. nucleatum* present in diseased tissue[11–13]. Subsequent studies confirmed a potential causative effect for *F. nucleatum* in tumor formation using an APC $^{min/-}$ mouse model of accelerated CRC pathogenesis[14]. In addition, human patients that had the highest detected levels of *F. nucleatum* within tumors had the lowest survival rate[15]. Invasive *F. nucleatum* strains can enter into epithelial and endothelial cells[16,17], which induces the secretion of proinflammatory cytokines that drive local inflammation as seen in colorectal cancer[14]. Previously characterized proteins involved in host cell binding and invasion include FadA (ATCC 25586, gene FN0264), a small helical adhesin that binds to E-cadherin and modulates prevalent colorectal cancer signaling pathways[18,19]; Fap2 (ATCC 25586, gene FN1449), a galactose inhibitable Type Va secreted autotransporter adhesin that binds Gal-GalNAc sugars[3,20–22]; and RadD (ATCC 25586, gene 1526), an arginine inhibitable Type Va autotransporter adhesin[20,23]. *F. nucleatum* also induces the production of human β-defensin 2 and 3 (hBD2, hBD3), which are secreted, cationic antimicrobial peptides that act as chemo-attractants to modulate adaptive immunity[24,25].

F. nucleatum is unique in that it does not harbor large, multi-protein secretion systems (Types I-IV, VI, and IX) to establish infections and alter host-signaling for survival[26]. However, invasive strains of *F. nucleatum* contain an overabundance of uncharacterized proteins containing type II membrane occupation and recognition nexus (MORN2) domains, and a genomic expansion of Type V secreted effectors known as autotransporters[17]. Autotransporters are large outer

membrane and secreted proteins that are divided into 5 classes (Type Va-Ve) based on their domain architecture, and are critical proteins in host cell adherence, invasion, and biofilm formation[27–30]. Autotransporter biogenesis and folding is driven by initial translocation through the SEC apparatus in the inner membrane, followed by the insertion of a C-terminal β-barrel domain in the outer membrane[30,31]. In a process that requires multiple chaperones (e.g. BAM complex), the large N-terminal passenger domains is that presented on the surface or cleaved and secreted after β-barrel translocation. The recent biochemical and structural characterization of the type Vd autotransporter PlpD from *Pseudomonas aeruginosa* revealed a secreted N-terminal patatin-like protein (PFAM: PF01734) with an α-β hydrolase fold containing a catalytic dyad (Ser, Asp) conferring phospholipase A1 activity (EC 3.1.1.32) through the hydrolysis of glycerophospholipid moieties at the *sn*-1 position to release a fatty acid[32,33]. In addition, PlpD contains a 16-strand C-terminal β-barrel domain of the bacterial surface antigen family (PFAM: PF01103) for outer membrane anchorage, and a (POTRA) domain potentially involved in protein folding and export of the phospholipase domain to the surface. The PlpD secreted phospholipase domain was able to disrupt liposomes and was also shown to bind the phosphoinositide class of human intracellular signaling lipids[34]. Our anlysis revealed that most *F. nucleatum* genomes each contain one gene (in strain ATCC 25586, gene FN1704, UniProtKB-Q8R6F6 - herein renamed *fplA*) encoding for a previously uncharacterized ~85 kDa type Vd autotransporter that is homologous to PlpD. Bioinformatic analysis of *F. nucleatum* strains reveals that most strains also contain a single gene encoding for an additional small patatin domain containing protein (~32 kDa) (FN0508, UniProtKB-Q8R6A1) that is not a Type Vd autotransporter and does not contain a predicted signal sequence for export from the bacterial cytoplasm.

While the role of Type Vd secreted phospholipases has not been determined, bacterial phospholipases play critical roles in the virulence of intracellular bacteria by promoting

phagosome survival, or by aiding in vacuole lysis to achieve liberation into the cytoplasm and subversion of host lysosomal induced death[35,36]. Bacterial pathogens including *Helicobacter*, *Listeria*, *Salmonella*, *Shigella*, *Pseudomonas, and Legionella* rely on phospholipases for virulence, survival, and some for intercellular spread[36]. PldA1 from *Helicobacter pylori* is a phospholipase that is involved in growth at low pH[37], colonization of the gastric mucosa[38], and hemolytic activity[38]. *Listeria monocytogenes* secretes two phospholipase C proteins (PI-PLC and PC-PLC) that are critical for late time point evasion of autophagy and establishment of an intracellular niche[39].

Here we present studies that probe the molecular mechanisms of the Type Vd secreted autotransporter phospholipase FplA using a diverse set of chemical and biological tools. These experiments have strengthened our understanding of the Type Vd secretion, and will aid in determining the role of FplA in *F. nucleatum* pathogenesis.

Materials and Methods

Bacterial Strains, Growth Conditions, and Plasmids:

Unless otherwise indicated, *E. coli* strains were grown in LB at 37°C aerobically, and *F. nucleatum* strains were grown in CBHK (Columbia Broth, hemin (5 µg/mL) and menadione (0.5 µg/mL)) at 37°C in an anaerobic chamber (90% N_2, 5% CO_2, 5% H_2). Where appropriate, antibiotics were added at the indicated concentrations: carbenicillin 100 µg/mL; thiamphenicol 5 µg/mL (CBHK plates), 2.5 µg/mL (CBHK liquid). For taxonomy verification of *Fusobacterium*, PCR amplification of a 1502bp region of the 16S rRNA gene sequence was carried out using the universal primers U8F and U1510R (**Table 4.3**) as previously described[40]. Sanger sequence analysis was carried out at the Advanced Analysis Center at the University of Guelph. Obtained DNA sequences were compared to the GenBank database (NCBI) using BLASTn.

Bioinformatic Analysis of FplA in Multiple *Fusobacterium* Strains:

The genome sequence of *F. nucleatum* strain ATCC 25586 (GenBank accession NC_003454.1) was used to predict all open reading frames using the Prodigal Bacterial Gene Prediction Server[41]. An open reading frame encoding for a 760 amino acid protein was identified using a HMMER model built from a seed alignment of the PFAM (EMBL-EBI website) patatin family (PF01734) and the stand alone HMMER 3.1 software package[42]. The identified gene contained an N-terminal patatin domain conferring phospholipase activity and a C-terminal bacterial surface antigen domain (PFAM: PF01103) that encodes for an outer membrane β-barrel domain. Cross referencing revealed this gene is FN1704 in *F. nucleatum* ATCC 25586, which was incorrectly predicted to be a serine protease in both the KEGG and Uniprot databases. The same method was used to search multiple *Fusobacterium* genomes resulting in the identification of only one protein with this structure in each strain. A PSI-BLAST search using FplA returned a close match to the

Pseudomonas aeruginosa protein PlpD, which was previously characterized as a class A1 phospholipase and labeled as the first in a new class of type Vd autotransporters[32,33]. Alignment of FplA proteins from seven strains of *Fusobacterium* shown in **Fig. 4.12** was performed using Geneious version 9.0.2[43].

Structure Prediction to Identify Domain Boundaries and Catalytic Residues in FplA:

Structure prediction was performed using the FplA sequence from *F. nucleatum* strain 25586 and the SWISS-MODEL Workspace[44]. Results showed a close match of the N-terminal phospholipase domain to PlpD from *Pseudomonas aeruginosa* (PDB: 5FYA) and the C-terminal POTRA and β-barrel domains to BamA from *Haemophilus ducreyi* (PDB: 4K3C) (**Fig. 4.1-4.2**). A composite predicted structure was assembled using the predicted phospholipase, POTRA, and β-barrel domain, which has the phospholipase domain exposed on the surface of the bacteria, which we confirmed biochemically as a recombinant protein in *E. coli* and a native protein in *F. nucleatum*. In addition, the modeled FplA phospholipase domain was aligned with ExoU (PDB: 4AKX) and VipD (PDB: 4AKF) (**Fig. 4.3**). Active site residues in FplA were identified as S98 and D243, and these were verified by multiple enzymatic and chemical biology methods presented in **Fig. 4.4** and **Fig. 4.6**. In close proximity to the active site is the oxyanion hole comprised of three consecutive glycine residues (G69, G70, G71). Graphical representations and alignments of all predicted structures were created using PyMOL Molecular Graphics System, Version 1.7.3 Schrödinger, LLC.

Cloning of FplA Constructs for Expression in *E. coli*:

All primers were ordered from IDT DNA and all plasmids and bacterial strains either used or created for these studies are described in **Table 4.1** (Bacterial Strains), **Table 4.2** (Plasmids), and **Table 4.3** (Primers). All restriction enzymes and T4 DNA Ligase, and Antarctic Phosphatase were from NEB (MA, USA). DNA purifications kits were from BioBasic (Markham, ON). Genomic DNA for *F. nucleatum* ATCC 25586 was purchased from ATCC (VA, USA) and used to create all recombinant FplA constructs for expression described herein. pET16b was used as the base expression vector for *E.coli* expression of FplA constructs. PCR products were then spin column purified and digested overnight at 37˚C with restriction enzymes described in **Table 4.3**. Digested PCR products were spin column purified and ligated by T4 DNA ligase into pET16b vector that had been restriction enzyme and Antarctic Phosphatase treated according to the manufacturer's recommended protocol. Ligations were transformed into Mix & Go! (Zymo Research, USA) competent *E. coli* and plated on LB 100 μg/ml carbenicillin (ampicillin), followed by verification of positive clones by restriction digest analysis using purified plasmid. Positive clones were then transformed into LOBSTR RIL[45] *E. coli* cells for protein expression.

Specifically, pDJSVT84 ($FplA_{20-350}$), pDJSVT43 ($FplA_{20-431}$), pDJSVT85 ($FplA_{60-350}$), and pDJSVT82 ($FplA_{60-431}$) all produce proteins with a C-terminal 6x-Histidine tag and are expressed in the cytoplasm because these constructs lack the N-terminal signal sequence used to export FplA through the Sec apparatus in *F. nucleatum*. pDJSVT60 ($FplA_{20-431}$ S98A) and pDJSVT61 ($FplA_{20-431}$ D243A) were created by using pDJSVT43 as a template for Quikchange mutagenesis PCR. Verification of mutants and all clones was performed by Sanger sequencing (Genewiz, USA). To facilitate the export of FplA to the surface of *E. coli*, a new inducible expression vector was created using pET16b as the backbone by incorporating the signal sequence from the *E. coli* protein OmpA (residues 1-27). In addition, this expression vector (pDJSVT86) contains an N-terminal 6x-

Histidine tag that remains on the expressed protein after residues 1-21 from OmpA are cleaved in the periplasm. This effectively creates an inducible vector for the expression of periplasmic and outer membrane proteins in *E. coli* that was customized with GC rich restriction sites (NotI, KpnI, XhoI) to facilitate enhanced cloning of AT rich (74%) genomes such as *F. nucleatum*. Using the pDJSVT86 expression vector, pDJSVT88 ($OmpA_{1-27}$, 6xHis, $FplA_{20-760}$) was created and shows efficient export of enzymatically active, full-length FplA to the surface of *E. coli* (**Fig. 4.8**).

Strain	Bacterial Species	Relevant genotype	Source or Reference
TOP10	*E. coli*	*mcrA*, Δ(*mrr-hsdRMS-mcrBC*), Phi80(*del*)*M15*, Δl*acX74*, *deoR*, *recA1*, *araD139*, Δ(*ara-leu*)7697, *galU*, *galK*, *rpsL*(*SmR*), *endA1*, *nupG*	Invitrogen
LOBSTR-BL21(DE3)-RIL	*E. coli*	*fhuA2* [*lon*] *ompT gal* (λ *DE3*) [*dcm*] Δ*hsdS* λ DE3 = λ *sBamHIo* Δ*EcoRI-B* *int::(lacI::PlacUV5::T7 gene1) i21 Δnin5 arnA*(H359S, H361S, H592S, H593S) *slyD*(1-150)	[45]
F. nucleatum nucleatum ATCC 23726	*F. nucleatum*	Wild Type	ATCC, [17,46–48]
DJSVT01	*F. nucleatum*	*F. nucleatum* ATCC 23726 Cm^r Tm^r ΔFN1704::*catP*	This Study
F. nucleatum nucleatum ATCC 25586	*F. nucleatum*	Wild Type	ATCC, [17,46–48]
F. nucleatum polymorphum 10953	*F. nucleatum*	Wild Type	ATCC, [17,46–48]
F. nucleatum vincentii ATCC 49256	*F. nucleatum*	Wild Type	ATCC, [17,46–48]
F. nucleatum vincentii 4_1_13	*F. nucleatum*	Wild Type	[17]
F. nucleatum animalis 4_8	*F. nucleatum*	Wild Type	[17]
F. nucleatum animalis 7_1	*F. nucleatum*	Wild Type	[17]

Table 4.1 Bacterial strains used for this study.

Plasmid	Description	Reference
pET16b	*E. coli* inducible expression vector	EMD Millipore
pJIR750	Base *C. perfringens-E. coli* shuttle vector to make *F. nucleatum* shuttle vectors.	[49]
pDJSVT43	*F. nucleatum* 25586 FN1704 (*fplA*) 20-431 C-6xHis cloned into pET16b	This Study
pDJSVT60	*F. nucleatum* 25586 FN1704 (*fplA*) 20-431 S98A C-6xHis cloned into pET16b	This Study
pDJSVT61	*F. nucleatum* 25586 FN1704 (*fplA*) 20-431 D243A C-6xHis cloned into pET16b	This Study
pDJSVT82	*F. nucleatum* 25586 FN1704 (*fplA*) 60-431 C-6xHis cloned into pET16b	This Study
pDJSVT84	*F. nucleatum* 25586 FN1704 (*fplA*) 20-350 C-6xHis cloned into pET16b	This Study
pDJSVT85	*F. nucleatum* 25586 FN1704 (*fplA*) 60-350 C-6xHis cloned into pET16b	This Study
pDJSVT86	*E. coli* inducible expression vector - pET16b with *E.coli* OmpA signal sequence (residues 1-27) followed by a 6xHis tag and multiple cloning site.	This Study
pDJSVT88	*F. nucleatum* 25586 FN1704 (*fplA*) 20-760 cloned into pDJSVT86 for expression of full length FplA on the surface of *E. coli*	This Study
pDJSVT100	Shuttle vector to make strain DJSVT01 (*Table S1*): *F. nucleatum* ATCC 23726 ΔFN1704::*catP* (*Cm*^{r} *Tm*^{r})	This Study

Cm^r = Chloramphenicol resistance

Tm^r = Thiamphenicol resistance

Table 4.2. Plasmids used in this study

Primer	Sequence 5' to 3'	Direction	Restriction Site	Tag	FplA Construct	Strain/Plasmid (*Table S1, S2*)
prDJSVT95	GCACTACCCATGGAAAATAT CGAATTAAAATCAAGAG	Forward	NcoI		AA 20-350, 20-431	pDJSVT43, pDJSVT84
prDJSVT96	CTAGTTCTCGAGTTAATGATG ATGATGATGATGTGCTTTTTC TCCATCTAAATATAAAAC	Reverse	XhoI	6xHis	AA 20-431, 60-431	pDJSVT43, pDJSVT82
prDJSVT135	CTATATAACAGGTACTGCTAT AGGAGCCTTTATTG	Forward			QuikChange: AA 20-431 S98A	pDJSVT60
prDJSVT136	CAATAAAGGCTCCTATAGCA GTACCTGTTATATAG	Reverse			QuikChange: AA 20-431 S98A	pDJSVT60
prDJSVT137	GGAAATATATGTTGCTGGTCT TGTTAGTAG	Forward			QuikChange: AA 20-431 D243A	pDJSVT61
prDJSVT138	CTACTAACAAGACCAGCAAC ATATATTTCC	Reverse			QuikChange: AA 20-431 D243A	pDJSVT61
prDJSVT153	CTAGTTCTCGAGTTAATCTAA TTTATATCCAATTG	Reverse	XhoI		OmpA 1-27 FplA 20-760	pDJSVT88
prDJSVT203	GCACTACGCGGCCGCGGAAA ATATCGAATTAAAATCAAGA G	Forward	NotI		OmpA 1-27 FplA 20-760	pDJSVT88
prDJSVT211	GCACTACCCATGGGAAATTT AAAAGTTGCTCTAGTTTTAAG	Forward	NcoI		AA 60-350, 60-431	pDJSVT82
prDJSVT214	CTAGTCTCGAGTTAGTGGTGG TGGTGGTGGTGCTTTTTATTA TCAGCTTTAGC	Reverse	XhoI	6xHis	AA 20-350, 60-350	pDJSVT84, pDJSVT85
prDJSVT215	GAGATATACCATGGGAATGA AAAAGACAGCTATCGCG	Forward	NcoI		OmpA 1-27 vector	pDJSVT86
prDJSVT216	GATCCTCGAGGGTACCCGCG GCCGCGTGGTGGTGGTGGTG GTGGGTGTTATCTTTCGGAG	Reverse	NotI, KpnI, XhoI	6xHis	OmpA 1-27 vector	pDJSVT86
prDJSVT259	GCATCGAATTCGAGATGTTGC TAAAATTTTAATAG	Forward	EcoRI		KO vector for strain 23726 Δ*fplA*	pDJSVT100
prDJSVT260	CGTAGCACTAGTCTAGAAAA CTTTGAAAGTACAC	Reverse	SpeI		KO vector for strain 23726 Δ*fplA*	pDJSVT100
prDJSVT295	CATTTTTAGCAGATTATGAAA GTG	Reverse			*catP* primer to confirm pDJSVT100 and Δ*fplA*	Strain DJSVT01
U8F	AGAGTTTGATYMTGGCTCAG	Forward			16s rRNA for *F. nucleatum* verification	*Fusobacterium* strains
U1510R	GGTTACCTTGTTACGACTT	Reverse			16s rRNA for *F. nuc.* verification	*Fusobacterium* strains

Table 4.3. Primers used for this study.

FplA Protein Expression and Purification:

Briefly, all FplA constructs in LOBSTR RIL[45] *E. coli* cells were grown in Studier auto-induction media[50] (ZYP-5052, 0.05% glucose, 0.5% lactose, 0.5% glycerol) at 37 ˚C, 250 rpm shaking, and harvested at 20 hours post inoculation by pelleting at 5 kG for 15 minutes at 4˚C. Pellets were weighed and resuspended in lysis buffer (20 mM tris pH 7.5, 20 mM imidazole, 400 mM NaCl, 0.1 % BOG, 1 mM PMSF) at 10 mL/gram of cell pellet. Bacteria were lysed by using 5 passes on an EmulsiFlex-C3 (Avestin, Germany), followed by removal of insoluble material and unlysed cells by pelleting at 15 kG for 15 minutes at 4˚C. The resulting supernatant containing 6xHis-tagged FplA constructs were gently stirred with 5 mL of $NiCl_2$ charged chelating sepharose beads (GE Healthcare, USA) for 30 minutes at 4˚C, followed by washing with 200 mL of wash buffer (20 mM Tris pH 7.5, 50 mM Imidazole, 400 mM NaCl, 0.1% BOG). After washing, FplA was eluted in 10 mL of elution buffer: (20 mM Tris pH 7.5, 250 mM Imidazole, 50 mM NaCl, 0.1% BOG). This protein was directly applied to a HiTrap Q FP anion exchange column (FplA construct theoretical PIs: 5.91-6.34) and purified on an ÄKTA pure system (GE Healthcare, USA) using a linear gradient between Buffer A (20 mM Tris, pH 8, 50 mM NaCl, 0.025% BOG) and Buffer B (20 mM Tris, pH 8, 1 M NaCl, 0.025% BOG). Fractions containing FplA as determined by SDS-PAGE analysis were pooled and further purified on a HiPrep 16/60 Sephacryl S-200 HR size exclusion column (GE Healthcare, USA) in 20 mM Tris pH 7.5, 150 mM NaCl, 10% glycerol. Protein concentrations were determined using a Qubit fluorimeter and BCA assays according to the manufacturer's recommended protocol. Protein purity was determined using ClearPage 4-20% gradient gels (CBS Scientific, USA) and determined to be greater than 95% pure for all constructs.

Antibody Production and Western Blotting to Detect FplA:

Purified $FplA_{20-431}$ was used to create a polyclonal antibody in rabbits (New England Peptide, USA). To purify the antibody, $FplA_{20-431}$ was coupled to CNBr-Activated Sepharose (Bioworld, USA) and Anti-$FplA_{20-431}$ antisera adjusted to pH 8.0 with 20 mM Tris-HCl was passed through the column to bind $FplA_{20-431}$ antibodies, followed by extensive washing in phosphate buffered saline (PBS) and elution in 2.7 mL of 100 mM Glycine, pH 2.8. To the eluted antibodies, 0.3 mL of 1M Tris-HCl pH 8.5 was added, for a final storage buffer of (10 mM Glycine, 100 mM Tris-HCl, pH 8.5).

For western blot detection of FplA, proteins were separated by SDS PAGE and subsequently transferred to PVDF membranes, blocked in 20 mL of TBST (20 mM Tris, 150 mM NaCl, 0.1% Tween 20) with 3% BSA for 15 hrs at 4˚C. After blocking, the membranes were incubated with rabbit anti-FplA antibody (1:10,000 for pure proteins, 1:2,500-1:1000 whole cells or lysates) in TBST 3% BSA for 1 hour (70 rpm shaking, 26˚C). After incubating with the primary antibody the membrane was washed with TBST, followed by incubation with goat anti-rabbit-HRP secondary antibody (Cell Signaling, USA) at 1:10,000 dilution in TBST 3% BSA for 30 minutes (70 rpm shaking, 26˚C). After the secondary antibody incubation, the membrane was washed in TBST, followed by incubation with ECL-Plus blotting reagents (Pierce, USA) and visualization using Lucent Blue X-ray film (Advansta, USA) developed on an SRX-101A medical film processor (Konica, Japan).

Development of an *F. nucleatum* 23726 ΔfplA Strain:

Single-crossover homologous recombination gene knockouts *F. nucleatum* 23726 have been previously reported, although like with all *Fusobacterium* mutagenesis strategies, efficiencies are quite low. Based on a previous method[51], we created an integration plasmid that will not

replicate in *F. nucleatum*, therefore only producing antibiotic resistant colonies for strains that incorporate the plasmid directly into the chromosome in the gene of interest during transformation and outgrowth. A central 1000bp region in the FN1704 (*fplA)* gene in *F. nucleatum* 23726 was amplified from genomic DNA by PCR, digested with *EcoRI* and *SpeI*, and ligated into pJIR750 that was digested with the same enzymes and subsequently treated with Antarctic phosphatase. The ligation was transformed into Mix & Go! competent *E. coli*, and plated on LB 10 μg/mL chloramphenicol, followed by selection of colonies, purification of plasmid DNA, and verification of positive clones by restriction digest analysis. A single positive clone was selected for all future studies, and DNA was initially purified by spin column (BioBasic, Canada), followed by additional purification of the DNA using glycogen and methanol precipitation, followed by resuspension in sterile deionized H_2O.

F. nucleatum 23726 was made competent by growing a 5 mL culture to mid-log phase (OD_{600} = 0.4) followed by spinning down cells at 14k G for 3 minutes, removal of media, and five successive 1 mL washes with ice cold 10% glycerol in diH_2O. Cells were then resuspened in a final volume of 100 μl of ice cold 10% glycerol (Final OD_{600}= ~20). Bacteria were transferred to cold 1 mm electroporation cuvettes (Genesee, USA) and 0.5-2.0 μg ([ ] > 500 ng/μl) of pDJSVT100 plasmid was added immediately before electroporating at 2.0 kV (20 kV/cm), 50 μF, 129 OHMs, using an Electro Cell Manipulator 600 (BTX, USA). To the cuvette, 1 mL of recovery media (CBHK, 1 mM $MgCl_2$) was added, and immediately transferred by syringe into a sterile, anaerobic tube via septum for incubation at 37˚C for 20 hours with no shaking. Post outgrowth, cells were spun down at 14 kG for 3 minutes, media removed, and resuspended in 0.1 mL recovery media, followed by plating on CBHK plates with 5 μg/mL thiamphenicol and incubation in an anaerobic 37˚C incubator for two days for colony growth. ~ 5 colonies/μg of DNA were achieved, and the *fplA* gene knockout was verified by PCR specific to the chromosome and *catP* gene that

was incorporated into the genome by the pDJSVT100 KO plasmid (Primers, **Table S3)**. In addition, western blots were used to confirm a loss of FplA protein expression (**Fig. 4.9 and 4.11**).

Enzymatic Assay Design, Data Collection, and FplA Kinetics:

Initial tests for FplA enzymatic activity were run using the EnzChek Phospholipase A1 and EnzChek Phospholipase A2 assay kits (ThermoFisher, USA) at 1 μM and 10 μM $FplA_{20-431}$ using the manufacturer's protocol (**Fig. 4.4A**). These assays showed that FplA has PLA_1, but not PLA_2 activity, which is consistent with data reported for the homologous enzyme PlpD. We then went on to further characterize its activity by developing a continuous kinetic assay using the PLA_1 specific substrate PED-A1 (ThermoFisher, USA) and determined the full kinetic parameters of FplA with this substrate as reported in **Fig. 4.4** and **Fig. 4.5**. In detail, FplA was used at 1 nM in the reaction and substrate (10 mM stock in 100% DMSO) dilutions (0-10 μM) and reactions were carried out in reaction buffer (50 mM Tris pH 8.5, 50 mM NaCl, 0.025% BOG). All samples including controls contained equal concentrations of DMSO. Reactions were run at 26˚C for 30 minutes with 3 seconds of shaking in between continuous fluorescent monitoring (Ex = 488 nm, Em 530 nm) every 2 minutes on a SpectraMax $M5^e$ plate reader (Molecular Devices, USA). Relative fluorescence units measured upon cleavage of substrate ester bonds and release of the acyl chain were converted to the concentration of product (BODIPY® FL C5) created by establishing a standard curve using pure BODIPY® FL C5 (ThermoFisher, USA). In all enzymatic reactions, controls containing no protein were run and the values were subtracted from the reactions containing protein during analysis.

We then developed a continuous fluorescent assay to characterize the phospholipase activity of FplA using the general lipase substrates 4-Methylumbelliferyl Butyrate (4-MuB) and 4-Methylumbelliferyl heptanoate (4-MuH) (Santa Cruz Biotechnology, USA). In detail, FplA

was used at 1 nM in the reaction and substrate (50 mM stock in 100% DMSO) dilutions (0-200 μM) and reactions were carried out in reaction buffer (50 mM Tris pH 8.5, 50 mM NaCl, 0.025% BOG). All samples including controls contained equal concentrations of DMSO (0.4%). Reactions were run at 26˚C for 30 minutes with 3 seconds of shaking in between continuous fluorescent monitoring (Ex = 360 nm, Em 449 nm) every 2 minutes on a SpectraMax M5^e plate reader. Relative fluorescence units measured upon cleavage of substrate ester bonds and release of the acyl chain were converted to the concentration of product (4-Methylumbeliferone, 4-Mu) created by establishing a standard curve using pure 4-Mu (Sigma Aldrich, USA).

The steady-state kinetic parameters for each substrate were determined using GraphPad Prism version 6 (Graphpad Software, USA) by fitting the initial rate data (n=2) to the Michaelis-Menten equation (**Equation 1)**:

$$v = V_{max}[S] / (K_M + [S]) \qquad (1)$$

to obtain the values reported in **Fig. 4.2** and **Fig. 4.10**.

Characterization of FplA Inhibitors:

We set out to characterize inhibitors that we could use as effective tools to test the role of FplA both *in vitro* and potentially *in vivo* by IC_{50} assays using a variety of inhibitor classes. Inhibitors shown in **Fig. 4.6** and **Fig. 4.7** were chosen based on their previous classification as inhibitors of a diverse set of phospholipase enzymes: Methylarachidonyl fluorophosphonate (MAFP), $PLA_{2[52]}$; Arachidonyl Trifluoromethyl Ketone (ATFMK), $cPLA_2$, $iPLA_{2[53]}$; Isopropyl Dodec-11-Enylfluorophosphonate (IDEFP), fatty acid amide hydrolase[54]; Palmityl Trifluoromethyl Ketone (PTFMK), $cPLA_2$, $iPLA_{2[55]}$; ML-211, LYPLA1, LYPLA2[56]; Isopropyl Dodecylfluorophosphonate (IDFP), fatty acid amide hydrolase, monoacylglycerol lipase[57];

LY311727, $sPLA_{2[58]}$; Manoalide, sPLA2, PLC[59,60]. All inhibitors were purchased from Cayman Chemical, USA.

For potent inhibitors, 0-25 μM concentrations were used in assays, and for compounds found to not inhibit efficiently, the concentration range was 0-100 μM. Inhibitors were diluted into reaction buffer (50 mM Tris pH 8.5, 50 mM NaCl, 0.025% BOG) containing 10 μM 4-MuH. To initiate the reaction, 1 nM final $FplA_{20-431}$ was added and reactions were run at 26˚C for 30 minutes with 3 seconds of shaking in between continuous fluorescent monitoring (Ex = 360 nm, Em 449 nm) every 2 minutes on a SpectraMax $M5^e$ plate reader. Raw data (n=2) for each reaction were analyzed in GraphPad Prism using a log(inhibitor) vs response using variable slope and a least squares (ordinary) fit model.

Use of Fluorescent Chemical Probes to Label and Detect FplA:

Purified recombinant FplA constructs or WT FplA from *F. nucleatum* strains were visualized using an ActivX TAMRA-FP probe (ThermoFisher, USA). This probe only binds to proteins with activated serine residues. For purified recombinant proteins, 5 μg of purified protein was incubated with either 100 μM of methylarachidonyl fluorophosphonate (MAFP) or PBS for 1 hour. Following preincubation with MAFP or PBS, 1 μM ActivX TAMRA-FP probe was added to the protein and incubated for 20 minutes at 26˚C followed by the addition SDS-PAGE running buffer to stop the reaction. 500 ng of protein was run on an SDS-PAGE gel at 210V for 60 minutes, followed by transferring proteins to PVDF membranes in transfer buffer (25 mM Tris, 190 mM Glycine, 20% methanol, pH 8.3) at 80V for 60 minutes. Fluorescent proteins were visualized using a G:Box XX6 system (SynGene, USA) using the TAMRA fluorescence filter.

For the detection of FplA in *F. nucleatum* whole cell mixtures, 5 ml of *F. nucleatum* 23726 or *F. nucleatum* 23726 Δ*fplA* cells at OD_{600} = 0.2 were pelleted, washed, and resuspended in 100

µL of PBS. ActivX TAMRA-FP was added at a final concentration of 2 µM and incubated at 26˚C for 20 minutes, followed by the addition of SDS buffer. 10 uL of this reaction (lysate from ~4.2 x 10^8 bacteria) was run per well on an SDS-PAGE gel at 210V for 60 minutes. Gels were then imaged on a Typhoon Trio (GE Healthcare, USA) using the TAMRA filter setting.

Detection of FplA on the Surface of E.coli by Microscopy, Enzymatic Activity, and Proteinase K Treatment:

Using the expression vector pDJSVT86 that is described in the cloning and expression section above, we cloned $FplA_{20\text{-}760}$ into the vector at the 3' end of the $OmpA_{1\text{-}27}$-6xHis signal sequence (pDJSVT88). This construct was expressed in LOBSTR RIL[45] *E. coli* in Studier autoinduction media at 37˚C for 20 hours with 250 RPM shaking. The empty vector pDJSVT86 was used as a negative control for FplA expression for both microscopy and enzymatic assays.

For microscopy, stationary phase bacteria from overnight expressions were washed in PBS pH 7.5, 0.2% gelatin and spun down at 5 kG for 5 minutes, followed by resuspending the bacteria at an OD_{600}=0.2. To the bacteria, a final 3.2% paraformaldehyde was added for 15 minutes at 26˚C for fixation, followed by washing in PBS pH 7.5, 0.2% gelatin. 500 µl of fixed bacteria were then added on top of a polylysine coated coverslip in a 6 well plates, and 2 mL of PBS was added for a final volume of 2.5 mL. Bacteria were then spun down onto the coverslips at 2,000x G for 10 minutes. Washed coverslips were submerged in 300 µl of PBS pH 7.5, 0.2% gelatin containing a 1:100 dilution of the anti-FplA antibody and incubated for 20 hours at 26˚C with light shaking. Coverslips were washed again in PBS pH 7.5, 0.2% gelatin and then incubated in the same buffer containing an anti-rabbit Alexa Fluor 488 conjugated secondary antibody for 30 minutes at 26˚C. Washed coverslips were mounted with Cytoseal 60 (ThermoFisher, USA) and visualized by

brightfield and fluorescence microscopy using the GFP channel on an EVOS FL microscope (Life Technologies, USA).

For the enzymatic activity assay, stationary phase bacteria from overnight expressions were washed in PBS pH 7.5 and spun down at 5 kG for 5 minutes, followed by resuspending the bacteria at an OD_{600}=0.2 in PBS pH 7.5. Bacterial samples were incubated with 10 μM MAFP or PBS pH 7.5 at RT for 60 minutes at 26˚C, followed by washing in PBS pH 7.5 and resuspension to the original OD_{600}=0.2 (2 x 10^8 CFU/mL in enzymatic assay buffer (50 mM Tris pH 8.5, 50 mM NaCl, 0.025% BOG). 2 x 10^6 bacteria were then added to reaction wells containing 10 μM 4-MuH fluorescent lipase substrate (Ex = 360 nm, Em 449 nm), followed by incubation at 37˚C for 30 minutes and detection of lipid cleavage and product formation with a Spectramax M5^e as seen in **Fig. 4.8B**. Activity was plotted as fluorescence units and statistical analysis was performed using a multiple comparison analysis by one-way ANOVA in GraphPad Prism.

To further validate the translocation of the PLA_1 domain of FplA to the surface of *E. c*oli, the non-specific and membrane impenetrable enzyme proteinase K (PK) was used to cleave FplA in a dose dependent manner. FplA expression was induced with 500 μM IPTG for four hours shaking at 37˚C. Bacteria were washed in PBS and adjusted to an OD_{600} = 0.2 in PBS with 1 mM $CaCl_2$ to activate PK. 100 μl of cells were added to tubes followed by the addition of 0, 100, 250, or 1000 nM PK and incubation at 26˚C for 15 minutes. Reactions were then quenched with protease inhibitors (Roche, USA) and samples were separated by SDS-PAGE and transferred to PVDF for western blot analysis with an anti-FplA antibody. As a control, *E. coli* with the empty vector pDJSVT86 were analyzed for FplA expression and cleavage. In addition, GAPDH was used a load control, and also as a control to show PK was not digesting intracellular proteins.

Lipid binding assays:

Binding of FplA to various lipids was performed with commercially available lipids spotted on membranes, or by our laboratory spotting fresh lipids on blots. For the first analysis, membrane lipid strips were purchased from Eschelon, Inc. The strips were blocked in 10 mL of TBST 3% BSA for 2 hours at 26˚C with 70 rpm shaking. After blocking, lipid strips were incubated with TBST 3% BSA containing 50 μg/mL of the indicated FplA construct at 4˚C for 15 hours. After incubation with FplA, lipid strips were washed with TBST and incubated with a 1:1000 dilution of rabbit anti-FplA antibody in 10 mL of TBST 3% BSA for 60 minutes at 26˚C with 70 rpm shaking. Lipid strips were washed with TBST and incubated with a 1:2000 dilution of goat anti-rabbit IgG-HRP linked antibody (Cell Signaling, USA) in 10 mL of TBST 3% BSA for 30 minutes at 26˚C with 70 rpm shaking. After secondary antibody incubation, the lipid strips were thoroughly washed in TBST, and ECL-Plus blotting reagents were added for visualization[61]. The membranes were visualized using a G:Box XX6 system (SynGene, USA) (**Fig. 4.13**)

For a more detailed analysis of FplA binding to phosphoinositides, we purchased various phosphoinositides from Avanti Polar Lipids, and then spotted them onto PVDF at concentrations from 0-200 picomols (pMol). We tested FplA binding to PI, PI(3)p, PI(4)p, PI(5)p, PI(3,4)p_2, PI(3,5)p_2, PI(4,5)p_2, PI(3,4,5)p_3, and cardiolipin. All steps for analysis were the same as described above, except the membranes were visualized using Lucent Blue X-ray film developed on a SRX-101A medical film processor (**Fig. 4.14**).

Results

FN1704 Encodes for a Type Vd Phospholipase Autotransporter

Fusobacterium phospholipase autotransporter (FplA, UniProtKB-Q8R6F6) was identified as the gene previously labeled FN1704 in *F. nucleatum* ATCC 25586. Domain identification was carried out using SignalP 4.1 to identify a signal sequence (residues 1-19), and the SWISS-MODEL[62] structure prediction server identified a patatin domain responsible for phospholipase activity (residues 60-350), a POTRA domain common in protein-protein interactions (residues 351-431), and a C-terminal β-barrel domain (residues 431-760) to insert FplA in the outer membrane (**Fig. 4.1**). In addition, we identified a unique 40 amino acid N-terminal extension (NTE, residues 20-59) that plays a role in the catalytic efficiency of the enzyme likely by being critical for proper protein folding and position of the active site residues, and not substrate binding. Structure prediction of this enzyme revealed the N-terminal patatin domain is highly similar to PlpD from *Pseudomonas aeruginosa* (PDB: 5FQU), and an alignment shows an overall fold in residues 60-343 (32% identity corresponding to PlpD residues 22-311) that align well, with a highly conserved active site containing a catalytic dyad (Ser98 and Asp243) and an oxyanion hole (Gly69/70/71) (**Fig. 4.2**). In addition, the next closest structural homologs of the FplA catalytic domain (residues 60-343) are predicted to be the non-autotransporter phospholipase A enzymes ExoU (Type III secreted) from *P. aeruginosa* (19.0% identity to residues 102-472, PDB: 4AKX, 3TU3) and VipD (Type IV secreted) from *Legionella pneumophila* (17.3% identity to residues 33-411, PDB: 4AKF) (**Fig. 4.3**).

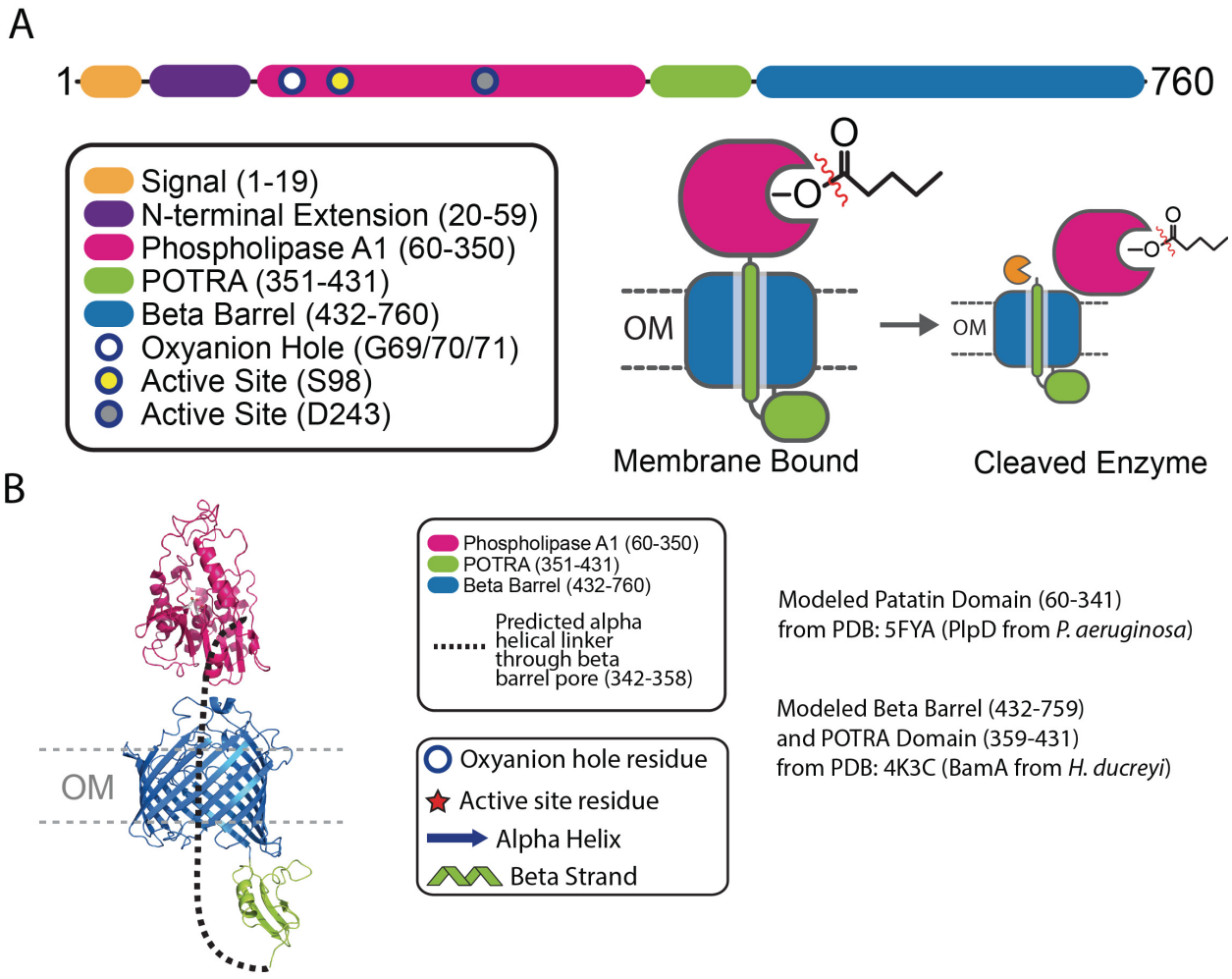

Figure 4.1 FplA is a Type Vd autotransporter phospholipase from *Fusobacterium nucleatum*. (A) Cartoon representation of FplA domains and their location in the periplasm, outer membrane, and surface exposure of the phospholipase A1 (PLA1) domain. Experimental data shows FplA to be cleaved in a select set of *F. nucleatum* species, but the phospholipase domain remains associated with the bacterium. POTRA: Polypeptide-Transport-Associated domain. (B) Structure prediction of FplA domains. Modeled Patatin Domain (60-341) from PDB: 5FYA (PlpD from *P. aeruginosa*). Modeled Beta Barrel (432-759) and POTRA Domain (359-431) from PDB: 4K3C (BamA from *H. ducreyi*).

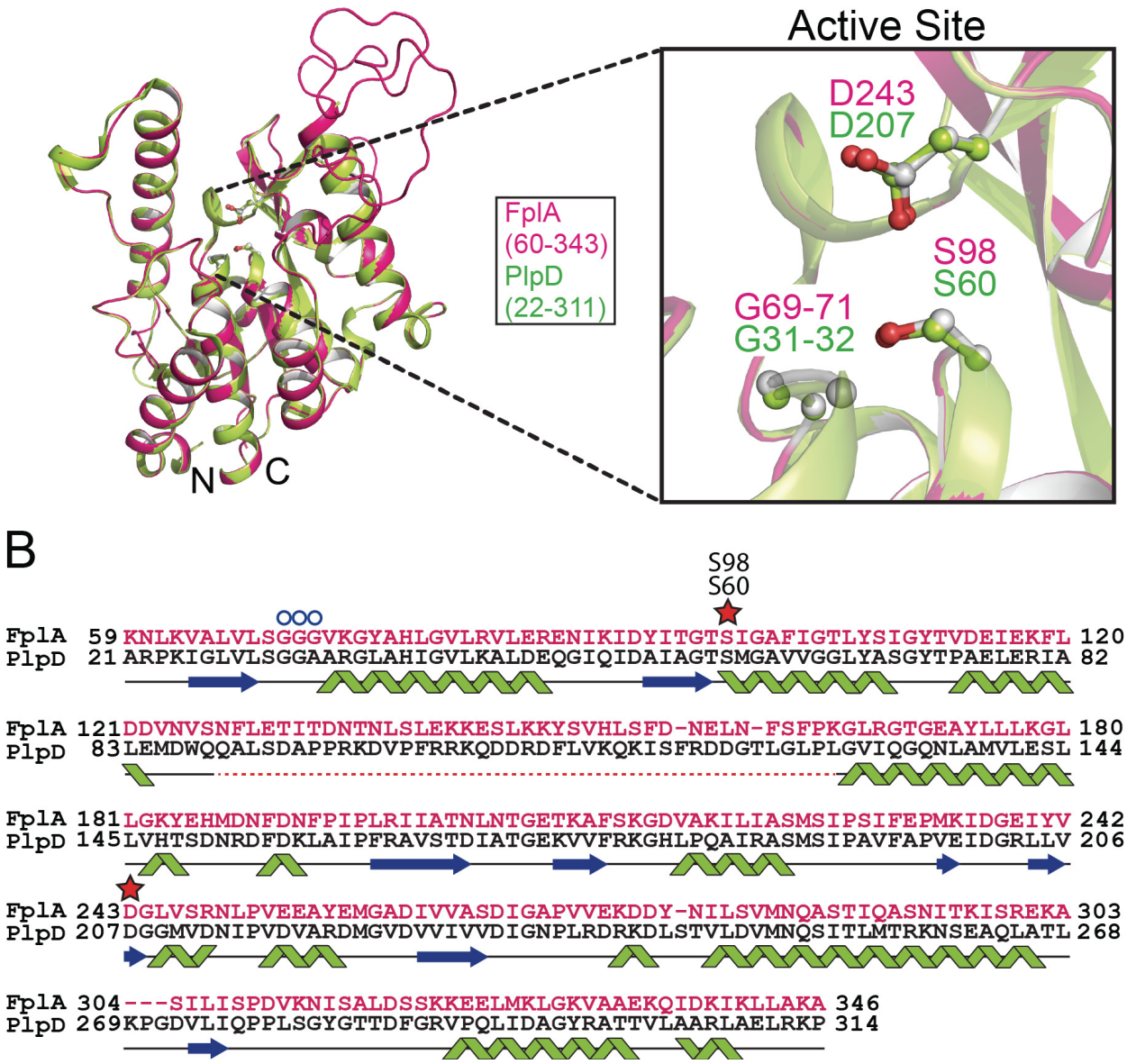

Figure 4.2 A predicted FplA structure is homologous to PlpD. (A) Alignment of a predicted FplA PLA1 domain structure with the crystal structure (PDB: 5FQU) of the homologous phospholipase A_1 enzyme PlpD from *Pseudomonas Aeruginosa*, with a magnified view of the catalytic dyad (S98, D243) and oxyanion hole (G69, G70, G71). (B) Alignment of amino acids from PlpD (Black) and FplA (Pink) from the predicted structures of the PLA1 domains. Dashed red line indicates this region was not predicted in the structure.

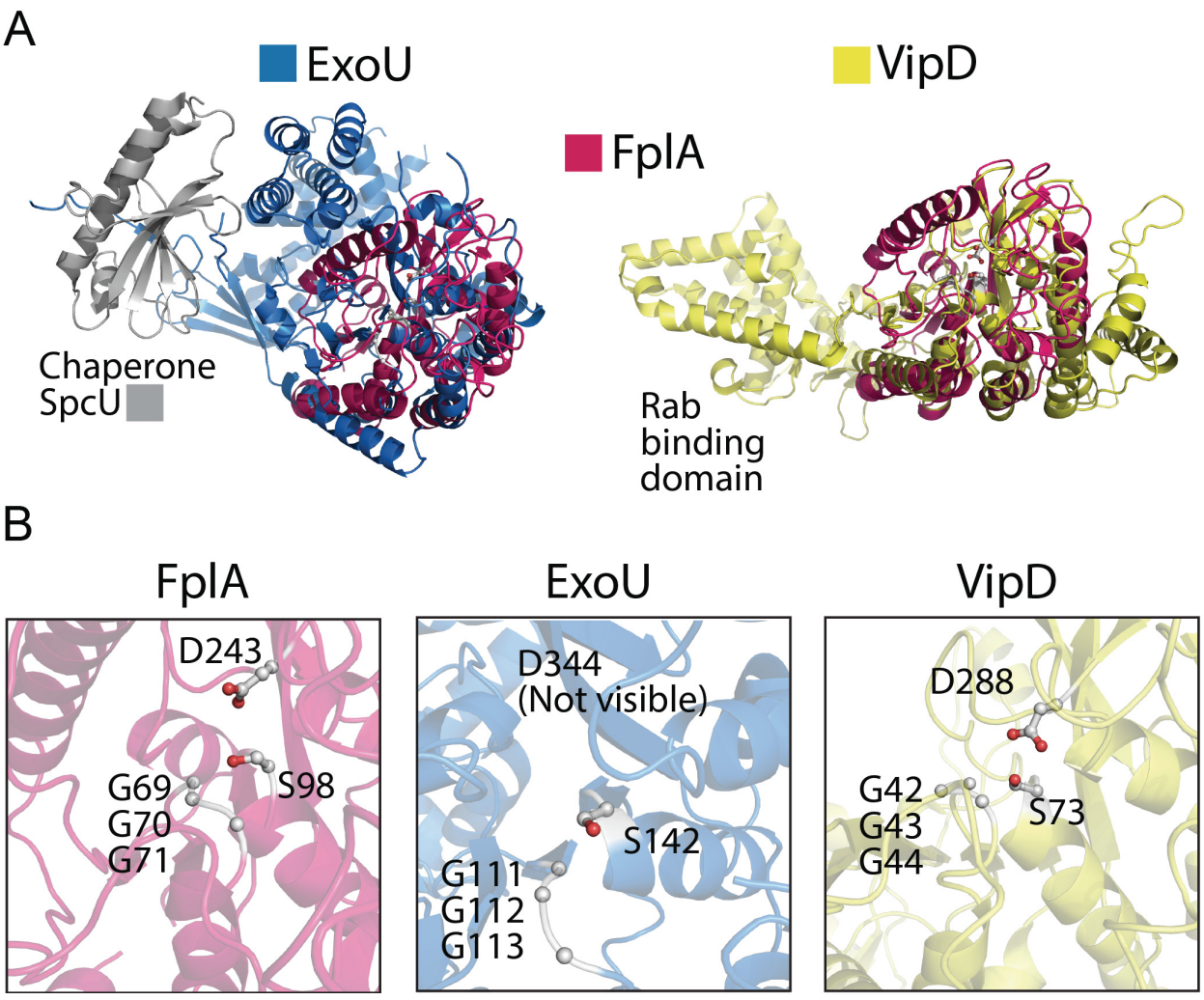

Figure 4.3 Alignment of predicted FplA patatin domain structure with characterized phospholipase virulence factors. (A) Predicted FplA structure (residues 60-431) aligned with with ExoU (*P. aeruginosa*)(PDB: 4AKX) and VipD (*L. pneumophila*)(PDB: 4AKF). (B) Zoomed in view of active sites after alignment showing similar architectures and residue placement of the catalytic dyad (Ser, Asp) and oxyanion hole (Gly, Gly, Gly)

Characterization of Fluorogenic Substrates to Probe the Phospholipase A1 (PLA_1) Activity of FplA

Multiple FplA constructs were cloned from the *F. nucleatum* 25586 genome and expressed in *E. coli*, including variations that lack a signal sequence for cytoplasmic expression (Residues 20-431, 20-350, 60-431, 60-350), and a full-length version in which we replaced the native signal sequence with an *E. coli* OmpA signal for more robust expression and surface presentation ($OmpA_{1-27}$-$FplA_{20-760}$). Constructs were tested for their phospholipase activity using substrates specific for either A1 or A2 class enzymes, as the homolog PlpD from *P. aeruginosa* showed specific A1 activity. We showed that FplA has only PLA_1 activity (**Fig. 4.4A**) using the PLA_1 specific substrate PED-A1, and further demonstrated that the general lipase substrates 4-Methyl Umbelliferyl Butyrate (4-MuB) and 4-Methyl Umbelliferyl Heptanoate (4-MuH) are robust tools for studies of FplA (**Fig. 4.4B-E**). In addition, we determined this enzyme is not dependent on calcium for activity (**Fig. 4.5A**), and that it is most active at pH 8.5 (**Fig. 4.5B**). The first full Michaelis-Menten kinetics for a Type Vd autotransporter were performed on each FplA construct using 4-MuH as a substrate, and indicated that amino acids 20-350, incorporating the N-terminal extension and catalytic PLA_1 domain, shows the most robust catalytic efficiency (k_{cat}/K_m = 3.2 x 10^6 s^{-1} M^{-1}) (**Fig. 4.4E, Fig. 4.5C-D**). Upon removal of the N-terminal extension, constructs had lower substrate turnover rates (k_{cat}), but the relative binding affinities (K_m) for 4-MuH was unchanged. We also show that tighter binding was seen with the substrate that most closely mimics a phospholipid (PED-A1, K_m=1.90 μM), and of the single acyl chain substrates, 4-MuH (7 carbon acyl chain) resulted in significantly tighter binding (K_m=19 μM) than with the 4 carbon acyl chain substrate 4-MuB (K_m=500 μM) (**Fig. 4.4C**). Mutation of the active site serine (S98A) and aspartate (D243A) residues that make up the catalytic dyad resulted in no detectable enzymatic activity

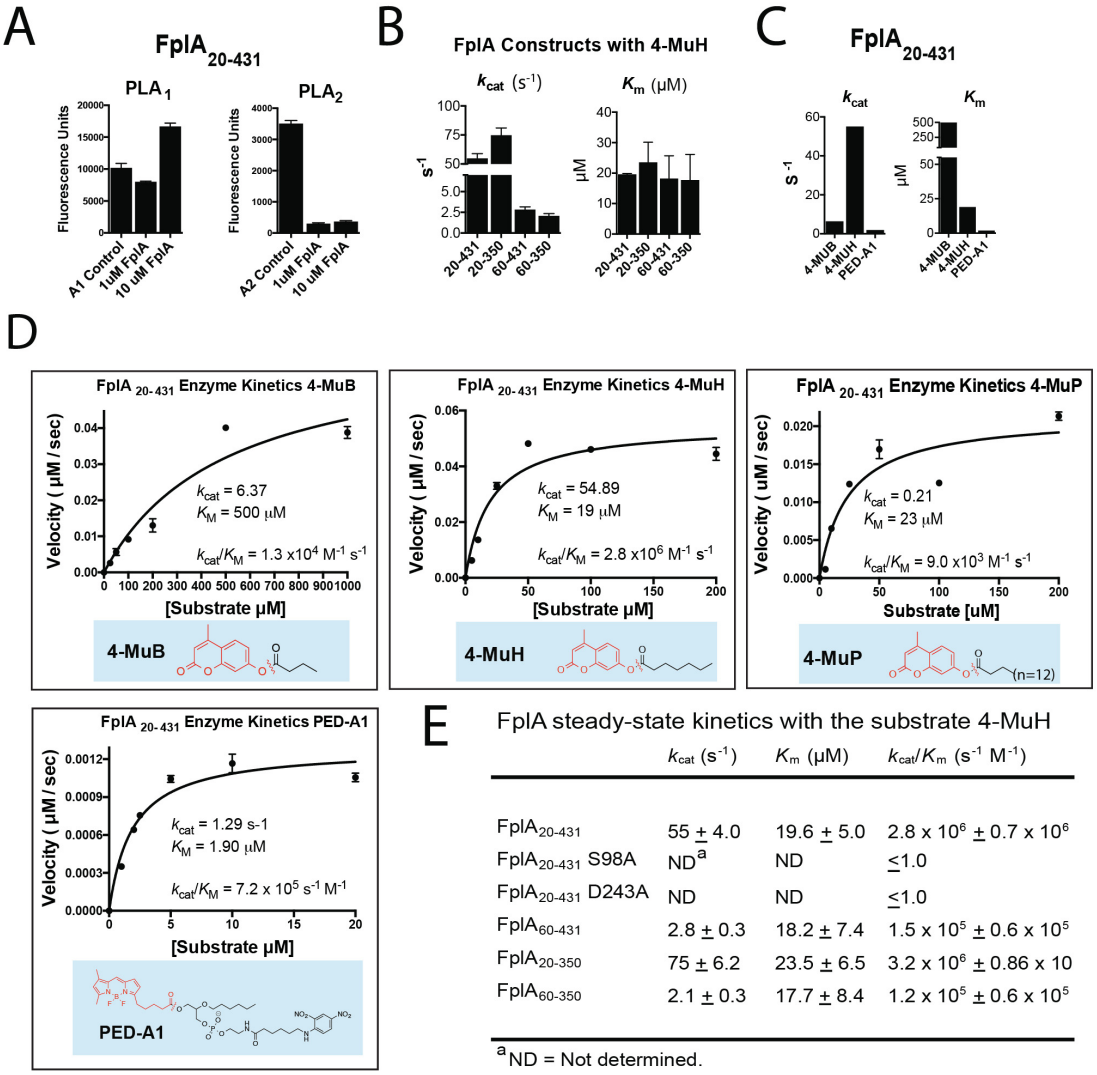

	k_{cat} (s^{-1})	K_m (μM)	k_{cat}/K_m (s^{-1} M^{-1})
$FplA_{20-431}$	55 ± 4.0	19.6 ± 5.0	2.8 x 10^6 ± 0.7 x 10^6
$FplA_{20-431}$ S98A	ND[a]	ND	≤1.0
$FplA_{20-431}$ D243A	ND	ND	≤1.0
$FplA_{60-431}$	2.8 ± 0.3	18.2 ± 7.4	1.5 x 10^5 ± 0.6 x 10^5
$FplA_{20-350}$	75 ± 6.2	23.5 ± 6.5	3.2 x 10^6 ± 0.86 x 10
$FplA_{60-350}$	2.1 ± 0.3	17.7 ± 8.4	1.2 x 10^5 ± 0.6 x 10^5

[a] ND = Not determined.

Figure 4.4 Characterization of FplA lipase activity with multiple fluorescent substrates. (A) Enzymatic assays show that FplA is a PLA1 specific enzyme with no PLA2 activity. (B) Steady-state kinetics of multiple FplA constructs with 4-MuH. (C) $FplA_{20-431}$ K_{cat} and K_m values vary greatly across substrates with various acyl chain lengths. (D-E) Characterization of FplA enzyme kinetics.

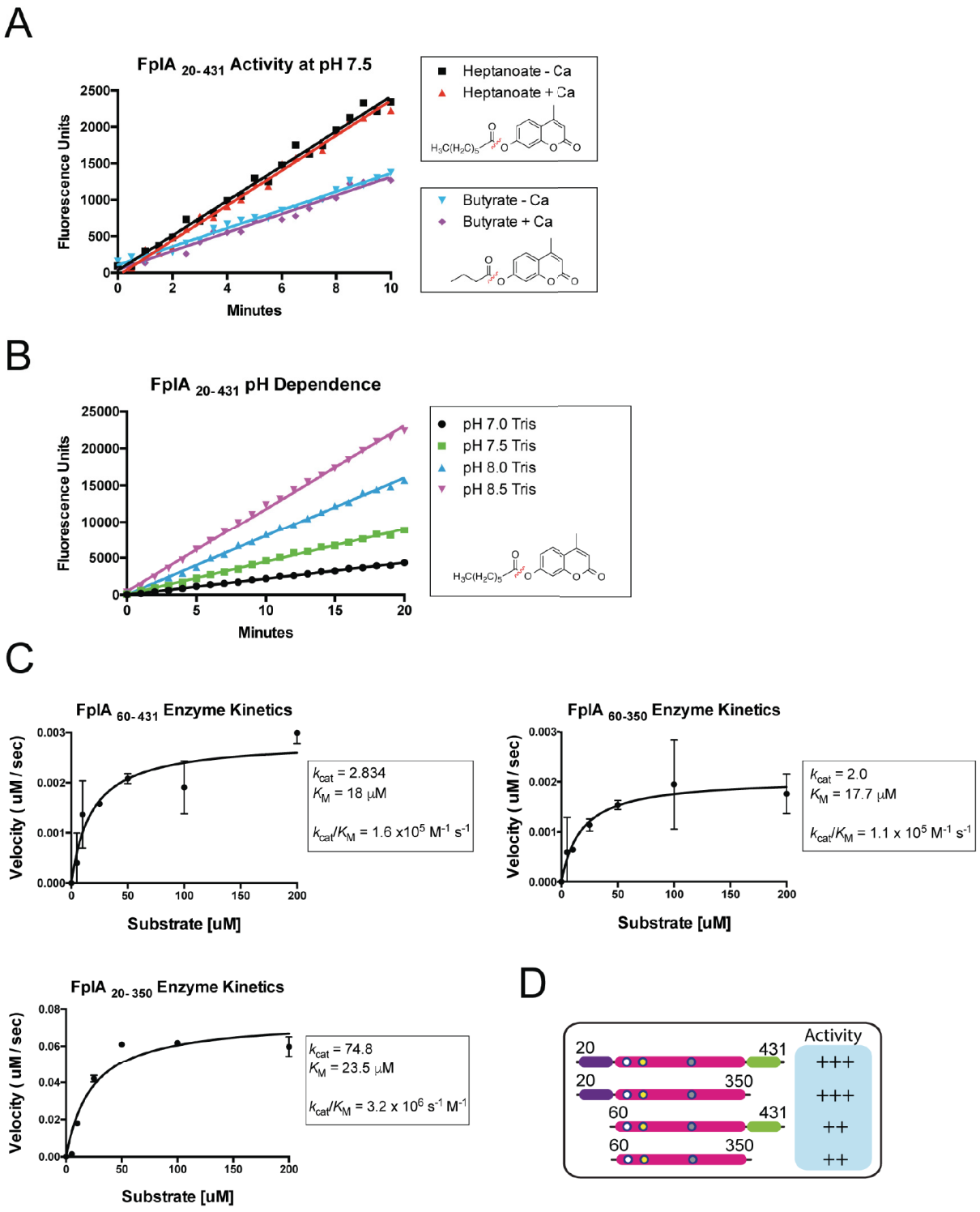

Figure 4.5 Enzymatic analysis of FplA$_{20\text{-}431}$. (A)FplA$_{20\text{-}431}$ does not need calcium for activity and is more active against the substrate 4-MuH than 4-MuB, indicating that longer acyl chains are critical for substrate binding. (B) pH dependent activity of FplA$_{20\text{-}431}$ using 4-MuH as a substrate shows maximal activity at pH 8.5. (C.) Enzyme kinetics and activity plots of FplA$_{60\text{-}431}$, FplA$_{60\text{-}350}$, and FplA$_{20\text{-}350}$ with 4-MuH. (D) Graphic representation of FplA construct activity and the importance of the N-terminal extension (NTE).

(**Fig. 4.4E**). In addition, the glycine rich stretch that constitutes the oxyanion hole (G69/70/71) was analyzed, but G→A single mutations or multiple glycine changes (G69/70/71A) rendered the proteins insoluble (unpublished data) and therefore could not be used for enzymatic analysis.

Identification of FplA Inhibitors and Chemical Probes for *in vitro* Enzyme Characterization

We present the first characterization of inhibitors for Type Vd autotransporter phospholipases. We show that the classic calcium-dependent PLA_2 inhibitor Methyl Arachidonyl Fluorophosphonate (MAFP) is the most potent for FplA with an IC_{50} of 11 nM[63]. Additional potent inhibitors contained a trifluoromethyl ketone head-group (ATFMK) which also covalently binds to active site serines within enzymes, or an enylfluorophosphonate group (**Fig. 4.6A-C**). We observed that IDEFP is a much more potent inhibitor than IDFP; these compounds differ by only a double bond at the end of the IDEFP acyl chain. In addition, MAFP is the most potent inhibitor and the arachidonyl portion of the molecule contains four double bonds, making it and ATFMK the most unsaturated substrates of the inhibitors tested. We therefore hypothesize that FplA binds and docks unsaturated acyl chain substrates and inhibitors with much higher affinity than saturated acyl chains, potentially because of angular changes within the molecule at double bonds. Additional inhibitors were tested that showed no significant activity against FplA (IC_{50} > 100 μM) and their analysis, as well as IC_{50} plots for all inhibitors are presented in **Fig. 4.7**.

An activity-based protein profiling (ABPP) probe (ActivX TAMRA-FP) that labels active site serines in serine hydrolases was used to label purified FplA constructs (**Fig. 4.6D**)[64,65]. ActivX TAMRA-FP labeled active FplA, but did not bind to the S98A or D243A mutants. We propose that in the absence of D243 which stabilizes substrate, the probe does not properly interact with S98 to initiate covalent labeling. In addition, in the presence of the competitive inhibitor

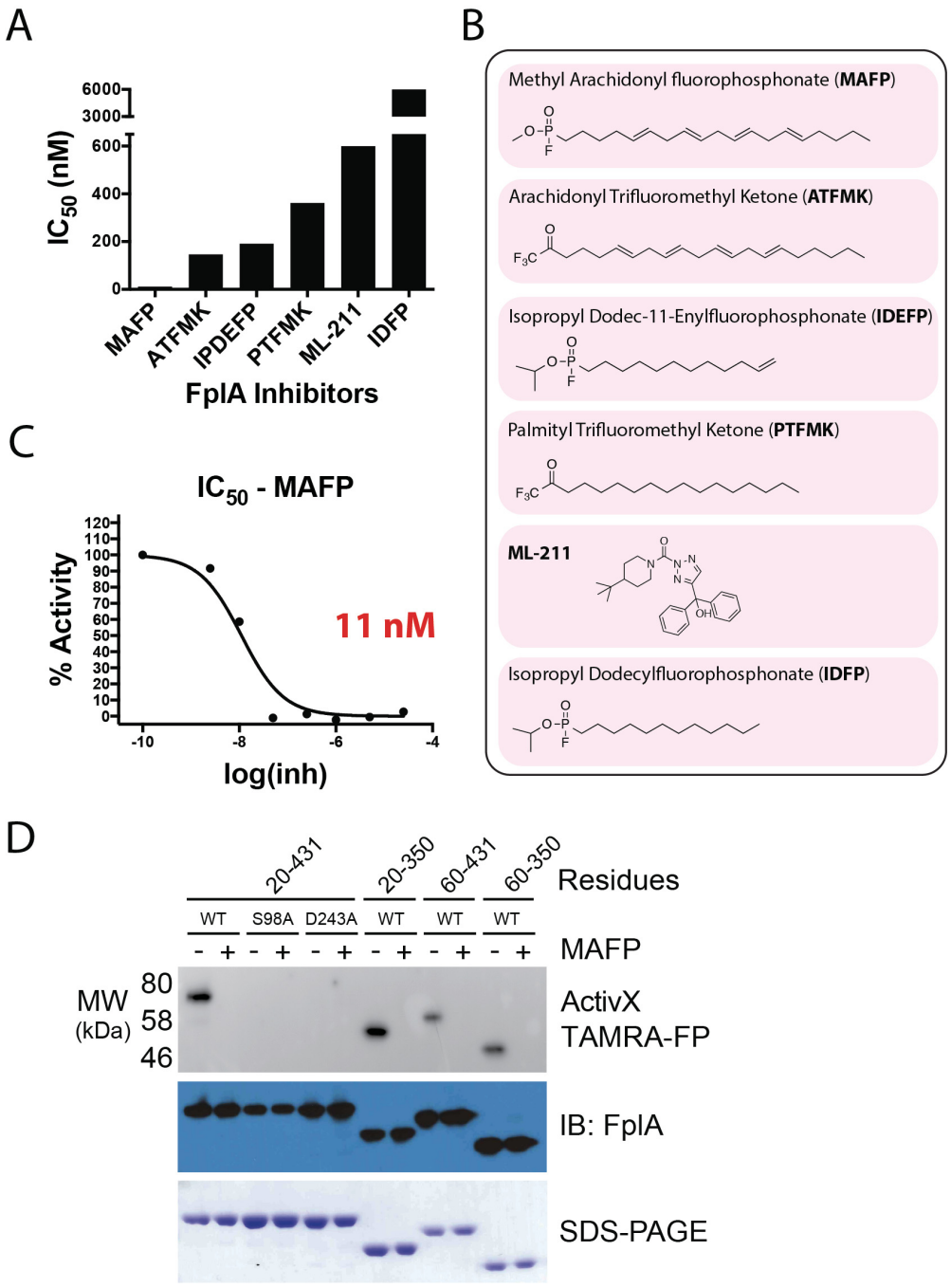

Figure 4.6 Characterization of FplA inhibitors. (A) IC_{50} assays showing varying degrees of inhibition towards FplA by inhibitors previously shown to inhibit a variety of lipases. (B) Structure and names of tested inhibitors. (C) IC_{50} plot of MAFP, the most potent (11 nM) FplA inhibitor characterized. (D) Analysis of the active site of FplA shows that the active site serine (S98) reacts with ActivX TAMRA-FP probe, but does not bind in the presence of the competitive inhibitor MAFP. S98A and D243A mutants will not bind the serine active site probe. Western blot and SDS-PAGE gels stained with Coomassie blue serve as load controls for all constructs.

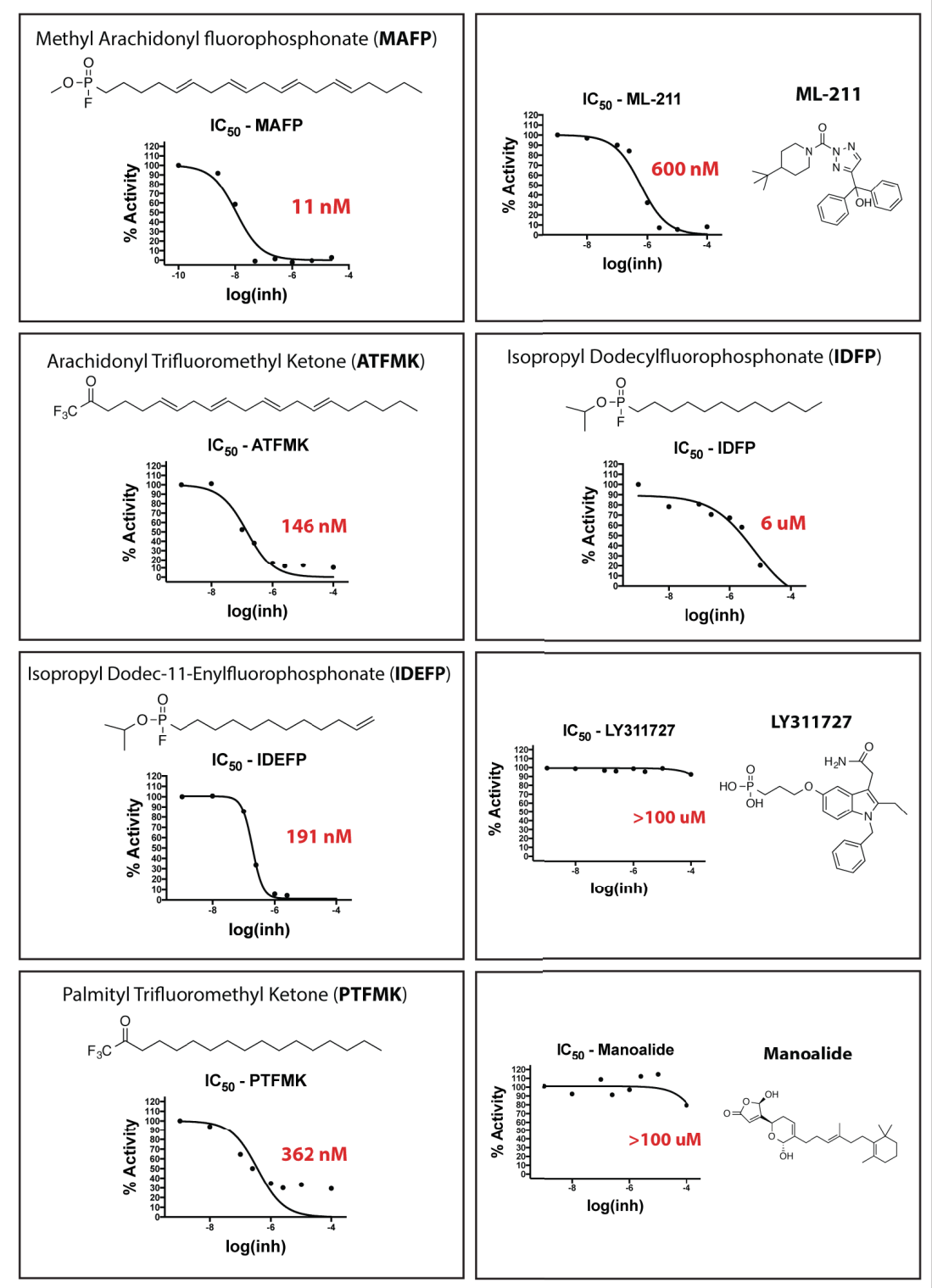

Figure 4.7 Analysis of multiple inhibitors previously shown to inhibit a diverse set of phospholipases. IC_{50} values equate to the concentration of inhibitor necessary to achieve 50% inhibition of $FplA_{20-431}$ using 4-MuH as a substrate.

MAFP, the ActivX TAMRA-FP probe is unable to bind to FplA due to competitive inhibition (**Fig. 4.6D**). We further demonstrated that load controlling is even by transferring the probe bound proteins to PVDF and immunoblotting using a custom $FplA_{20-431}$ antibody.

Expression of Full-length FplA on the Surface of *E. coli*

We created a FplA construct from *F. nucleatum* 25586 for recombinant expression in *E. coli* that removed the native signal sequence (residues 1-19) and replaced it with the signal sequence from *E. coli* OmpA (residues 1-27). This resulted in more robust expression of FplA on the surface of *E. coli* when compared with using a native signal sequence, which may not be recognized as efficiently by the *E. coli* Sec machinery (native signal sequence data not shown). We demonstrated that FplA can be efficiently exported through the Sec apparatus, assembled in the outer membrane, and the PLA_1 domain of FplA is present and functional on the surface of *E. coli*. In **Fig. 4.8A** we show that full-length FplA was detected on the surface of *E. coli* by fluorescence microscopy. FplA on the surface was active as addition of whole live bacteria to a reaction containing the fluorogenic substrate 4-MuH resulted in cleavage of the lipid substrate and a subsequent increase in fluorescence, which was inhibited by the addition of MAFP (**Fig. 4.8B**). To further prove that full-length FplA is expressed on the surface of E. coli, we confirm that treatment with the non-specific and cell-impermeable protease, Proteinase K (PK), cleaves FplA from the surface, but does not cleave the cytoplasmic control GAPDH (**Fig. 4.8C-D**).

Attempts to detect FplA on the surface of *F. nucleatum* 23726 and *F. nucleatum* 25586 by fluorescence microscopy were unsuccessful, which we attribute to the low abundance of this protein as indicated by the need to use large cell quantities in order to see the protein via western blot. It is possible that this is because FplA is such a potent phospholipase that high expression of

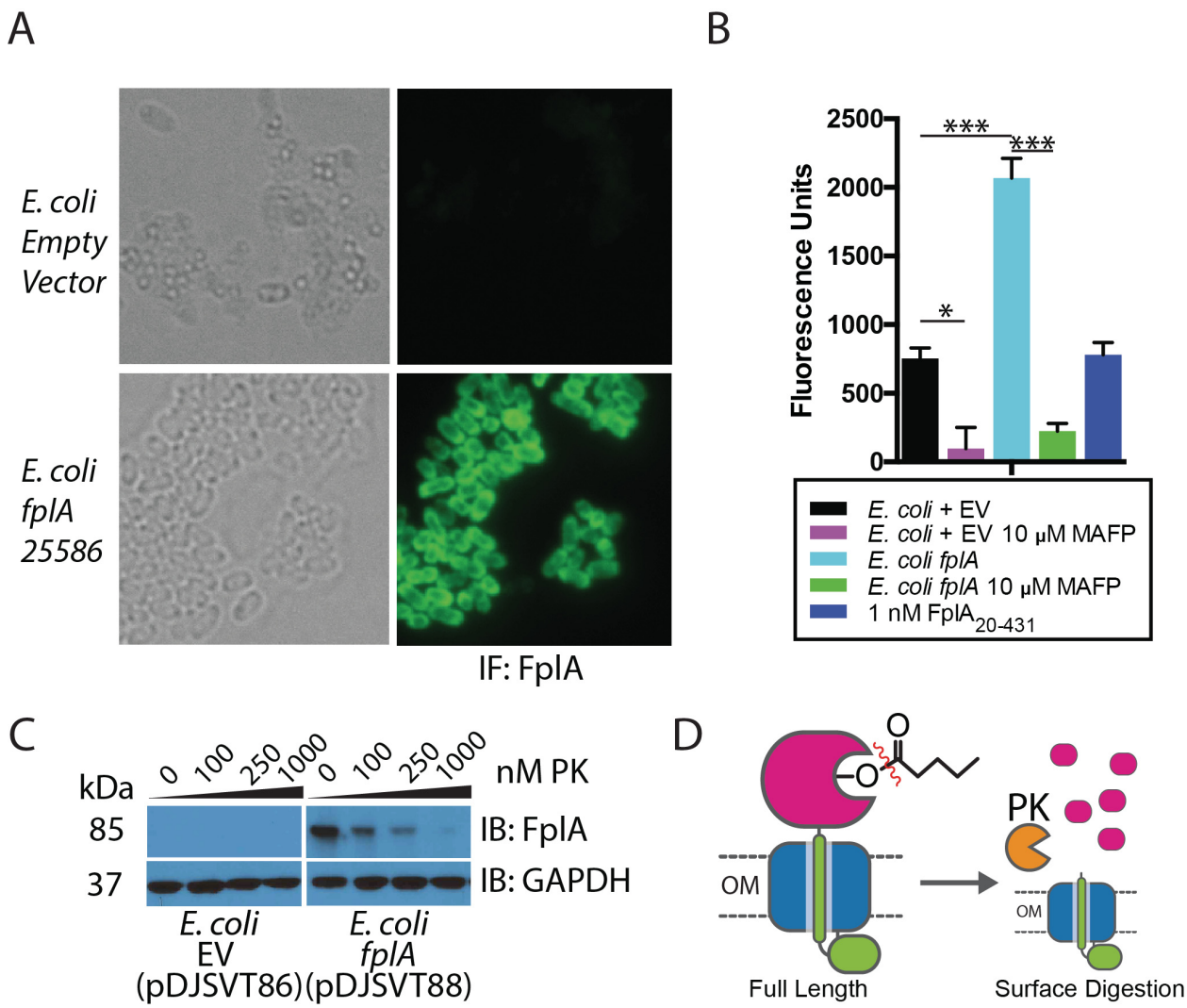

Figure 4.8 Expression of Full length FplA in *E. coli* and functional analysis. (A) An $OmpA_{1-27}$ signal sequence allows for robust expression of $FplA_{20-760}$ on the surface of *E. coli* as seen by fluorescence microscopy with an anti-FplA antibody. (B) Enzymatic activity of FplA when live *E. coli* are added to reactions containing 4-MuH as a fluorescent substrate (C) Proteinase K (PK), a cell impenetrable non-specific protease, is able to digest surface exposed FplA, but not the cytoplasmic protein GAPDH. (D) Schematic of PK cleavage of full-length FplA from the surface of *E. coli*. EV = Empty vector. Statistical analysis was performed using a multiple comparison analysis by one-way ANOVA. p-values: * = ≤ 0.05, *** = ≤ 0.0005.

the enzyme could be detrimental to *F. nucleatum*, as it could result in self-lysis and cell death. Additionally, we were unable to detect enzymatic activity by placing wild-type *F. nucleatum* 23726 directly in a mixture of 4-MuH substrate (results not shown). Neither of these negative results for activity are surprising considering the low amount of FplA present; such a lack of activity at the surface is not uncommon for other outer membrane phospholipases in Gram-negative bacteria. For example, outer membrane phospholipase A (OMPLA) from *E. coli* displays no activity in the absence of outer membrane destabilization compounds such as polymyxin B[66].

Creation of an *fplA* Deletion Strain in *F. nucleatum* 23726

Genetic manipulation of *Fusobacterium* spp. is technically challenging, and of the seven strains used for analysis in this manuscript, only *F. nucleatum* 23726 and 10953 have been successfully mutated by gene deletion[51]. A single homologous crossover plasmid (pDJSVT100, **Table S2**) that we developed from a *Clostridium* shuttle vector[49] using a recombination method previously established for *F. nucleatum[51]* was used to create a Δ*fplA* strain (Gene HMPREF0397_1968) (Strain DJSVT01, **Table S1**) marked with chloramphenicol resistance (**Fig. 4.9A-B**). We verified by PCR that the *fplA* gene was disrupted by the chromosomally-inserted plasmid, and further showed expression of the protein had been abolished by a fluorescent probe and western blots probed with an anti-FplA antibody (**Fig. 4.9C**). As phospholipases have been shown to play a role in bacterial membrane maintenance, we tested *F. nucleatum* 23726 Δ*fplA* for changes in growth rates and cell size, and found that when compared to wild-type *F. nucleatum* 23726, there were no changes in these physical parameters when grown under standard laboratory conditions (**Fig. 4.10**).

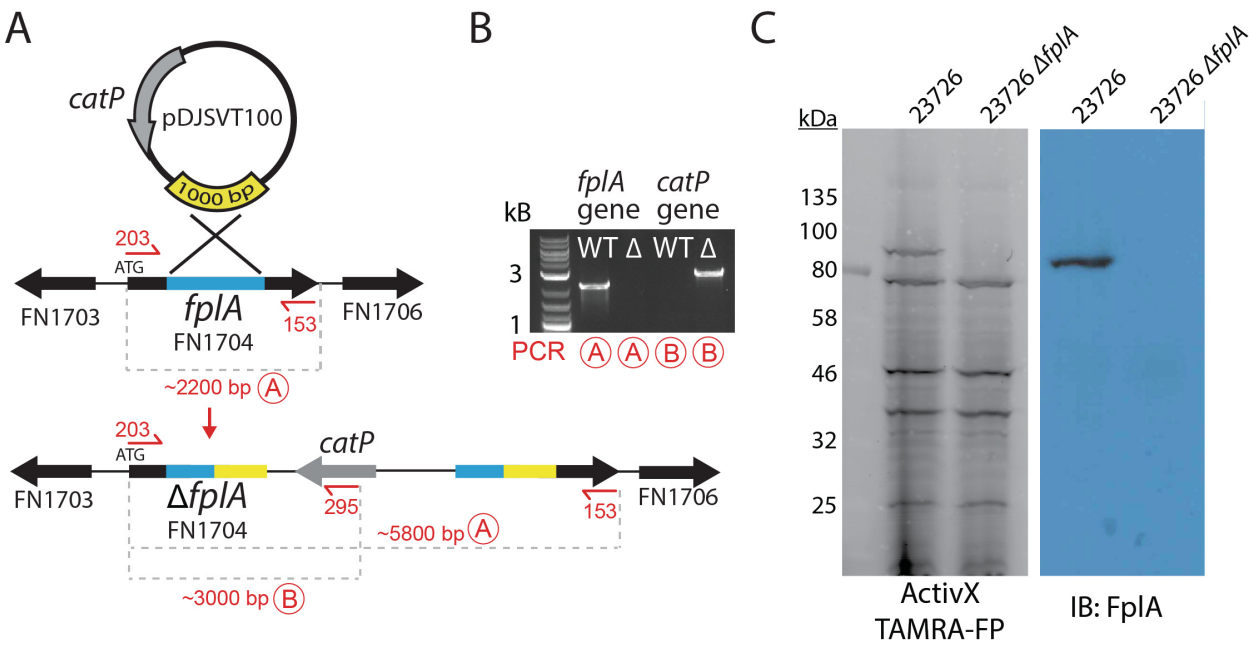

Figure 4.9 Creation of an *F. nucleatum* 23726 Δ*fplA*. (A) pDJSVT100 is a single-crossover integration plasmid for disruption of the *fplA* gene. Primers are labeled in red for PCR reactions A and B to confirm plasmid integration and gene knockout. (B) PCR confirmation of the *F. nucleatum* 23726 Δ*fplA* strain. (C) Analysis of FplA protein (85.6 kDa) in WT and Δ*fplA* by fluorescent chemical probe (ActivX TAMRA-FP) to label all active site serine enzymes in the bacteria (Also serves as a load control), followed by transfer to PVDF for western blot analysis by probing with an anti-FplA antibody.

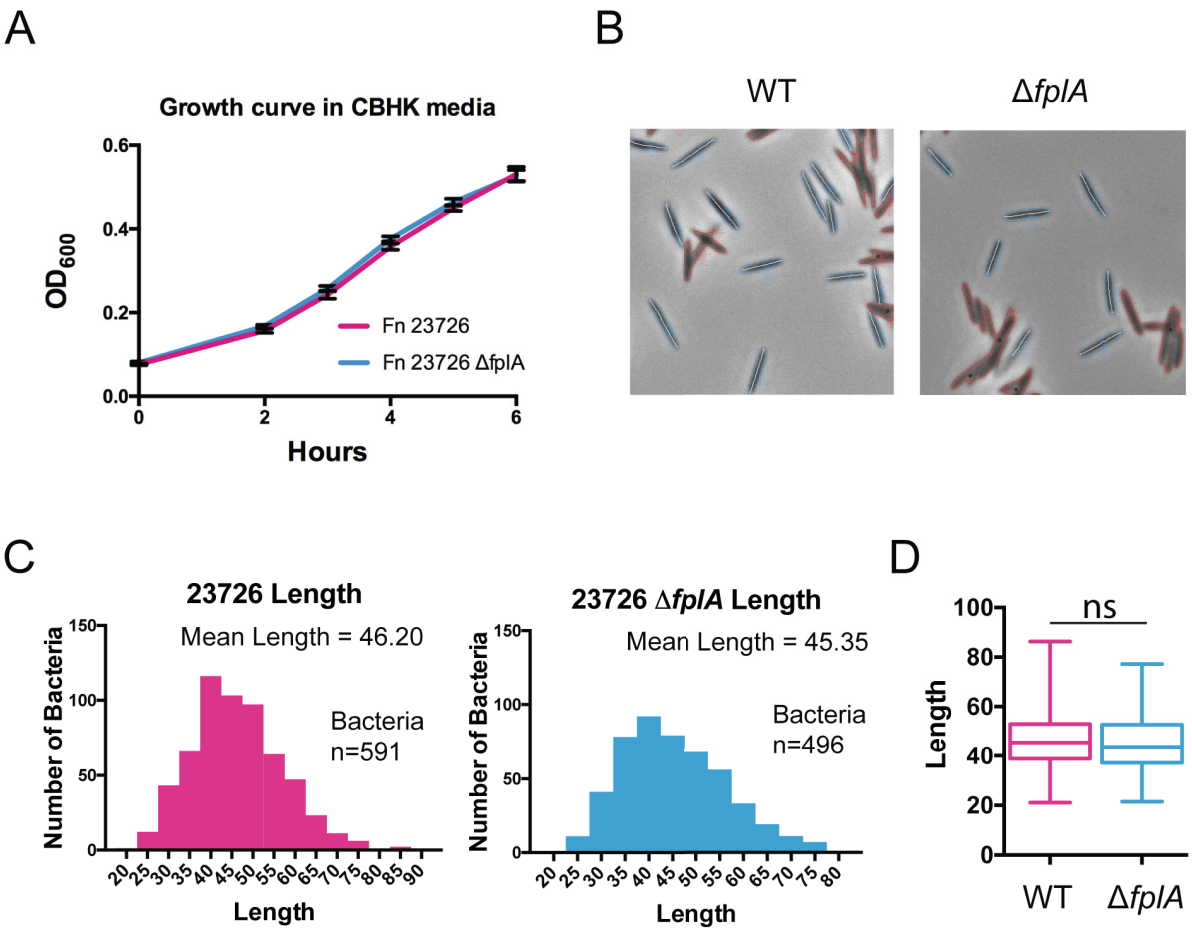

Figure 4.10 Analysis of Cell bacterial growth and morphology in WT and mutant *F. nucleatum*. (A) Analysis of a Δ*fplA* mutation on *F. nucleatum* growth in rich CBHK shows no growth defect in the absence of FplA. (B-C) Loss of FplA does not alter bacterial cell shape or length as determined by analyzing n=~500 bacteria using the MicrobeJ plugin from ImageJ. Statistical analysis was performed using an unpaired t-test. n.s.=not significant (p-value = 0.195).

F. nucleatum Strains Express FplA as a Full-length Outer Membrane Protein or as a Cleaved Phospholipase Domain That Remains Associated with the Bacterial Surface

Our initial results showed that FplA from *F. nucleatum* 23726 was expressed as a full-length 85 kDa protein, with no apparent release of the PLA_1 domain from the β-barrel domain. Since PlpD from *P. aeruginosa* is a Type Vd autotransporter that releases the PLA_1 domain into the media, we sought to see if FplA from seven different *F. nucleatum* strains had different expression patterns or actual physical differences in the size or location of expressed and/or secreted domains. Various FplA proteins were expressed as either a full-length 85 kDa proteins (Strains 23726 and 25586) or as a truncated phospholipase domain (FplA antibody developed against the PLA_1 and POTRA domains) around 25-30 kDa for strains 10953, 4_8, 4_1_13, 49256, and 7_1 when expressed in either mid-exponential (OD_{600} = 0.7) or stationary phase (OD_{600} = 1.2) (**Fig. 4.11A**). Interestingly, we could not detect any secreted FplA in the spent culture media, as was previously seen for PlpD from *P. aeruginosa* (**Fig. 4.11B**). We then tested for the presence of full length FplA in 10953 (cleaved) and 23726 (uncleaved) in early exponential growth (OD_{600} = 0.2) and found that we could detect full length and truncated FplA from 10953, indicating that upon increases in bacterial cell density, FplA is cleaved from the surface by an unknown protein and mechanism (**Fig. 4.11C**). It is possible that FplA cleavage from the surface results in an active PLA_1 domain that remains associated with the surface until released by undetermined host factors (pH, molecular cues, etc.) while colonizing specific regions of the human body.

While the FplA amino acid sequences from the seven tested strains are highly similar (>95% identity), we identified two regions in *F. nucleatum* 23726 and *F. nucleatum* 25586 at the intersection of the end of the N-terminal extension and just before the end of the PLA_1 domain, which could correspond to potential protease processing sites (**Fig. 4.11D**, **Fig. 4.12**). The

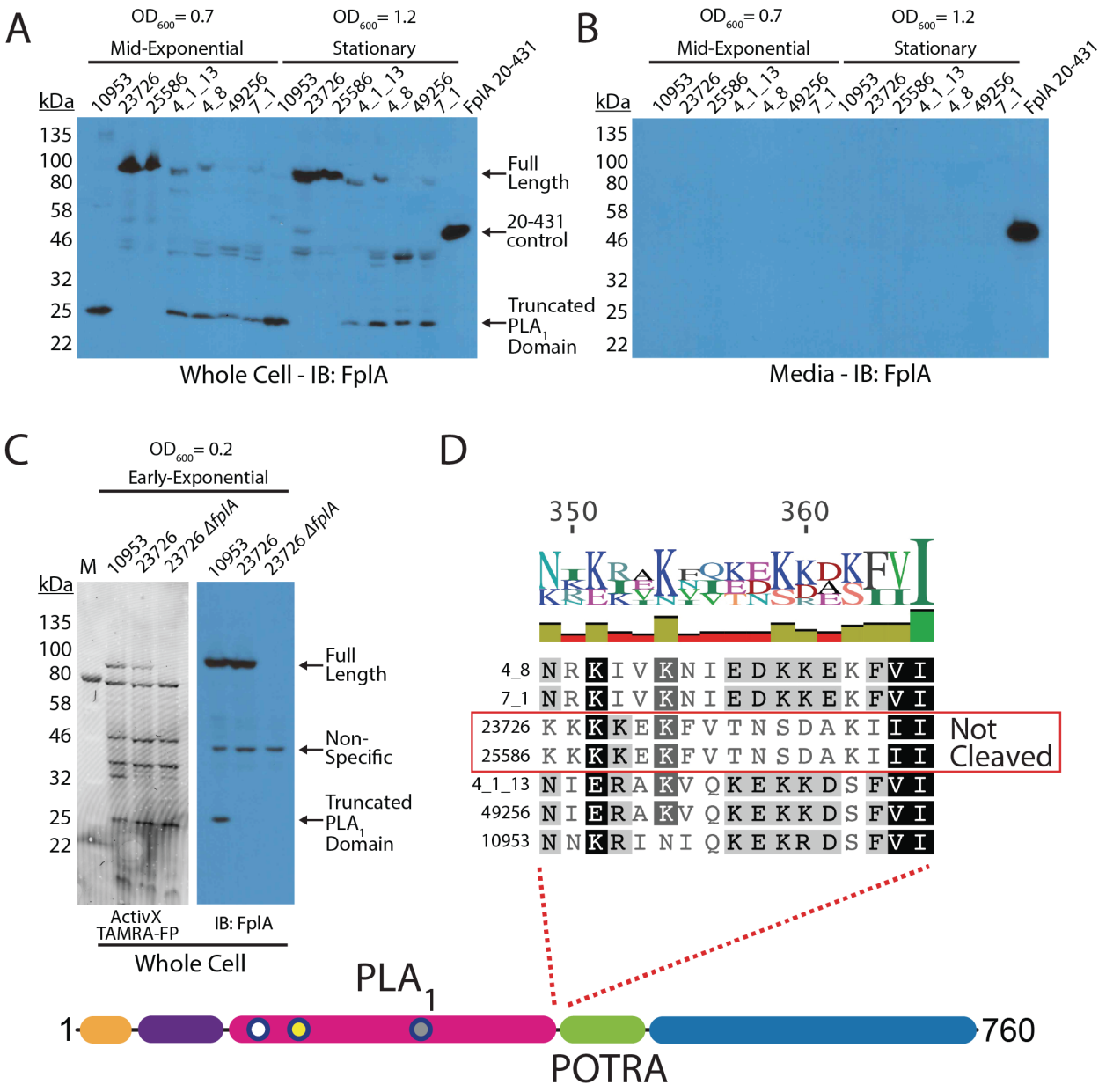

Figure 4.11 Western blot analysis of FplA in multiple *Fusobacterium* strains. (A) Initial characterization of FplA expression and protein size in mid-exponential phase (OD_{600} = 0.7) and stationary phase (OD_{600} = 1.2) shows that several strains produce a truncated form of FpA that consists of the PLA_1 domain to which the FplA antibody was raised. (B) Western blot of media from *Fusobacterium* growths shows that while truncated, FplA is not released into the media and remains associated with the bacteria. (C) Analysis of FplA expression during early exponential phase growth (OD_{600} = 0.2) reveals that strain 10953, which is cleaved in mid-exponential and stationary phase, is still in full-length state with a portion beginning to be cleaved. (D) Sequence alignment reveals that all FplA sequences from cleaved strains contain a highly charged motif at the PLA_1/POTRA hinge region as a potential site for an unidentified protease, with the exception being the non-cleaved FplA proteins from 23726 and 25586, which contain a drastically different neutral motif.

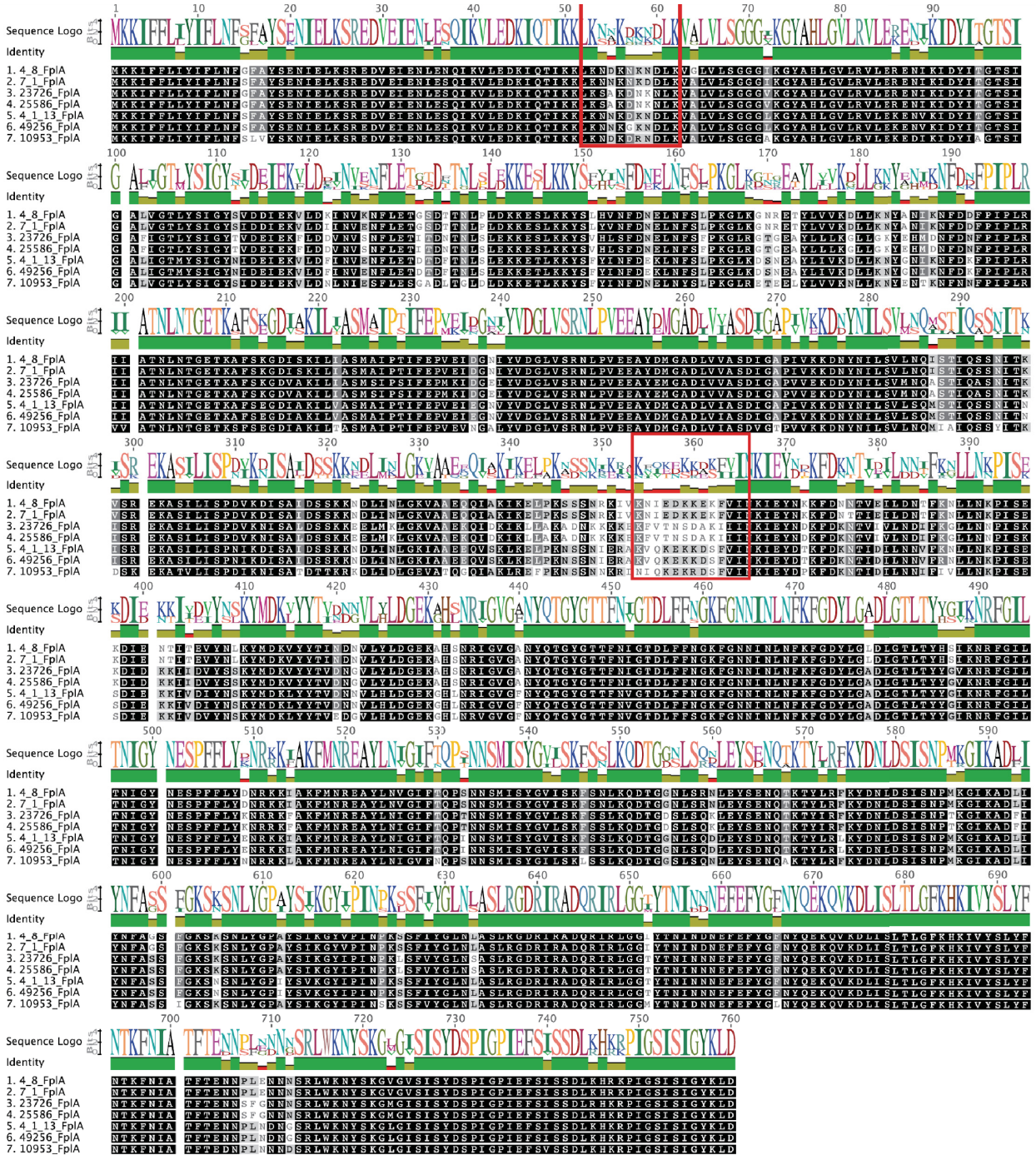

Figure 4.12 Alignment of full-length FplA from 7 strains of *Fusobacterium*. Potential cleavage sites for release of the PLA_1 domain are outlined in red and were determined based on differences seen in the 23726 and 25586 strains (not cleaved) when compared to the remaining five strains that are cleaved.

suspected cleavage site in *F. nucleatum* 23726 and *F. nucleatum* 25586 flanking the PLA_1 domain is switched from a highly-charged motif (consensus sequence: KNIEDKKEKF), to a more neutral motif (consensus sequence: KFVTNSDAKI) that could be more protease resistant, resulting in retention of the full-length protein. In addition, to arrive at the 25 kDa product seen in five strains, a second cleavage event could occur at the end of the N-terminal extension, as strains 23726 and 25586 differ in this region by substitution of an alanine for charged and polar residues (**Fig. 4.12)**.

FplA Binds Phosphoinositide Signaling Lipids

We tested FplA for binding to lipids found in human cells and found that it preferentially binds to human phosphoinositides, as was previously seen when characterizing the homologous enzyme PlpD from *P. aeruginosa[33]* (**Fig. 4.13**). Upon incubation with a more diverse and freshly-prepared library of PIs, FplA was found to preferentially bind to $PI(4,5)p_2$, and with even stronger affinity to $PI(3,5)p_2$, and $PI(3,4,5)p_3$ lipids (**Fig. 4.14**). This is consistent with structurally homologous enzymes binding PIs, and implicates a role for this enzyme in an intracellular environment.

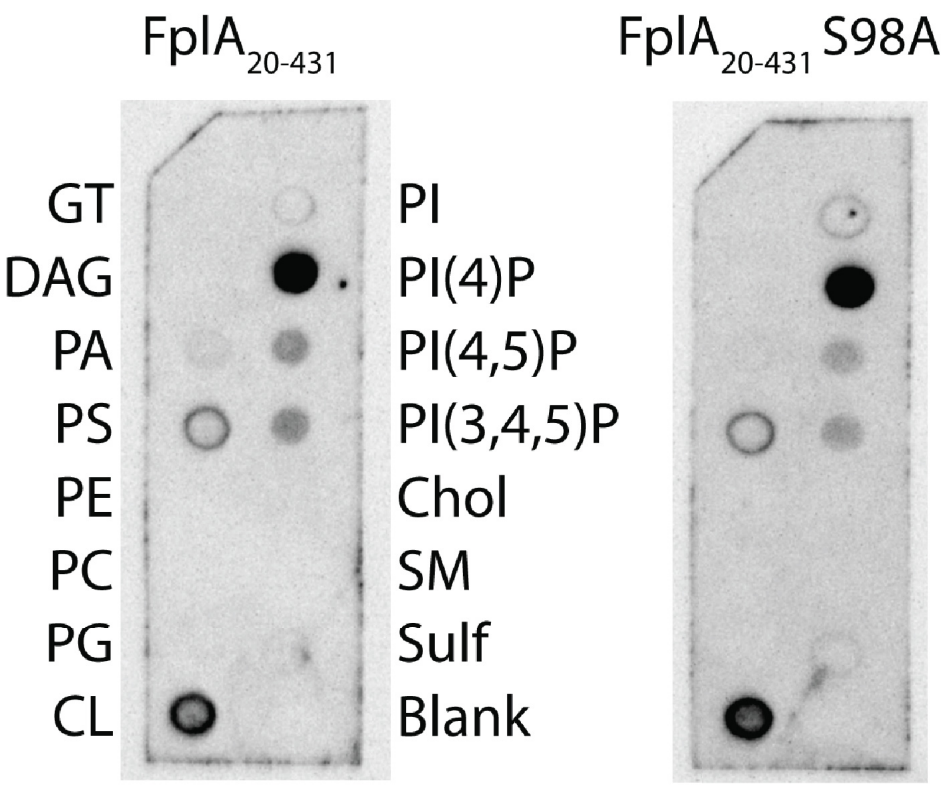

Figure 4.13 Initial analysis of $FplA_{20-431}$ and $FplA_{20-431}$ S98A lipid binding using commercially available lipid strips from Echelon Biosciences. Subsequent analysis using freshly blotted lipids (Avanti Polar Lipids) and revealed strong affinity for phosphoinositides, but not PI(4)p as seen here (See figure 4.14)

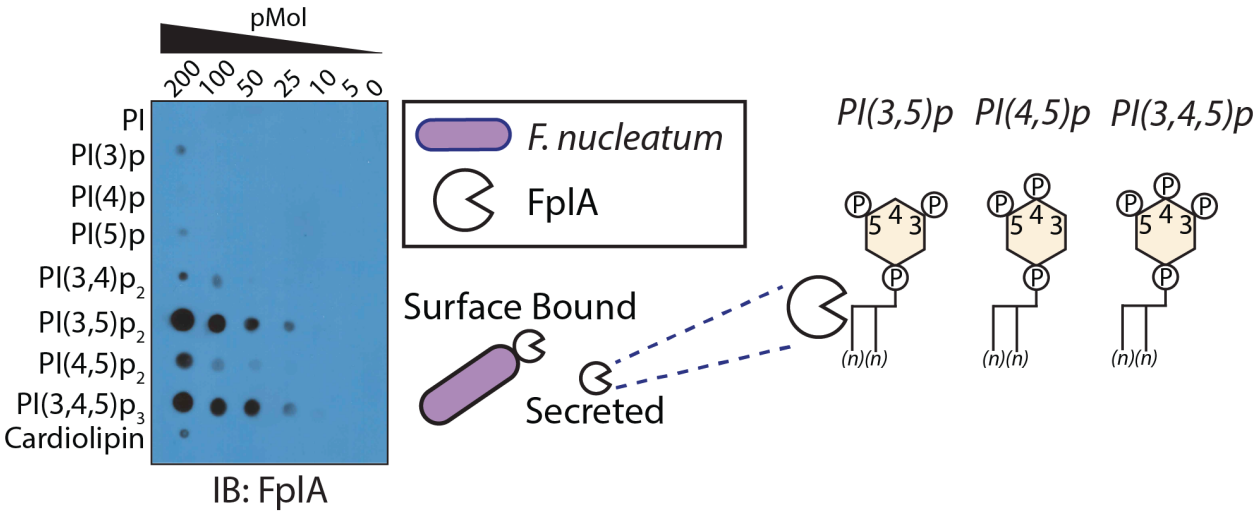

Figure 4.14 FplA lipid affinity profile. FplA binds with high affinity to phosphoinositide signaling lipids that are critical for multiple cellular processes in a human host.

Discussion

Fusobacterium is quite unique amongst Gram-negative bacteria in that the most recent and complete tree of life depicts a genetic lineage of *Fusobacterium* closer to high GC content Gram-positive bacteria (e.g. *Actinobacteria*) and Gram-negative *Bacteroidetes,* in which *Bacteroides fragilis* has multiple FplA homologs[67,68]. In addition, several *F. nucleatum* genes involved in metabolism are evolutionarily similar to that of gram-positive *Clostridium* spp.[69]. This unique combination of both Gram-positive and Gram-negative features could be an evolutionary clue as to why *Fusobacterium* lacks most Gram-negative specific secretion systems other than Type V.

Seminal studies by multiple groups have shown a repertoire of both small (FadA, ~15 kDa) and large (Fap2, >300 kDa, Type Va secreted) *F. nucleatum* adhesins that are critical for host cell binding, invasion, and inflammation[3,18]. We set out to probe the role of a potential Type Vd virulence factor that we predicted to have phospholipase activity. We characterized the gene FN1704, which we have renamed *fplA* for *Fusobacterium* phospholipase autotransporter (FplA). Our *in vitro* studies were focused on identifying tools and methods to characterize Type Vd secreted autotransporters to determine their role in virulence in a diverse set of Gram-negative bacteria; many such autotransporters have been identified in intracellular pathogens[32]. We created a *F. nucleatum* 23726 Δ*fplA* strain which will allow us to next probe the role of this enzyme through the first *in vivo* studies of Type Vd autotransporter phospholipases in infection. Our analyses indicate that deletion of the *fplA* gene from *F. nucleatum* does not alter growth or cell size and shape under laboratory growth conditions, adding to our hypothesis that FplA is a potential virulence factor and not a bacterial maintenance protein.

Determining that different *F. nucleatum* strains express mature FplA proteins of varying molecular weights was a surprising result that made us question which form of the enzyme may be involved during specific *in vivo* niches within the human host. Because of the well-known

genetic intractability of most *Fusobacterium* spp., we have not been able to delete copies of *fplA* in strains that we predicted to have a truncated yet surface-associated version of the protein. The development of more robust genetic systems for *Fusobacterium* has the potential to open doors to fill a critical knowledge gap in the role of Type Vd secretion in a variety of clinically isolated *F. nucleatum* strains.

Our initial results showed that FplA does not bind with high affinity to PA, PC, and PE, but these results do not rule out potential cleavage of these lipids in experiments that better simulate an environment found in infection. FplA could be involved in cleaving lipids in a mucous-rich environment found in the human oral cavity or gut. To add to the role of bacterial phospholipases cleaving lipids found in structural membranes, ExoU plays a major role in *P. aeruginosa* entry into the bloodstream upon leaving the lungs[70], and strains lacking ExoU are cleared more efficiently in mouse models of pneumonia[71,72]. Since cases of *Fusobacterium* bacteremia are frequently documented (*F. nucleatum* comprises 61% of cases)[73], and a wide array of bodily locations have been reported for *F. nucleatum* infections (brain[74], liver[75], lungs[6], heart[76]), it will be critical to use our newly created *fplA* deletion strain to test the role of this enzyme in the previously established hematogenous spread[3].

As there are an impressive number of phosphoinositide modulating enzymes secreted by bacteria to alter host signaling and induce colonization, it will be important to develop a robust set of chemical and molecular tools to determine the role of Type Vd surface bound or secreted PLA_1 enzymes in bacterial virulence. In summary, we have used chemical and biochemical tools to show that FplA is the lone Type Vd PLA_1 enzyme found in *F. nucleatum* and is a potential virulence factor that modulates host-pathogen interactions.

Acknowledgements

We thank the following individual for help and guidance with these studies: S. Melville (Virginia Tech) for critical critical insight into bacterial mutagenesis and for providing the pJIR750 plasmid; C. Caswell (Virginia Tech) for critical conversations regarding bacterial genetics; W. Lewis (WUSTL) for help with the *Fusobacterium* electroporation protocol; M. Klemba (Virginia Tech) for reagents and critical phospholipase insights. Funding for this work was partially provided by Virginia Tech new faculty start-up funds and a seed grant from the Institute for Critical Technology and Applied Science (ICTAS, Virginia Tech) to DJS. Partial funding for this work was provided through an Innovation grant to EAV from the Canadian Cancer Society Research Institute.

Author Contributions

MAC and CCY designed, performed, analyzed experiments, and wrote the manuscript. HBS purified protein and performed kinetic experiments. AJD grew fusobacterium and created the *fplA* knockout strain. KC prepared and sequenced all strains of Fusobacterium used in the study. ACV purified protein and performed kinetic experiments. EAV analyzed and wrote the manuscript. DJS designed, performed, analyzed experiments, and wrote the manuscript. All authors analyzed the results and approved the final version of the manuscript.

Competing Interests

The authors declare that they have no conflicts of interest with the contents of this article.

References

1. Signat B, Roques C, Poulet P, Duffaut D. Fusobacterium nucleatum in periodontal health and disease. Curr Issues Mol Biol. 2011;13: 25–36.
2. Han YW, Redline RW, Li M, Yin L, Hill GB, McCormick TS. Fusobacterium nucleatum induces premature and term stillbirths in pregnant mice: implication of oral bacteria in preterm birth. Infect Immun. 2004;72: 2272–2279.
3. Abed J, Emgård JEM, Zamir G, Faroja M, Almogy G, Grenov A, et al. Fap2 Mediates Fusobacterium nucleatum Colorectal Adenocarcinoma Enrichment by Binding to Tumor-Expressed Gal-GalNAc. Cell Host Microbe. 2016;20: 215–225.
4. Dahya V, Patel J, Wheeler M, Ketsela G. Fusobacterium nucleatum endocarditis presenting as liver and brain abscesses in an immunocompetent patient. Am J Med Sci. 2015;349: 284–285.
5. Rashidi A, Tahhan SG, Cohee MW, Goodman BM. Fusobacterium nucleatum infection mimicking metastatic cancer. Indian J Gastroenterol. 2012;31: 198–200.
6. Gedik AH, Cakir E, Soysal O, Umutoğlu T. Endobronchial lesion due to pulmonary Fusobacterium nucleatum infection in a child. Pediatr Pulmonol. 2014;49: E63–5.
7. Shammas NW, Murphy GW, Eichelberger J, Klee D, Schwartz R, Bachman W. Infective endocarditis due to Fusobacterium nucleatum: case report and review of the literature. Clin Cardiol. 1993;16: 72–75.
8. Swidsinski A, Dörffel Y, Loening-Baucke V, Theissig F, Rückert JC, Ismail M, et al. Acute appendicitis is characterised by local invasion with Fusobacterium nucleatum/necrophorum. Gut. 2011;60: 34–40.
9. Han YW. Fusobacterium nucleatum: a commensal-turned pathogen. Curr Opin Microbiol. 2015;23: 141–147.
10. Gauthier S, Tétu A, Himaya E, Morand M, Chandad F, Rallu F, et al. The origin of Fusobacterium nucleatum involved in intra-amniotic infection and preterm birth. J Matern Fetal Neonatal Med. 2011;24: 1329–1332.
11. Castellarin M, Warren RL, Freeman JD, Dreolini L, Krzywinski M, Strauss J, et al. Fusobacterium nucleatum infection is prevalent in human colorectal carcinoma. Genome Res. 2012;22: 299–306.
12. Warren RL, Freeman DJ, Pleasance S, Watson P, Moore RA, Cochrane K, et al. Co-occurrence of anaerobic bacteria in colorectal carcinomas. Microbiome. 2013;1: 16.
13. Kostic AD, Gevers D, Pedamallu CS, Michaud M, Duke F, Earl AM, et al. Genomic analysis identifies association of Fusobacterium with colorectal carcinoma. Genome Res. 2012;22: 292–298.
14. Kostic AD, Chun E, Robertson L, Glickman JN, Gallini CA, Michaud M, et al. Fusobacterium nucleatum potentiates intestinal tumorigenesis and modulates the tumor-immune microenvironment. Cell Host Microbe. 2013;14: 207–215.
15. Flanagan L, Schmid J, Ebert M, Soucek P, Kunicka T, Liska V, et al. Fusobacterium nucleatum associates with stages of colorectal neoplasia development, colorectal cancer and disease outcome. Eur J Clin Microbiol Infect Dis. 2014;33: 1381–1390.
16. Strauss J, Kaplan GG, Beck PL, Rioux K, Panaccione R, Devinney R, et al. Invasive potential of gut mucosa-derived Fusobacterium nucleatum positively correlates with IBD status of the host. Inflamm Bowel Dis. 2011;17: 1971–1978.
17. Manson McGuire A, Cochrane K, Griggs AD, Haas BJ, Abeel T, Zeng Q, et al. Evolution of invasion in a diverse set of Fusobacterium species. MBio. 2014;5: e01864.

18. Rubinstein MR, Wang X, Liu W, Hao Y, Cai G, Han YW. Fusobacterium nucleatum promotes colorectal carcinogenesis by modulating E-cadherin/β-catenin signaling via its FadA adhesin. Cell Host Microbe. 2013;14: 195–206.
19. Xu M, Yamada M, Li M, Liu H, Chen SG, Han YW. FadA from Fusobacterium nucleatum utilizes both secreted and nonsecreted forms for functional oligomerization for attachment and invasion of host cells. J Biol Chem. 2007;282: 25000–25009.
20. Kaplan CW, Ma X, Paranjpe A, Jewett A, Lux R, Kinder-Haake S, et al. Fusobacterium nucleatum outer membrane proteins Fap2 and RadD induce cell death in human lymphocytes. Infect Immun. 2010;78: 4773–4778.
21. Gur C, Ibrahim Y, Isaacson B, Yamin R, Abed J, Gamliel M, et al. Binding of the Fap2 protein of Fusobacterium nucleatum to human inhibitory receptor TIGIT protects tumors from immune cell attack. Immunity. 2015;42: 344–355.
22. Coppenhagen-Glazer S, Sol A, Abed J, Naor R, Zhang X, Han YW, et al. Fap2 of Fusobacterium nucleatum is a galactose-inhibitable adhesin involved in coaggregation, cell adhesion, and preterm birth. Infect Immun. 2015;83: 1104–1113.
23. Kaplan CW, Lux R, Haake SK, Shi W. The Fusobacterium nucleatum outer membrane protein RadD is an arginine-inhibitable adhesin required for inter-species adherence and the structured …. Mol Microbiol. Wiley Online Library; 2009; Available: http://onlinelibrary.wiley.com/doi/10.1111/j.1365-2958.2008.06503.x/full
24. Gupta S, Ghosh SK, Scott ME, Bainbridge B, Jiang B, Lamont RJ, et al. Fusobacterium nucleatum-associated beta-defensin inducer (FAD-I): identification, isolation, and functional evaluation. J Biol Chem. 2010;285: 36523–36531.
25. Bhattacharyya S, Ghosh SK, Shokeen B, Eapan B, Lux R, Kiselar J, et al. FAD-I, a Fusobacterium nucleatum Cell Wall-Associated Diacylated Lipoprotein That Mediates Human Beta Defensin 2 Induction through Toll-Like Receptor-1/2 (TLR-1/2) and TLR-2/6. Infect Immun. 2016;84: 1446–1456.
26. Desvaux M, Khan A, Beatson SA, Scott-Tucker A, Henderson IR. Protein secretion systems in Fusobacterium nucleatum: genomic identification of Type 4 piliation and complete Type V pathways brings new insight into mechanisms of pathogenesis. Biochim Biophys Acta. 2005;1713: 92–112.
27. Henderson IR, Nataro JP. Virulence functions of autotransporter proteins. Infect Immun. 2001;69: 1231–1243.
28. Wells TJ, Tree JJ, Ulett GC, Schembri MA. Autotransporter proteins: novel targets at the bacterial cell surface. FEMS Microbiol Lett. 2007;274: 163–172.
29. Fan E, Chauhan N, Udatha DBRKG, Leo JC, Linke D. Type V Secretion Systems in Bacteria. Microbiol Spectr. 2016;4. doi:10.1128/microbiolspec.VMBF-0009-2015
30. Albenne C, Ieva R. Job contenders: roles of the β-barrel assembly machinery and the translocation and assembly module in autotransporter secretion. Mol Microbiol. 2017; doi:10.1111/mmi.13832
31. Rossiter AE, Leyton DL, Tveen-Jensen K, Browning DF, Sevastsyanovich Y, Knowles TJ, et al. The essential β-barrel assembly machinery complex components BamD and BamA are required for autotransporter biogenesis. J Bacteriol. 2011;193: 4250–4253.
32. Salacha R, Kovacić F, Brochier-Armanet C, Wilhelm S, Tommassen J, Filloux A, et al. The Pseudomonas aeruginosa patatin-like protein PlpD is the archetype of a novel Type V secretion system. Environ Microbiol. 2010;12: 1498–1512.
33. da Mata Madeira PV, Zouhir S, Basso P, Neves D, Laubier A, Salacha R, et al. Structural Basis of Lipid Targeting and Destruction by the Type V Secretion System of Pseudomonas aeruginosa. J Mol Biol. 2016;428: 1790–1803.

34. Pizarro-Cerdá J, Cossart P. Subversion of phosphoinositide metabolism by intracellular bacterial pathogens. Nat Cell Biol. Nature Publishing Group; 2004;6: 1026–1033.
35. Istivan TS, Coloe PJ. Phospholipase A in Gram-negative bacteria and its role in pathogenesis. Microbiology. 2006;152: 1263–1274.
36. Flores-Díaz M, Monturiol-Gross L, Naylor C, Alape-Girón A, Flieger A. Bacterial Sphingomyelinases and Phospholipases as Virulence Factors. Microbiol Mol Biol Rev. 2016;80: 597–628.
37. Tannaes T, Bukholm IK, Bukholm G. High relative content of lysophospholipids of Helicobacter pylori mediates increased risk for ulcer disease. FEMS Immunol Med Microbiol. 2005;44: 17–23.
38. Dorrell N, Martino MC, Stabler RA, Ward SJ, Zhang ZW, McColm AA, et al. Characterization of Helicobacter pylori PldA, a phospholipase with a role in colonization of the gastric mucosa. Gastroenterology. 1999;117: 1098–1104.
39. Birmingham CL, Canadien V, Gouin E, Troy EB, Yoshimori T, Cossart P, et al. Listeria monocytogenes evades killing by autophagy during colonization of host cells. Autophagy. 2007;3: 442–451.
40. Muyzer G, de Waal EC, Uitterlinden AG. Profiling of complex microbial populations by denaturing gradient gel electrophoresis analysis of polymerase chain reaction-amplified genes coding for 16S rRNA. Appl Environ Microbiol. 1993;59: 695–700.
41. Hyatt D, Chen G-L, Locascio PF, Land ML, Larimer FW, Hauser LJ. Prodigal: prokaryotic gene recognition and translation initiation site identification. BMC Bioinformatics. 2010;11: 119.
42. Eddy SR. Profile hidden Markov models. Bioinformatics. 1998;14: 755–763.
43. Kearse M, Moir R, Wilson A, Stones-Havas S, Cheung M, Sturrock S, et al. Geneious Basic: an integrated and extendable desktop software platform for the organization and analysis of sequence data. Bioinformatics. 2012;28: 1647–1649.
44. Arnold K, Bordoli L, Kopp J, Schwede T. The SWISS-MODEL workspace: a web-based environment for protein structure homology modelling. Bioinformatics. 2006;22: 195–201.
45. Andersen KR, Leksa NC, Schwartz TU. Optimized E. coli expression strain LOBSTR eliminates common contaminants from His-tag purification. Proteins. 2013;81: 1857–1861.
46. Knorr M. Über die fusospirilläre Symbiose, die Gattung Fusobacterium (KB Lehmann) und Spirillum sputigenum. Zugleich ein Beiträg zür Bakteriologie der Mundhohle. II. Mitteilung Die Gattung Fusobacterium I Abt Orig Zentralbl Bakteriol Parasitenkd Infektionskr Hyg. 1922;89: 4–22.
47. Knorr M. Ueber die fusospirilläre symbiose, die Gattung Fusobacterium (KB Lehmann) und Spirillum sputigenum. II Mitteilung. Die Gattung Fusobacterium. Zentbl Bakteriol Parasitenkd Infekt Hyg Abt. 1923;1: 4–22.
48. Dzink JL, Sheenan MT, Socransky SS. Proposal of three subspecies of Fusobacterium nucleatum Knorr 1922: Fusobacterium nucleatum subsp. nucleatum subsp. nov., comb. nov.; Fusobacterium nucleatum subsp. polymorphum subsp. nov., nom. rev., comb. nov.; and Fusobacterium nucleatum subsp. vincentii subsp. nov., nom. rev., comb. nov. Int J Syst Evol Microbiol. Microbiology Society; 1990;40: 74–78.
49. Bannam TL, Rood JI. Clostridium perfringens-Escherichia coli shuttle vectors that carry single antibiotic resistance determinants. Plasmid. 1993;29: 233–235.
50. Studier FW. Protein production by auto-induction in high density shaking cultures. Protein Expr Purif. 2005;41: 207–234.
51. Kinder Haake S, Yoder S, Gerardo SH. Efficient gene transfer and targeted mutagenesis in Fusobacterium nucleatum. Plasmid. 2006;55: 27–38.

52. Huang Z, Liu S, Street I, Laliberte F, Abdullah K. Methyl arachidonyl fluorophosphonate, a potent irreversible cPLA2 inhibitor, blocks the mobilization of arachidonic acid in human platelets and …. Mediators Inflamm. 1994;
53. Street IP, Lin HK, Laliberté F, Ghomashchi F, Wang Z, Perrier H, et al. Slow- and tight-binding inhibitors of the 85-kDa human phospholipase A2. Biochemistry. 1993;32: 5935–5940.
54. Segall Y, Quistad GB, Sparks SE, Nomura DK, Casida JE. Toxicological and structural features of organophosphorus and organosulfur cannabinoid CB1 receptor ligands. Toxicol Sci. 2003;76: 131–137.
55. Ackermann EJ, Conde-Frieboes K, Dennis EA. Inhibition of Macrophage Ca-independent Phospholipase A by Bromoenol Lactone and Trifluoromethyl Ketones. J Biol Chem. 1995;270: 445–450.
56. Adibekian A, Martin BR, Speers AE, Brown SJ, Spicer T. Optimization and characterization of a triazole urea dual inhibitor for lysophospholipase 1 (LYPLA1) and lysophospholipase 2 (LYPLA2). ncbi.nlm.nih.gov; 2013; Available: https://www.ncbi.nlm.nih.gov/books/NBK133440/
57. Nomura DK, Blankman JL, Simon GM, Fujioka K, Issa RS, Ward AM, et al. Activation of the endocannabinoid system by organophosphorus nerve agents. Nat Chem Biol. 2008;4: 373–378.
58. Schevitz RW, Bach NJ, Carlson DG, Chirgadze NY, Clawson DK, Dillard RD, et al. Structure-based design of the first potent and selective inhibitor of human non-pancreatic secretory phospholipase A2. Nat Struct Biol. 1995;2: 458–465.
59. Randazzo A, Debitus C, Minale L, García Pastor P, Alcaraz MJ, Payá M, et al. Petrosaspongiolides M-R: new potent and selective phospholipase A2 inhibitors from the New Caledonian marine sponge Petrosaspongia nigra. J Nat Prod. 1998;61: 571–575.
60. Bennett CF, Mong S, Wu HL, Clark MA, Wheeler L, Crooke ST. Inhibition of phosphoinositide-specific phospholipase C by manoalide. Mol Pharmacol. 1987;32: 587–593.
61. Maffei M, Perez Y, Maffei M, Amata I, Arbesú M, Pons M. Lipid Binding by Disordered Proteins. Protocol Exchange. 2013; doi:10.1038/protex.2013.094
62. Biasini M, Bienert S, Waterhouse A, Arnold K, Studer G, Schmidt T, et al. SWISS-MODEL: modelling protein tertiary and quaternary structure using evolutionary information. Nucleic Acids Res. 2014;42: W252–8.
63. Lio YC, Reynolds LJ, Balsinde J, Dennis EA. Irreversible inhibition of Ca(2+)-independent phospholipase A2 by methyl arachidonyl fluorophosphonate. Biochim Biophys Acta. 1996;1302: 55–60.
64. Liu Y, Patricelli MP, Cravatt BF. Activity-based protein profiling: the serine hydrolases. Proc Natl Acad Sci U S A. 1999;96: 14694–14699.
65. Simon GM, Cravatt BF. Activity-based proteomics of enzyme superfamilies: serine hydrolases as a case study. J Biol Chem. 2010;285: 11051–11055.
66. Dekker N, Tommassen J, Lustig A, Rosenbusch JP, Verheij HM. Dimerization regulates the enzymatic activity of Escherichia coli outer membrane phospholipase A. J Biol Chem. 1997;272: 3179–3184.
67. Hug LA, Baker BJ, Anantharaman K, Brown CT, Probst AJ, Castelle CJ, et al. A new view of the tree of life. Nat Microbiol. 2016;1: 16048.
68. Wilson MM, Anderson DE, Bernstein HD. Analysis of the outer membrane proteome and secretome of Bacteroides fragilis reveals a multiplicity of secretion mechanisms. PLoS One. 2015;10: e0117732.

69. Kapatral V, Anderson I, Ivanova N, Reznik G, Los T, Lykidis A, et al. Genome sequence and analysis of the oral bacterium Fusobacterium nucleatum strain ATCC 25586. J Bacteriol. 2002;184: 2005–2018.
70. Howell HA, Logan LK, Hauser AR. Type III secretion of ExoU is critical during early Pseudomonas aeruginosa pneumonia. MBio. 2013;4: e00032–13.
71. Machado G-BS, de Assis M-C, Leão R, Saliba AM, Silva MCA, Suassuna JH, et al. ExoU-induced vascular hyperpermeability and platelet activation in the course of experimental Pseudomonas aeruginosa pneumosepsis. Shock. 2010;33: 315–321.
72. Allewelt M, Coleman FT, Grout M, Priebe GP, Pier GB. Acquisition of expression of the Pseudomonas aeruginosa ExoU cytotoxin leads to increased bacterial virulence in a murine model of acute pneumonia and systemic spread. Infect Immun. Am Soc Microbiol; 2000;68: 3998–4004.
73. Afra K, Laupland K, Leal J, Lloyd T, Gregson D. Incidence, risk factors, and outcomes of Fusobacterium species bacteremia. BMC Infect Dis. 2013;13: 264.
74. Heckmann JG, Lang CJG, Hartl H, Tomandl B. Multiple brain abscesses caused by Fusobacterium nucleatum treated conservatively. Can J Neurol Sci. 2003;30: 266–268.
75. Ahmed Z, Bansal SK, Dhillon S. Pyogenic liver abscess caused by Fusobacterium in a 21-year-old immunocompetent male. World J Gastroenterol. 2015;21: 3731–3735.
76. Brook I. Infective endocarditis caused by anaerobic bacteria. Arch Cardiovasc Dis. 2008;101: 665–676.

Chapter 5

Conclusions

Fusobacterium nucleatum is an anaerobic, Gram-negative member of the oral microbiome. As a resident of the mouth it is a major cause of periodontitis. It also causes life-threatening disease in locations throughout the body including the lungs, liver, heart, brain and placenta, where it induces preterm birth. Recent high-impact studies have implicated *Fusobacterium* in the development and progression of colorectal cancer (CRC). Despite these important associations, the molecular mechanisms underlying these phenotypes remain largely unknown. This knowledge gap is largely due to the lack of both an effective gene deletion system and molecular tools with which to study key host-pathogen interactions. This has caused a bottleneck in the field of *F. nucleatum* biology and, in particular, studies probing the mechanisms underlying the interactions with its human host. Breakthroughs presented in this work have largely focused on developing these tools to lay the foundation for the future study of *Fusobacterium* in relation to human health and disease.

To address this fundamental gap in knowledge, we created a unique marker-less gene deletion system capable of generating in-frame deletion mutants in any gene of interest. A benefit of this system is that it results in mutants with no antibiotic sensitivity. This permits the creation of bacterial strains with multiple genes deletions in parallel, which allows us to overcome potential confounding effects arising from virulence factor cooperativity or redundant protein systems. Our methodology takes advantage of an initial selection based on antibiotic sensitivity to ensure plasmid incorporation onto the chromosome and a secondary selection exploiting sugar sensitivity conferred by the plasmid to select for in-frame deletion mutants. This system has allowed us to screen a number of genes for their roles in *Fusobacterium*'s ability to invade human epithelial cells for the first time. This genetic system has allowed us to generate in-frame gene deletion strains of *fap2*, *fadA* and a strain with both genes deleted in parallel. Our results support a revised model of

F. nucleatum pathogenesis (**Figure 5.1**). Previously, FadA was presumed to be a main driver of *F. nucleatum* invasion along with Fap2. However, while we confirm that Fap2 is a significant contributor to invasion, our results suggest that the role of FadA in invasion should be further explored. We also show that WT *F. nucleatum* expressing increases IL-8 production in cancerous human epithelial cells, but this is greatly suppressed in a Δ*fap2* mutant. IL-8 is a known modulator of the tumor microenvironment with increased amounts corresponding to increased tumorigenicity, angiogenesis and metastasis. Our findings further corroborate the notion that Fap2 is a key player in the involvement of *F. nucleatum* in CRC.

In this body of work, we have also developed recombinant protein technologies to combine with our genetic system to probe the role of large autotransporter proteins in *F. nucleatum*. These proteins are prime candidates for therapeutic targets as they are present at the host-pathogen interface and have the potential to interact with and manipulate host cell machinery. We have developed molecular cloning technology to facilitate *Fusobacterium* protein expression in *E. coli* for *in vitro* studies including enzymatic characterization, protein secretion dynamics and host molecule interactions. The importance of these breakthroughs cannot be overstated. Similar technologies were employed in other pathogenic bacteria to elucidate crucial aspects of their disease-causing processes. This has helped the scientific and medical community to better understand bacteria that infect thousands of people per year.

In addition to studying the surface adhesins of *F. nucleatum,* Fap2 and FadA, we provided the first characterization of FplA, a surface bound phospholipase enzyme. Until, further studies are performed in *F. nucleatum*, we have put the current understanding of FplA in the context of human cell signaling modulating virulence factors of more well studied bacteria (**Figure 5.2**). ExoU of *P. aeruginosa* acts as a PLA2 and cleaves phosphatidylinositol (PI) 4, 5-P_2 that ultimately results elevated inflammation mediated through increased IL-8 signaling.

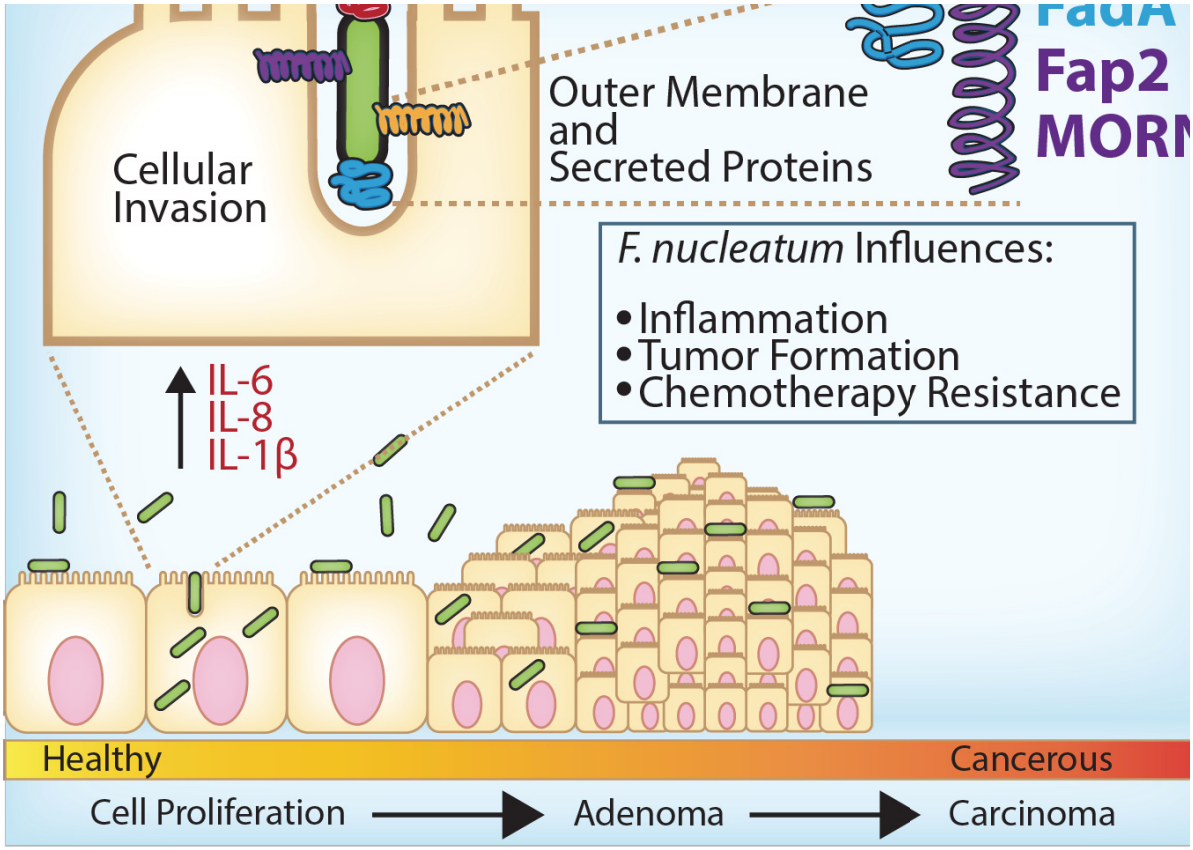

Figure 5.1 An updated model of *F. nucleatum* invasion. Our results suggest that Fap2, and not FadA, drive invasion of epithelial cells. IL-6, IL-8 and IL-1β all are increased leading to a microenvironment conducive to tumor formation.

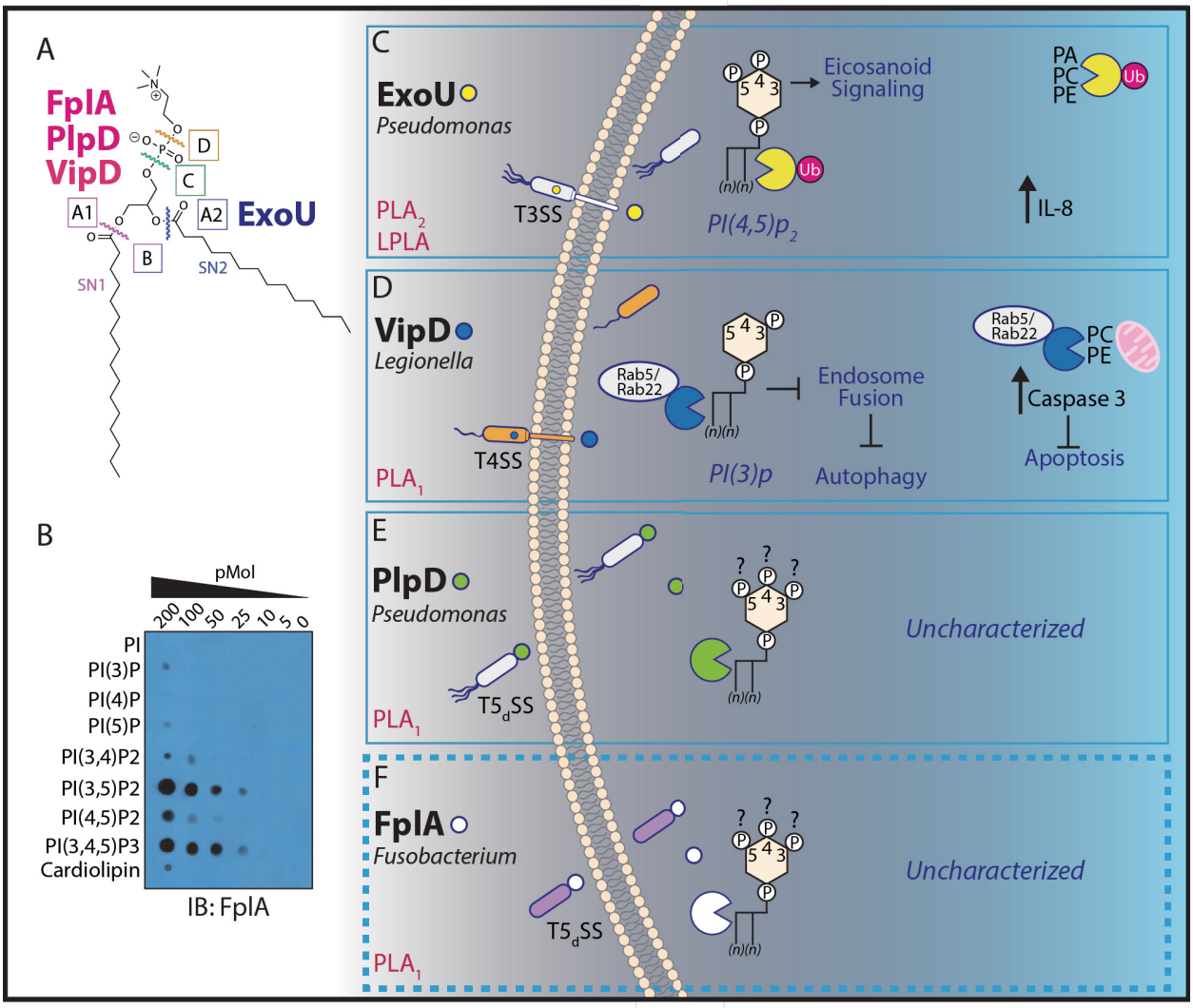

Figure 5.2 An overview of phospholipases as virulence factors. A model PI illustrating the hydrolysis point of each class of phospholipase is shown. FplA, PlpD, and VipD cleave ester bonds in the SN1 position. ExoU is a PLA2, cleaving bonds in the SN2 position (A). FplA demonstrates potent PI binding activity, with the strongest affinity shown for PI-3, 5-P_2 and PI-3, 4, 5-P_3 (B). Current knowledge in the field of PI interaction virulence factors is shown in the context of a cell. Much is known about ExoU and VipD's role in modulating inflammation and the autophagic/apoptotic pathways respectively (C-D). There is still much to be learned about the roles PlpD and FplA in bacterial virulence, however substrate affinities have been ascertained (E-F).

VipD of *Legionella pneumophila* cleaves PI-3-P which results in decreased autophagic and apoptotic activity. This ultimately enhances bacterial survival by keeping the host cell alive while preventing destruction of the bacteria's intracellular niche. We have demonstrated, *in vitro*, that FplA does indeed possess phosphatidylinositol interaction capacity. Lipid binding assays show that FplA interacts strongly with PI-3, 5-P_2 and PI-3, 4, 5-P_3. While it is impossible to speculate on which specific signaling pathways may be affected by *F. nucleatum* as these molecules are implicated in numerous pathways, the potential importance of FplA is abundantly apparent.

Using our genetic and recombinant protein expression breakthroughs, we have uncovered numerous details of *Fusobacterium* biology. We have revised the current invasion model of *F. nucleatum* 23726 by showing that Fap2 and not FadA drives invasion of host cells. Additionally, we show that Fap2 is mediates increased IL-8 production by host cells, which has been shown to be a tumor microenvironment regulator. This bolsters previous findings that *F. nucleatum* is implicated in the development and progression of colorectal cancer. We have also identified a potential lipid signaling interactor in *F. nucleatum* via the autotransporter phospholipase, FplA.

The methodologies and technologies presented in this dissertation effectively lay the foundation for repeatable, facile molecular studies of *Fusobacterium*-host interaction dynamics. Future experiments can exploit these technologies to better understand protein families that are likely involved in virulence. These include members of the Type 5a, b, and c autotransporter pathways. Their roles in virulence and substrate preferences can now be ascertained using whole bacterial cells as well as recombinant protein methodologies. This will shed new light on understudied protein families in *F. nucleatum*. We also established a launching point for probing these interactions with the initial biochemical characterization of FplA, which is a prime candidate to modulate host cell biology upon *Fusobacterium* invasion of human cells. The potential impact

of studies using these techniques is significant, and the future of the field of *Fusobacterium* biology is bright.